INFORMATION TO USERS

This manuscript has been reproduced from the microfilm master. UMI films the text directly from the original or copy submitted. Thus, some thesis and dissertation copies are in typewriter face, while others may be from any type of computer printer.

The quality of this reproduction is dependent upon the quality of the copy submitted. Broken or indistinct print, colored or poor quality illustrations and photographs, print bleedthrough, substandard margins, and improper alignment can adversely affect reproduction.

In the unlikely event that the author did not send UMI a complete manuscript and there are missing pages, these will be noted. Also, if unauthorized copyright material had to be removed, a note will indicate the deletion.

Oversize materials (e.g., maps, drawings, charts) are reproduced by sectioning the original, beginning at the upper left-hand corner and continuing from left to right in equal sections with small overlaps. Each original is also photographed in one exposure and is included in reduced form at the back of the book.

Photographs included in the original manuscript have been reproduced xerographically in this copy. Higher quality 6" x 9" black and white photographic prints are available for any photographs or illustrations appearing in this copy for an additional charge. Contact UMI directly to order.

UMI®

Bell & Howell Information and Learning
300 North Zeeb Road, Ann Arbor, MI 48106-1346 USA
800-521-0600

REPAIR OF A SITE-SPECIFICALLY PLACED PSORALEN CROSSLINK, PSORALEN MONOADDUCT, AND DOUBLE STRAND BREAK IN THE YEAST *SACCHAROMYCES CEREVISIAE*

By

ROSS GREENBERG

A dissertation submitted to the Graduate Faculty in Biochemistry in partial fulfillment of the requirements for the degree of Doctor of Philosophy, The City University of New York.

2001

UMI Number: 9997092

Bell & Howell Information and Learning Company
300 North Zeeb Road
P.O. Box 1346
Ann Arbor, MI 48106-1346

This manuscript has been read and accepted for the Graduate Faculty in Biochemistry in satisfaction of the dissertation requirement for the degree of Doctor of Philosophy.

1/25/01
Date

Wilma Saffran
Chair of Examining Committee
Prof. Wilma Saffran, Queens College

1/26/2001
Date

Horst Schultz
Executive Officer
Prof. Horst Schultz

Prof. Corrine A. Michels, Queens College

Prof. Carol Moore, City College

Prof. Maria Tomaz, Hunter College

Prof. Rodney Rothstein, Columbia University

Supervisory Committee

The City University of New York

ABSTRACT

REPAIR OF A SITE-SPECIFICALLY PLACED PSORALEN CROSSLINK, PSORALEN MONOADDUCT, AND DOUBLE STRAND BREAK IN THE YEAST *SACCHAROMYCES CEREVISIAE*

By
Ross Greenberg

Advisor: Professor Wilma Saffran

Repair substrates carrying a single site-specifically placed psoralen crosslink, monoadduct, or double strand break were synthesized and used to compare repair, recombination, and gene conversion induced from each form of damage. The damage was located at the *BsiWI* site of a *his3* allele carried on a plasmid. Damaged plasmids were introduced into yeast for in vivo repair. Genetic and physical analysis of colonies carrying repaired plasmids was performed.

The overall level of recombination and gene conversion induced from a DSB and a crosslink were similar. Monoadducts were non-recombinogenic. Similarities were observed for many of the properties of recombination and gene conversion induced by crosslinks and DSBs. These properties include the levels of reciprocal recombination, conversion tract length, the levels of uni- and bi-directional tracts, and the levels of discontinuous tracts. During crosslink and DSB induced gene conversion, the undamaged chromosomal allele was the primary donor of genetic information. The major difference in damage-induced

recombination between crosslinks and DSBs was in the polarity of gene conversion tracts.

Gene conversion tracts induced from crosslinks exhibited a directional polarity, preferentially extending upstream from the damage site. Conversion tracts induced from a DSB also exhibited a polarity, but in the downstream rather than the upstream direction. The results show that the form of damage initiating the conversion influences the direction of the conversion tract and offer evidences that conversion tract polarity is linked to physical and/or mechanistic properties of the repair intermediate.

An additional difference between crosslinks and DSBs was in the occurrence of induced mutations. A psoralen crosslink, in addition to error-free repair, was a substrate for error-prone repair. Mutations at the damage site occurred in 9.1% of the non-reciprocal products. Mutations were not detected in the reciprocal products of crosslink repair. DSBs were non-mutagenic. These repair patterns indicate that there are two branches of crosslink repair. An error-free pathway is initiated by nucleotide excision repair, which processes crosslinks to DSBs. These DSBs are repaired by homologous recombination. An alternate, error-prone pathway also acts on crosslinks, and competes with the error-free branch for crosslink substrate. This error-prone branch generates targeted mutations.

Acknowledgments

I wish to thank my mentor, Dr. Wilma Saffran, for the guidance, support, and patience you have shown me and I thank the members of my dissertation committee for your assistance and encouragement.

I wish to extend my gratitude to Eduardo Sanz-Navares, Lirong Wong, Wei Cheng, and Evan Mintzer for their help with the physical analysis.

My deepest gratitude goes to my wife Elaine for her understanding, patience, love, and financial support of our family, to my daughter Ilana whose glance can make me smile when things are at their worst, and to my mother Natalie for her love, mental support, and financial assistance. You are all the most important treasures I have; I love you all.

The love and support from my sister Reina and her family, as well as from my in-laws Millie and Jack was more important to me than any positive result obtained during these experiments and I thank you all.

Finally I wish to dedicate this work to the loving memories of my father Stanley, my granny Yetta, and my grampa Sam. I wish you were all here to share this with me. I miss you.

Table of Contents

List of Tables

List of Figures

Introduction

The cellular maintenance of genomic integrity is a fundamental principle of life. In order to survive, organisms have evolved complex strategies to cope with exogenous and endogenous factors that induce damage to the genome. Factors that induce damage to DNA include UV and ionizing radiation as well as chemical agents that impose their genotoxic effects through mutagenic, clastogenic, recombinogenic, and carcinogenic end points.

The factors that damage DNA produce lethal effects by direct and indirect mechanisms. Clastogenic factors that produce extensive breakage of DNA and factors producing chemical modification in excess of cellular repair capacities prevent replication and transcription, leading to direct cell death or to apoptosis. Damage in limiting quantity can still elicit lethal effects by inducing either recombination resulting in deletions, rearrangements, and gene amplification or by inducing mutations resulting in loss of function of critical gene products. In higher eukaryotes damage-induced genotoxicity has been implicated in the formation of many cancerous and non-cancerous diseases.

The genes that mediate the signaling and regulation of cell growth and division, involved in neoplastic transformation, fall into two major catagories: proto-oncogenes, and tumor suppressors. Positive mutations, causing hyper-activity of the gene product and/or overexpression of normal cellular proto-oncogenes, may induce transformation into the oncogenic state, releasing the cell

from the normal restraints on growth. Oncogenic mutations are dominant, inducing transformation upon mutation of only one allele of the proto-oncogene.

Tumor suppressor genes, in contrast to oncogenes, induce the pathogenic process through negative mutation. Mutations that result in the loss of function of the gene product account for transformation in these cells. Tumor suppressor mutations are recessive, requiring loss of function of both alleles to induce transformation.

The p53 gene encodes a tumor suppressor protein that is believed to sense DNA damage within the cell and arrest the cell cycle until the damage is repaired (Lee and Bernstein 1993). If the DNA damage of the cell is too extensive for the cellular repair mechanism(s), apoptosis involving the p53 gene product occurs, killing the potential tumor cell line. Loss of p53 function is believed to influence the pathogenic pathway by allowing cells that have DNA damage, and are therefore potential tumor cells, to divide prior to effective repair. The loss of apoptosis control of the p53 protein also allows potential tumor cells to survive and give rise to malignant cell lines. Alteration or inactivation of the p53 gene product by mutation of the p53 gene has been reported as the most common genetic change in human cancer (Levine *et al.*, 1991). Most cancer cell lines carry a mutation in the p53 gene. Both transition and transversion mutations in the p53 gene have been found in diverse types of cancers (Hollstein *et al.*, 1991a; 1991b). In squamous cell carcinomas of the skin, CC-to-TT double base changes were

identified in the p53 gene (Brash *et al.*, 1991). This form of transition is induced only by UV radiation.

Mutations, translocation, amplification and deletions of other proto-oncogenes of higher eukaryotes such as the Ras, Myc, and Src genes are all implicated in the pathogenic pathway leading to cancer.

Aetiological studies have identified a large number of known or suspected carcinogens, many of which are known to directly bind to DNA (Summary of the 8th report on Carcinogens, U.S. Department of Health and Human Services). While the pathogenic pathway of these carcinogens is not completely understood it is generally accepted that DNA lesions produced by the direct attack of these agents induce cellular repair processes (both error-free and error-prone pathways) leading to the genetic alterations that may induce neoplastic transformation of normal cells. It is therefore important to study the cellular repair processes induced by carcinogens to understand the mechanisms involved in the pathogenic process of cancer formation.

Psoralen:

Psoralens, tricyclic planar furocoumarins, constitute an important class of photochemical compounds that have been used to study biological aspects of nucleic acids (Song and Tapley 1979, Cimino *et al.*, 1985). The ability of psoralen modification to freeze helical regions of DNA and RNA has allowed the isolation of various nucleic acid molecules to study the structures found therein. Detailed information on chromatin structure (Hanson *et al.*, 1976; Cech and Pardue, 1977;

Cech and Karrer, 1980; Hallick *et al.*, 1980), cruciform structure (Sinden *et al.*, 1983), torsional tension (Sinden *et al.*, 1980; Sinden and Pettijohn 1981) secondary structure of ssDNA and RNA (Shen and Hearst 1976,1979; Thompson and Hearst 1983) and the presence of D-loops and Holliday structures (DeFrancesco and Attardi 1981; Sogo *et al.*, 1986) have been obtained by the use of psoralen modification to DNA and RNA. As a chemotheraputic agent psoralen plus ultraviolet A light (PUVA) is used clinically for the treatment of psoraisis, vitiligo, and other skin diseases (Van Scott, 1975; Rodighiero and Dall'Acqua, 1976,1986). Recently, photochemical processes have been developed for the inactivation of viruses and bacteria in platelet concentrates using psoralens (Lin *et al.*, 1993, 1997). PUVA therapy, however, has been reported as a known carcinogen in mice and humans (Report on carcinogens, 8^{th} edition) and is responsible for the formation of epidermal papillomas, squamous cell carcinoma, fibrosarcomas, basal cell tumors and melanomas.

The adducts that psoralens form within the double helix of DNA have been extensively characterized (Hearst *et al.*, 1984). Use of various natural or synthetic derivatives along with controlled photo-reaction parameters enables high control over the amounts and distributions of the photo-lesions that the compounds form within DNA. Psoralen modification of DNA leads to repair products that exhibit similar genetic alterations to those observed in transformed neoplastic cells. These factors make psoralens a useful tool to study repair and mutagenesis in bacteria, yeast, and mammalian cells.

Psoralen Chemistry:

Psoralens are bifunctional, photo-reactive compounds that form covalent bonds with pyrimidine bases of DNA. Structurally, psoralens are tricyclic linear fusions of a furan ring to a coumarin. The structure of psoralen and two derivatives and the covalent bonding of psoralens with thymine bases are shown in figure 1. The planar compound intercalates into the double helix in a dark reaction. Covalent photocycloaddition at either the furan or pyrone end occurs with light in the 320 - 400 nm range, producing either a furan-ended monoadduct or a pyrone-ended monoadduct (Kanne *et al.*, 1982). A second photon of light can convert the monoadduct into a crosslink. The bifunctional reactivity of linear psoralens, accounting for their crosslinking ability, arises from the 4',5' double bond on the furan moiety and, on the opposite end of the molecule, from the 3,4 double bond of the pyrone moiety.

The photoactivation of psoralen is not fully understood. There are two possible types of electronic excitation in the UV and near UV (200-400nm) region of the spectrum (Song and Baba 1974; Song and Fugate 1975). The first excitation state occurs when a nonbonding electron in the carbonyl group of the pyrone moiety is excited to the anti-bonding π^* molecular orbital, producing the n,π^* excited state (Song and Gordon 1970; Song 1984). The second excited state occurs when a π electron from the psoralen ring structure is excited to an antibonding π^* molecular orbital (π,π^*) (Mantulin and Song 1973). Different spin

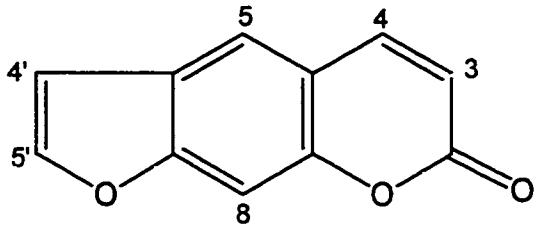

psoralen

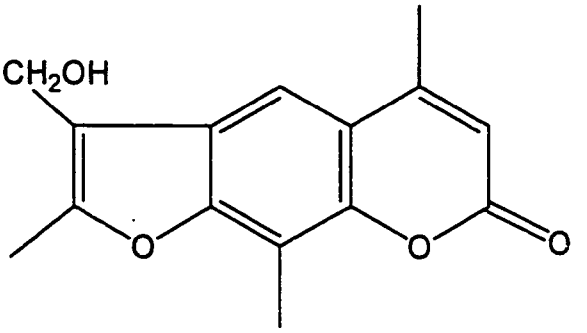

4'-hydroxymethyl-4,5',8-trimethylpsoralen
(HMT)

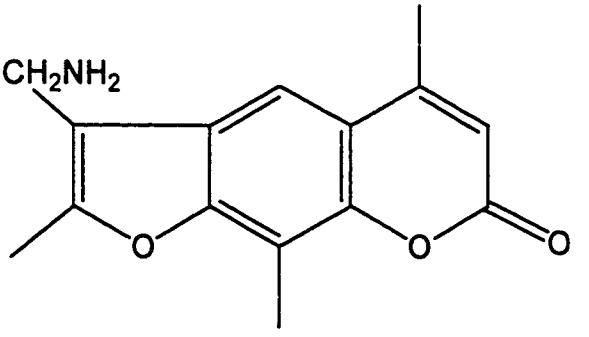

4'-aminomethyl-4,5',8-trimethylpsoralen
(AMT)

Figure 1a. Psoralen and two derivatives.

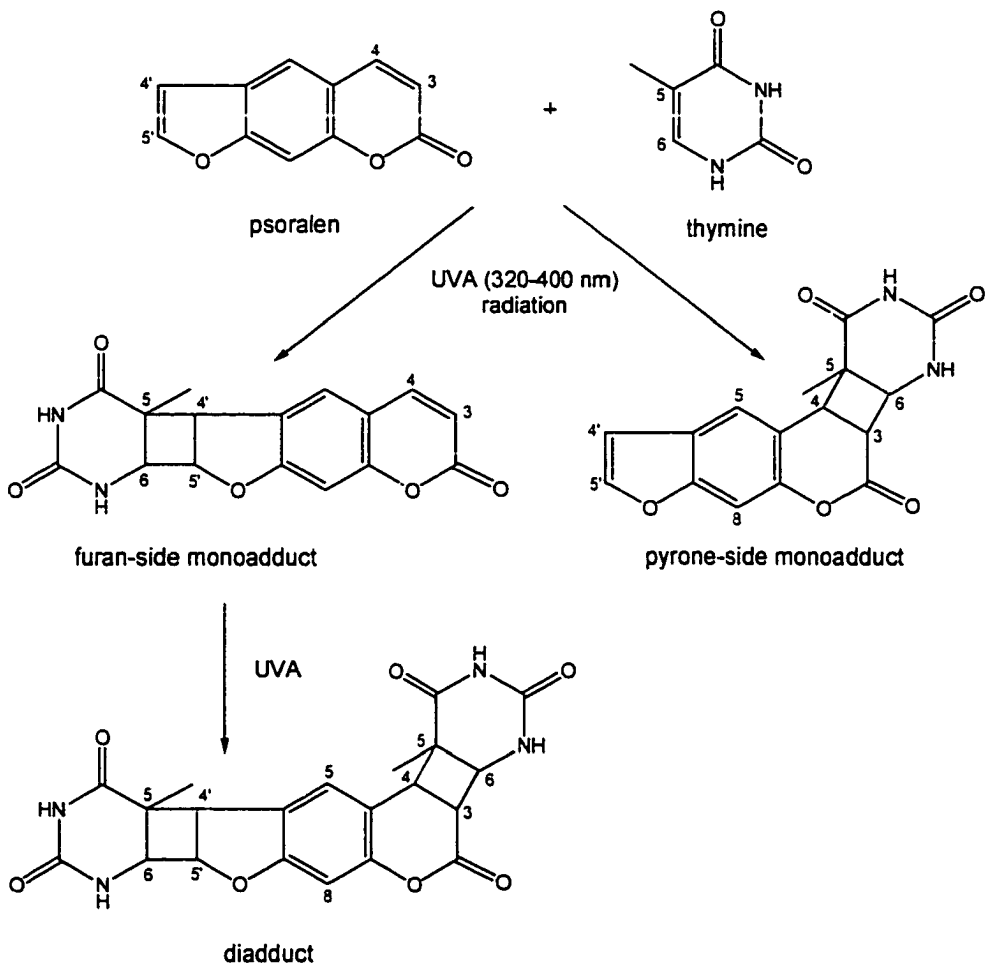

Figure 1b. Photoreaction products of psoralen with thymine bases

configurations of the unpaired electrons in the excited molecule give rise to either the singlet excited state or the triplet excited state (Song and Gordon 1970; Moore *et al.*, 1976; Knox *et al.*, 1988). The n,π^* singlet state has been localized to the carbonyl group of the pyrone (Song *et al.*, 1971). The triplet π,π^* state has been localized to the carbon-carbon double bond of the pyrone and is predicted to be the reactive state (Mantulin and Song 1973). Triplet quenching has been observed upon the addition of DNA to excited psoralens (Song and Gordon 1970; Salet *et al.*, 1980). Local excitation of the 4',5' double bond of the furan moiety has not been directly observed. Activation of this bond is believed to arise due to intramolecular charge transfer through the π electron system of the ring structure. The 3,4 double bond of the pyrone has been shown to possess higher charge transfer character than the 4',5' double bond of the furyl group (Mantulin and Song 1973; Song 1984) and it has been suggested that the photoreactivity resides, or initiates, within the pyrone (Song *et al.*, 1971; Song 1984).

Psoralens containing a variety of chemical substituents, attached to various carbons of the ring system, have been either isolated from natural sources or produced by organic synthesis (Isaacs *et al.*, 1977; Gia *et al.*, 1992a). The nature and positioning of these chemical groups have been shown to affect the reactivity of the various compounds. The substituents introduce steric, kinetic, and electronic factors that influence excitation lifetime and charge transfer of the excited species, as well as affecting the accessibility and alignment with respect to

the substrate DNA. Solvent effects also play a role in the reactivity of psoralens with DNA.

Excited (triplet π,π^*) psoralens undergo [2+2] cycloaddition with the 5,6 double bond of thymine bases (Song *et al.*, 1971; Cadet *et al.*,1990). The isolated photo-products formed from psoralen with nucleotide bases indicate that the 3,4 double bond of the pyrone is more photo-reactive than the 4',5' double bond of the furan (Shim and Kim 1983; Shim *et al.*, 1983). However, the distribution of products isolated from reactions with DNA is different from the distribution of products observed from the reaction of psoralen with free thymine (Gaboriau *et al.*,1987; Peckler *et al.*, 1982). Three major photoproducts are produced by the reaction of psoralens with DNA: the furan side thymidine-psoralen monoadduct, the pyrone side thymidine-psoralen monoadduct, and the thymidine-psoralen-thymidine diadduct or crosslink (Bankmann and Brendel 1989). The distribution of these products depends on the psoralen derivative (molecular geometry and substituents), the wavelength of irradiation, the time of the irradiation, and the DNA sequence.

The photoreaction of psoralens with DNA has been simplified into 3 distinct steps (Isaacs *et al.*, 1977). Psoralen intercalates between adjacent base pairs to form a noncovalent complex with DNA. The dissociation constants of the various psoralen derivatives are in the range of 10^{-3} to 10^{-6} mol/L (Isaacs *et al.*, 1984). The low dissociation constants enable the short-lived excited state to be effectively trapped by the DNA. The number of intercalation sites in DNA has

been reported to be 2-6 per 100 bases (Song and Tapley 1979). DNA sequence, solvent interactions, and the substituents on the derivative influence the efficiency of the forces of intercalation. A preference for intercalation at sequences with alternating purine and pyrimidine bases has been reported (Dall'acqua *et al.*, 1978; Tessman *et al.*, 1985). The intercalation complex that forms at each intercalation site governs the stereospecifity and the distribution of adducts produced.

Following intercalation, psoralens are activated by irradiation and undergo cycloaddition with an adjacent pyrimidine base. The photoproducts formed during the photoreaction depend on the specific derivative in use and the control of the wavelength and time of the irradiation. Derivatives with a methyl group at the C4 position of the pyrone, such as in 4,5',8-trimethylpsoralen (TMP) or 4' hydroxymethyl-4,5',8-trimethylpsoralen (HMT), form as little as 2% pyrone side monoadducts due to steric interference of the C4 methyl group with the C5 methyl group of the thymidine (Kanne *et al.*, 1984). 8-methoxypsoralen (8-MOP) lacks the C4 methyl group and forms pyrone adducts up to 20% (Kanne *et al.*, 1982). Formation of 4',5' furan monoadducts with 8-MOP is greatly enhanced if the wavelength is above 380nm. The major products formed with 8-MOP and TMP are diastereomeric furan side monoadducts.

Furan end monoadducts can absorb a second photon and convert to a covalent interstrand crosslink through cycloaddition of the pyrone end with a thymine base on the opposite strand. Pyrone end monoadducts are incapable of crosslink conversion, presumably because the photoreactive center has been

disrupted by the cycloaddition that forms the monoadduct at this end. Pyrone end monoadducts have been shown to lack absorbance in the 300-400nm region, required for photoactivation, further suggesting that the triplet reactive state initiates at the pyrone moiety (Cimino *et al.*, 1985). A 15ns pulse of 347nm laser irradiation was shown to produce only monoadducts (Johnston *et al.*, 1977). Subsequent pulses convert some of the monoadducts to crosslinks in the absence of unbound psoralen, exemplifying the concerted mechanism of crosslink formation. Not all furan end monoadducts convert to crosslinks. The geometry of the psoralen molecule, substituent group(s), and DNA sequence all influence the conversion of a furan end monoadduct to a crosslink.

A preference for reaction with the 3' face of thymidine has been observed. 72% of 8-MOP adducts are formed at crosslinkable sites, 69% of which are at 5'TpA (Tessman *et al.*,1985). It has been suggested that this preference is due to favorable intercalation at these sites. The overall quantum yield of initial binding of psoralens to DNA, however, is relatively low due to the low probabilities of activation of the molecule to the correct photoreactive state and positioning to the correct geometric alignment for cycloaddition.

The 5'TpA sequence is considered the preferential site of psoralen adduct formation (figure 2) (Boyer *et al.*, 1988; Kittler and Lober 1995). This sequence is a crosslinkable site. A 3 fold increase of adduct formation at 5'-GTAC has been reported over 5'-GATC and both 5'-TATA and 5'-TATG have been shown to be hotspots of psoralen reactivity (Gia *et al.*, 1992b). The 5'-TpA sequence provides

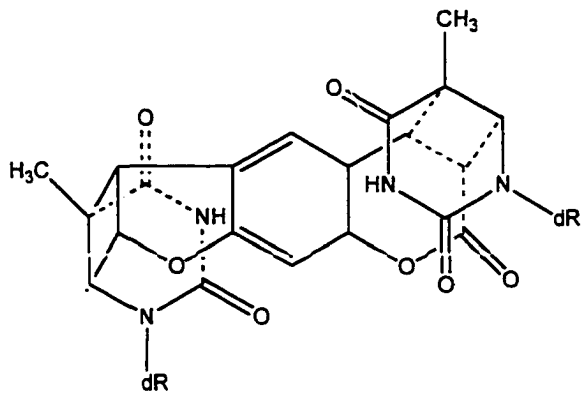

Interstrand crosslink

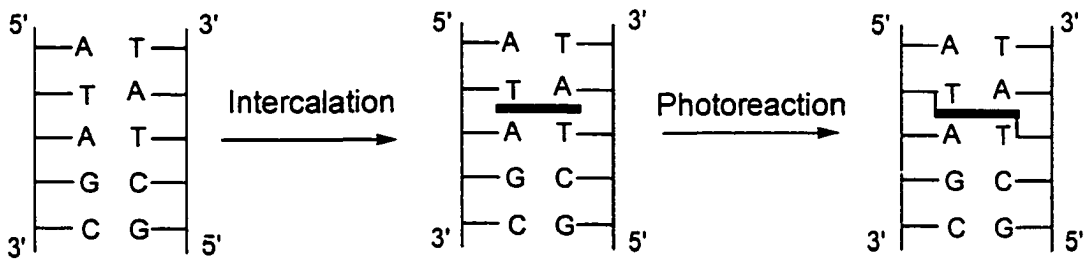

The preferred sites of psoralen photoreaction are at 5'-TpA-3' sequences.

Figure 2. Structure of interstrand crosslink.

the favored orientation for the two reactive ends of psoralen to undergo cycloaddition with the 3' face of the two adjacent thymidines. However, it has been reported that 5'-CATG restores photoreactivity of psoralens to the same level as 5'-GTAC and it has been suggested that preferential sites may only require alternating pyrimidine-purine sequences (Ramaswamy and Yeung 1984).

The covalent modification of DNA by psoralen monoadducts and crosslinks introduces physical alterations to the continuity of the double helix (Pearlman *et al.*, 1985; Wiesehahn and Hearst 1978). In vitro studies with 3-carbethoxypsoralen (3-CP) monoadducts in salmon sperm DNA have suggested that a single monoadduct introduces helix unwinding at the site of modification to the extent of 7 base pairs (Gaboriau *et al.*, 1989). ^{1}H NMR spectroscopy and restrained molecular dynamics studies on the structures of both psoralen monoadduct and crosslink adducts in an 8 base oligonucleotide has indicated that both forms of adduct induced local distortion of the helix (Spielmann *et al.*, 1995a). Furan end monoadducts were shown to induce a 34° unwinding twist in the helix while crosslinks induced a 25° unwinding twist. No significant bend in the helix axis was detected from either adduct, and bases containing both forms of adducts adopted Watson-Crick type base pairing geometry. In similar studies it was shown that base stacking in the helix is unaffected by either adduct, but conformational changes and increased flexibility in the sugar-phosphate backbone of the helix are induced by both (Spielmann *et al.*, 1995b,c). It has been suggested that the induced changes in the sugar-phosphate backbone may act as the signal

for the recognition of psoralen damage by the cellular repair machinery, and may be a general motif for the recognition of lesions caused by many DNA damaging agents.

Repair pathways of *S. cerevisiae*

The introduction of covalent lesions to DNA produces immediate lethal effects by blocking replication and transcription. To cope with such damage, organisms have developed systems to remove the blocking lesions and efficiently repair any lost genetic information. However, there are circumstances where repair processes are incapable of processing error-free repair of the genome. These circumstances can lead to cell death or, in higher eukaryots, to the induction of pathogenic pathways that result in cancers.

Much of what is known of the mechanisms of DNA repair, recombination and mutagenesis has come from studies in the yeast *Saccharomyces cerevisiae.* This lower eukaryote provides an ideal system for study due to the ease of genetic manipulation and growth conditions, its stability, and the homology, both genetic and mechanistic, to the repair systems in humans. Many of the genes involved in nucleotide excision repair and recombination pathways in yeast have homologs in higher eukaryotes, including humans (Sancar, 1996). While tumorogenesis does not occur in this lower eukaryote, the mechanisms involved in damage induced repair result in products that exhibit the same alterations found in human cancer cell lines.

In *S. cerevisiae*, there are 3 major pathways that mediate damage-induced repairs of the cell's genome. The nucleotide excision repair pathway is responsible for the physical cutting of DNA containing either chemical adducts or dimerized bases. The recombinational repair pathway functions when the template activity to direct repair synthesis in the damage-containing DNA region is lost. This pathway provides an intact template by means of recombination with a homologous sequence. The third pathway is a composite of mechanisms collectively referred to as the damage tolerance pathways, which has error-free and error-prone branches and also mediates post-replicative repair. All 3 repair pathways in yeast mediate the repair of psoralen modification.

Nucleotide excision repair:

The cellular response to covalent modification of DNA bases is to excise the modified bases by incision of the damaged strand(s). In yeast, the excision of afflicted bases is catalyzed by a complex of proteins that assemble on the basal transcription initiation factor TFIIH converting it into a repairosome.

The genes that mediate nucleotide excision repair in *S. cerevisiae* belong to the *RAD3* epistasis group. Mutations in the genes of the *RAD3* group display sensitivity to UV irradiation and chemical agents that produce bulky lesions in DNA. The mechanism of nucleotide excision repair includes the recognition of the damaged base(s), incision on both sides of the damaged area, and the release of the afflicted base(s) contained within an oligonucleotide. Repair synthesis and strand ligation complete the process. Eighteen genes involved in nucleotide

excision repair have been determined to be epistatic to the *RAD3* group through mutational analysis (reviewed in Friedberg *et al.*, 1995). Many of these genes have been cloned, sequenced, and shown to be homologous to the NER genes of higher eukaryotes including humans. The products of a number of the genes that are essential for DNA incision have been purified. Biochemical assays have determined the biological and enzymatic function of these proteins in the excision pathway. A summary of these proteins is shown in table 1.

Minimum requirements for NER:

Highly purified components of the nucleotide excision repair complex have been combined to reconstitute in vitro bimodal incision of UV damaged DNA (Guzder *et al.*, 1995). The components required to produce in vitro incision include Rad1-Rad10 complex, TFIIH, Ssl2, Rad2, Rad4-Rad23 complex, Rad14, and RPA (replication protein A). Negative supercoiling of UV damaged plasmid substrates was relaxed by the incision complex only in the presence of ATP or dATP indicating a requirement for ATP hydrolysis for the activity. Undamaged plasmids remained supercoiled when treated with the in vitro incision components. Incision of plasmids carrying N-acetoxy-2 aminoacetyl fluorene adducts occurred to the same degree as with UV irradiated substrate. Both the Rad1/Rad10 complex and the Rad2 protein were required to produce incision. Supercoiling was not relieved when either component was omitted suggesting that a complete repair complex is required to mediate incision activity. DNA fragments ranging in size from 24 to 27 nucleotides were released from substrates after incision.

Table 1.

Components of Yeast NER

Nucleotide excision repair factor	Gene product	Sequence motif	Activity	Role in repair	Ref.
NEF1	Rad14	Zinc finger	DNA binding	Damage recognition	a
	Rad1/Rad10		Nuclease	5'-incision, End processing in recombination	b-f
NEF2	Rad4		DNA binding	Damage recognition	g,h
	Rad23	Ubiquitin		Putative recycling of Repairosome	i, j
NEF3 (TFIIH)	Rad25	ATPase, Helicase	SsDNA-dependent ATPase, 3'→5' Helicase		k
	Rad3	ATPase, Helicase	SsDNA-dependent ATPase, 5'→3' Helicase		l-n
	Tfb1				o-q
	Tfb2				"
	Tfb3				"
	Ssl1				"
	Rad2		Nuclease	3'-Incision	r,s
RPA	RPA		DNA binding	Damage recognition	t

[a]Bankmann *et al.*, 1989. [b]Sung *et al.*, 1993. [c]Bardwell *et al.*, 1994. [d]Davies *et al.*, 1995. [e]Fishman-Lobel and Haber 1992. [f]Rodriguez *et al.*, 1996. [g]Guzder *et al.*, 1998. [h]Jansen *et al.*, 1998. [i]Watkins *et al.*, 1993. [j]Schauber *et al.*, 1998. [k]Gudzer *et al.*, 1993. [l]Reynolds *et al.*, 1985. [m]Sung *et al.*, 1987a. [n]Sung *et al.*, 1987b. [o]Buratowski,S. 1994. [p]Conaway R.C., and J.W.Conaway 1993. [q]Feaver *et al.*,1993. [r]O'Donovan *et al.*, 1994. [s]Habraken *et al.*, 1993. [t] Alani *et al.*, 1999

Recombinational Repair:

When both strands of a DNA sequence are damaged, the genetic information that is required for proper repair by template directed repair synthesis is lost. Cells can mediate error-free repair of such damage if a homologous sequence donates the genetic information lost in the damaged region. The mechanism by which cells utilize a homologous sequence to direct repair of missing genetic information is known as homologous recombinational repair.

There are three major events that are associated with general recombination in yeast: meiotic recombination during sporulation, mitotic recombinational repair, and mating type switching at MAT. While these events are unrelated with respect to their biological application, it has been known since the 1960's that the same family of genes, the *RAD52* epistasis group, mediates the pathways leading to these events.

The *RAD52* epistasis group comprises the genes governing the homologous recombination pathway (Game and Mortimer 1974; Resnick 1968; Cox and Parry 1968). This group includes *RAD50-55, RAD57, XRS2, MRE11.* Mutations in genes of the *RAD52* epistasis group confer sensitivity to ionizing radiation, sensitivity to chemical agents that bind to DNA, and are defective in meiosis and sporulation (Game and Mortimer 1974; Cox and Parry 1968). Mutant strains carrying alleles of *RAD50*, *RAD*52, and *RAD*57 all sporulate but produce inviable spores and show a large decrease in cell viability (Game *et al.*, 1980). These strains are also severely defective in meiotic gene conversion. Mutations in

RAD52 have been shown to block mitotic heteroallelic recombination induced by ionizing radiation (Prakash *et al.*, 1980; Resnick and Martin, 1976). *RAD51* mutants are defective in DSB repair, spontaneous and radiation-induced mitotic recombination, and are defective in the formation of viable spores during meiosis (Game *et al.*, 1980). The Rad51 protein is a homologue of the *E.coli* RecA protein, which catalyzes strand exchange during recombination. In addition, mutants of seven genes of the *RAD52* family (*RAD50, RAD51*, *RAD52*, *RAD54*, *RAD55*, *RAD56*, and *RAD57*) which are all defective in meiotic recombination show increased sensitivity to psoralen damage (Henriques and Moustacchi 1980).

The catalytic functions of the *RAD52* group genes are not all known. However recent purification of some of the gene products of the *RAD52* group has been accomplished and biochemical dissection of these proteins are underway. Once the gene products are isolated and their catalytic function determined a better understanding of the mechanisms involved during recombination will be achieved.

Most of what is known about the general mechanism of recombination comes from analysis of meiotic gene conversion products and from analysis of the products formed during double strand break repair. Phenotypic segregation patterns determined from asci dissection have been used to extrapolate back to intermediate structures of recombination that can account for the observed conversion patterns. Gene conversion patterns determined from genetic and physical analysis of double strand break repair products from substrate/strain systems carrying well defined genetic markers has been used to extrapolate back

to recombination intermediates. Models of recombination have been drawn on the basis of these proposed intermediate structures. Both the products and intermediate structures of recombination deduced from damage-induced repair and meiotic gene conversion outcome display similarities, suggesting that the two events may occur by the same mechanism.

The canonical double strand break repair model of recombination:

The canonical double strand break repair model of recombination (Szostak *et al.*, 1983) and its variations (Sun *et al.*,1991; Gilbertson and Stahl 1996) has gained the widest acceptance as the general model of recombination on the basis of experimental evidence obtained from both meiotic gene conversion analysis and double strand break induced repair and recombination. The model is diagrammed in figure 3. In both meiotic gene conversion and double strand break repair, recombination initiates with a double strand break (fig 3B). The terminal ends of the break are processed by a 5'-to-3' endonuclease, to produce 3' overhangs on each end (fig 3C). One overhang invades an undamaged homolog, displacing a D-loop and forming a stretch of asymmetric heteroduplex DNA (fig 3D). Repair synthesis primed from the annealed 3' end occurs using the undamaged strand incorporated in the heteroduplex DNA as a template to direct repair. As a consequence of repair synthesis, DNA polymerase causes extension of the D-loop allowing the second overhang to anneal to the loop forming a second region of asymmetric DNA (fig 3E). A second round of template directed repair synthesis is

The DSB repair model of recombination

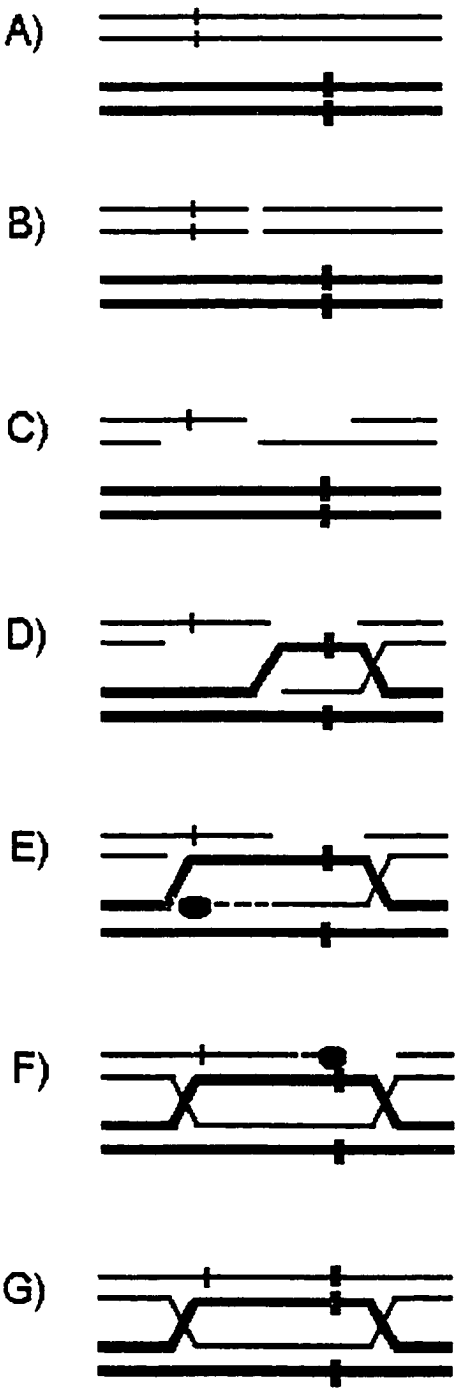

Figure 3 . The canonical double strand break model of recombination.

primed from the second 3' overhang end (fig 3F). The two regions of asymmetric heteroduplex DNA are formed on separate chromatids, and on opposite sides of the break. The recombination intermediate contains two Holliday junctions. Branch migration of the Holliday junctions can give rise to symmetric heteroduplex DNA on one or both sides of the double Holliday junction. In the absence of branch migration heteroduplex DNA remains asymmetric.

Gene conversion, the transfer of non-homologous genetic information between the two homologous alleles, is a consequence of recombination. The DSB repair model of recombination predicts that most or all gene conversion arises by mismatch repair of hDNA during both double strand break induced repair and meiotic gene conversion. Double strand break induced gene conversion has been extensively studied in various recombination systems. The products of DSB-induced gene conversion reveal common trends that are observed during meiotic gene conversion. Broken alleles are typically the recipient of genetic information (reviewed in Nickoloff and Hoekstra 1997). Conversion tract lengths have been observed to be limiting, exhibiting a distance gradient (Nelson *et al.*,1996). Tracts are predominately continuous and bidirectional in chromosomal borne direct repeats (Cho *et al.*, 1998). However, polarity of gene conversion has been observed in many systems (Detloff *et al.*, 1992; Malone *et al.*, 1992; Lamb 1998). Discontinuous tracts and unidirectional tracts have been observed in plasmid x chromosome recombination systems (Sweetser *et al.*, 1994; Cho *et al.*, 1998).

Resolution of the recombination intermediate can lead to either a crossover product, where flanking ends of the DNA molecules involved in the recombination are exchanged, or a non-crossover product exhibiting retention of the flanking sequences (fig 4). The pattern of resolution of the recombination intermediate leads to either the crossover or non-crossover product. If same–sense cutting of the Holliday junctions occurs (cutting of both junctions on the same strand) the product will be non-crossover (fig 4B). Opposite-sense cutting (cutting of different strand at the two junctions) results in a crossover product (fig 4C). In plasmid/chromosome recombination systems, crossover recombination leads to incorporation of the plasmid sequences into the genome (plasmid integration). Plasmids remaining extra-chromosomal arise from non-crossover events.

Nicks produced by resolution of the recombination intermediate create possible entry sites for mismatch repair enzymes. The canonical model accounts for two different mechanisms of gene conversion. Gene conversion events arise by either repair synthesis of the gaps produced by resectioning (fig 3G), or by mismatch repair of heteroduplex DNA (fig 4D and F).

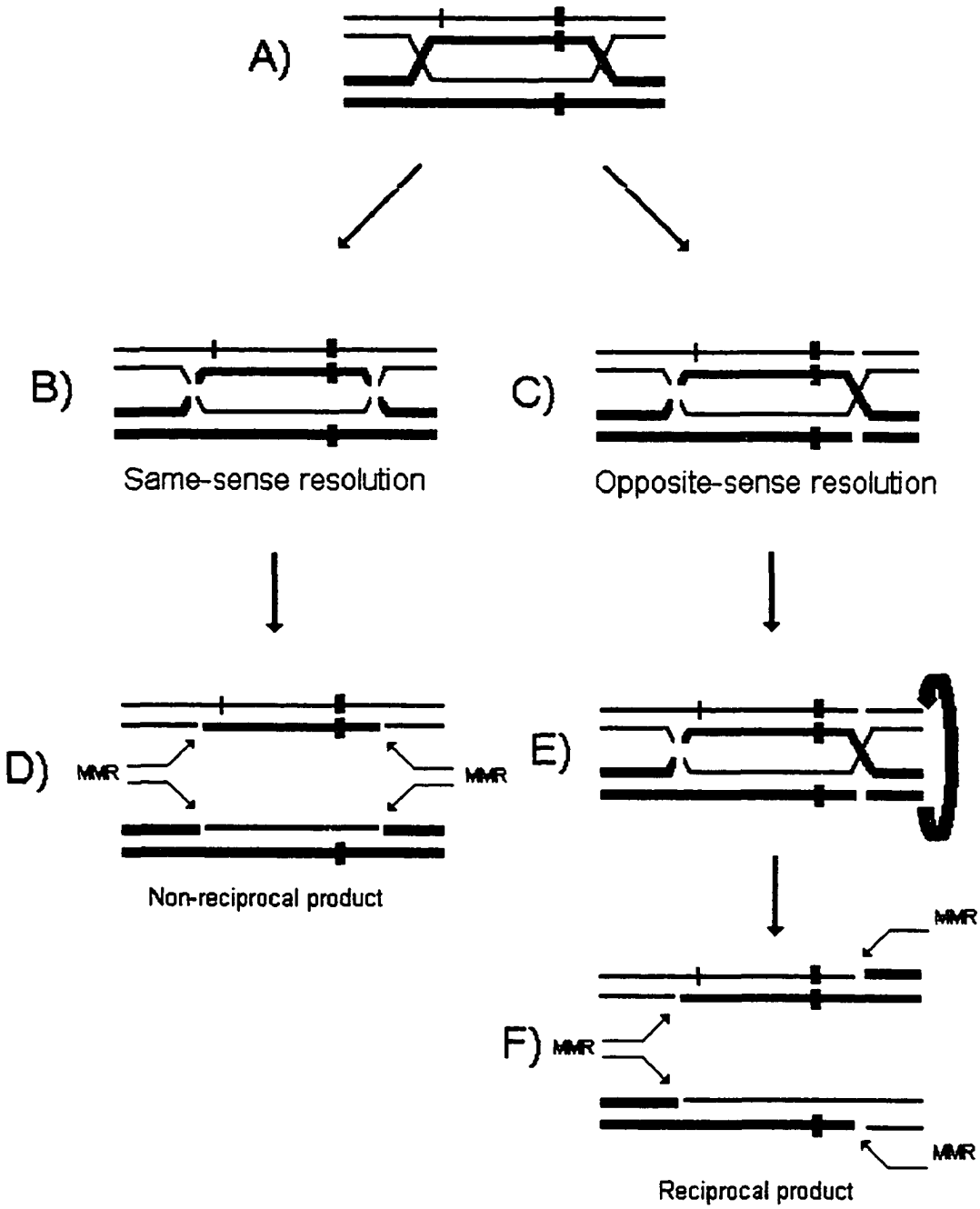

Figure 4. Crossover and non-crossover recombination products arise from different resolution patterns of the recombination intermediate.

Damage Tolerance Pathways:

The repair mechanisms mediated by the *RAD6* epistasis group comprise the damage tolerance pathways. The pathways of this group consist of mutagenic repair, damage avoidance pathways, and post-replicative repair. Of the three major repair groups in yeast, the least is known about these pathways. Many of the genes mediating these processes have been cloned, sequenced and analyzed by genetic and mutational techniques but most of the gene products have not been isolated and the mechanisms that are involved in these processes are not understood in detail. Generalized mechanisms have been proposed based on the genetic data for these processes, but roles of the gene products and the sequential steps of these pathways are not known.

The pathway believed responsible for most, if not all, induced mutations is the translesion synthesis pathway (TLS) (Friedberg *et al.*, 1995). When encountering damage inflicted bases, the normal cellular replication machinery stalls to allow error-free repair processes to ensue. If error-free repair mechanisms can process the damage, replication resumes. If the damage overwhelms the error-free processes replication is terminated. TLS allows replication recovery by enabling replication to occur through the damaged region. The information of the afflicted base(s), which may have altered base pairing due to the lesion, is copied resulting in a mutation.

Some of the genes involved in TLS have been identified. *REV3* and *REV7* code for the nonessential DNA polymerase designated Polζ, believed to be the

polymerase involved in TLS (Nelson *et al.*, 1996a; Lawrence and Hinkle 1996). Additionally the *REV1* gene product has been shown to insert cytosine allowing TLS repair synthesis to continue along a template containing an abasic lesion (Nelson *et al.*, 1996b).

In addition to the error-prone repair branch of the damage tolerance pathway, error-free branches exist. Damage avoidance mechanisms, which include the use of an undamaged homologous strand for template directed repair synthesis (Recombinational strand transfer) or use of a newly synthesized daughter strand from the undamaged complementary sequence (copy choice/strand switch) to direct repair synthesis have been proposed (Rupp and Flanders 1968; Higgins *et al.*, 1976)

Biological Effects and Repair of Psoralen Modification:

The toxic effects of psoralens arise directly from their reaction with DNA and RNA. Both crosslinks and monoadducts inhibit DNA and RNA synthesis. Crosslinks prevent strand separation during synthesis reactions and monoadducts block polymerase progression and recycling. The template activity of modified DNA is more sensitive to crosslinks than monoadducts (Ou *et al.*, 1978; Song and Tapley 1979). Psoralen modification also inhibits protein synthesis. Crosslink and monoadduct modification induce conformational alterations that inactivate tRNA and rRNA and activated psoralens cause clastogenic inactivation of

ribosome activity through the production of singlet oxygen (Ou and Song 1978). Both forms of modification have been shown to induce gene conversion and crossover recombination, and both cause mutations. At equal number of adducts, crosslinks have been shown to produce higher genotoxic effects than monoadducts (Averbeck et al., 1987).

Lethality of Psoralen Modification:

Photokilling induced by crosslinks and monoadducts has been extensively studied in prokaryotic and eukaryotic systems. In yeast, the monofunctional psoralen 3-carbethoxypsoralen (3-CPs) has been shown to bind to DNA at levels 16 times higher than 8-MOP (Averback *et al.*, 1978). Treatment of cells with these reagents produces in vivo binding ratios of one 3-CPs adduct/2 pyrimidine bases and one 8-MOP adduct/30 pyrimidine bases. While the binding of 3-CPs is higher than 8-MOP, the latter has been shown to be 6 times more lethal than 3-CPs. The lethal effect of crosslinks was shown to increase exponentially with increasing dose while the lethality of monoadducts shows a linear increase with increasing dose (Henriques and Moustacchi 1980). The LD_{10} 3-CPs/LD_{10} 8-MOP has been reported at 2.5 for these two reagents (lethal dose for 10% survival) and the LD_1 (4.5 kJm^{-2}) of 8-MOP has been reported to be less than the LD_{10} (6.0 kJm^{-2}) of 3-CPs. Similar results have been observed for various derivative of psoralen (Averbeck 1985).

Psoralen toxicity is a function of the repair pathways in both prokaryotic and eukaryotic systems. In *E. coli*, wild-type cells are able to survive modification

that produces 55-70 crosslinks in the genome (Cole 1971). Strains carrying muations in excision repair (*uvr*$^-$) or recombinational repair (*recA*$^-$) show an increased sensitivty to crosslinks, capable of recovery from the introduction of only 5-20 crosslinks per genome. A single crosslink is lethal in a double mutant carrying defective *uvr*$^-$ and *recA*$^-$.

Psoralen Repair in *E. coli*:

Repair-incubation profiles of *E. coli* DNA exposed to psoralen plus light, isolated from wildtype and *recA*$^-$ strains, were prepared by alkaline sucrose sedimentation and alkaline CsCl density gradients (Cole 1973). The profiles showed that psoralen crosslinks are partially excised in both wildtype and *recA*$^-$ strains in a *uvrA* and *uvrB* dependent step. The sedimentation patterns of the denatured excision products indicated that the repair intermediates contained single strand gaps opposite psoralen monoadducts, which were formed at the sites of crosslink modification. In wildtype cells the gaps were repaired after extended incubation but in *recA*$^-$ cells the gapped DNA was degraded into smaller pieces. It was proposed that a three-strand repair intermediate is formed during the repair of psoralen crosslinks in *E. coli* which is produced by the combined activities of the *uvr* nucleotide excision repair pathway and the *recA* recombinational pathway.

Through isolation and purification of the components of *E. coli* NER and reconstitution of an in-vitro nucleotide excision system, the proposed repair intermediate and mechanism of psoralen crosslink repair have been validated. Crosslinks are recognized by the UvrABC endonuclease complex, which catalyzes

bimodal incision on one strand flanking the crosslink. Incision preferentially occurs on the DNA strand modified with the furan ring of the psoralen molecule (Van Houten *et al.*, 1986). The 5'→3' exonuclease activity of DNA polymerase I widens a gap from the 3' incision exposing a single strand region (Sladek *et al.*, 1989). RecA mediates strand exchange between the damaged duplex and a homologous sequence that provides an intact base sequence complementary to the strand still carrying the partially excised crosslink. Following restoration of the gap sequence and resolution of the recombining sequences, the second arm of the crosslink is excised releasing the damage (Cheng *et al.*, 1988). The combined activities of DNA polymerase I, helicase II, and DNA ligase complete the process.

Psoralen Repair in Yeast:

The specific molecular mechanism of psoralen crosslink repair in *S. cerevisiae* is not known. However, many properties of psoralen repair have been determined through genetic and physical analysis of repaired products.

Strains carrying mutations in genes of the 3 major epistasis groups involved in repair of DNA damage (*RAD3*, *RAD6*, and *RAD52*) show increased sensitivity to psoralen modification (Averbeck and Moustacchi 1975, Averbeck *et al.*, 1978, Henriques and Moustacchi 1980). It is widely accepted that all three major repair pathways (nucleotide excision, DNA damage tolerance systems, and recombinational repair) function during the repair of psoralen damage.

The nucleotide excision repair system (*RAD3*) was shown to mediate psoralen monoadduct and crosslink removal (Jachymczyk *et al.*, 1981). Alkaline and neutral sucrose gradient profiles indicate that monoadducts are removed from DNA, producing single strand breaks in the DNA strands, while crosslink removal occurs with the accumulation of double strand breaks. Mutational analysis reveals that both the removal of psoralen molecules and production of broken DNA strands depends on *RAD3* function. The rejoining of broken DNA molecules, the double strand break intermediates produced from crosslink removal, depends on the recombinational pathway (*RAD51*). However, repair of single strand breaks, produced from monoadduct excision, is not affected by the *rad51* mutation.

Similar results from strains carrying mutations in the genes of the RAD3 epistasis group, (*rad1-2, rad2-5, rad3-2, rad4-4, rad10-2, mms19-1, rad14-2* and *rad16-1*) (Miller *et al.*, 1982) and the RAD52 epistasis group, (*rad50-1, rad51-1,* and *rad52-1*) provided further evidence that NER and recombination are required as complete pathways during the repair of psoralen modification. However, the incision of DNA induced from psoralen damage was not affected in a *rad6-1* mutant (Miller *et al.*, 1982).

The formation of double strand breaks as a result of psoralen crosslink removal during post-treatment incubation has more recently been confirmed by pulsed-field gel electrophoresis (Dardalhon and Averbeck 1995). Low-dose psoralen monoadduct modification did not lead to double strand break formation.

Crosslink induced double strand break formation and rejoining were shown to depend on *RAD2* and *RAD52* function but were independent of *RAD6* function.

Nucleotide excision has recently been duplicated in an in vitro system using highly purified yeast Rad proteins (Guzder *et al.*, 1995). Super-coiled, UV damaged plasmids were relaxed in the presence of the protein components and ATP and evidence of a bimodal incision mechanism was obtained. However, experiments using psoralen-damaged substrates have not been reported and the sequential order of steps during NER have not been determined.

The early steps of the excision of psoralen monoadducts and crosslinks by mammalian excision pathways have been examined using extracts for rodent and human cell lines (Bessho *et al.*, 1997). Monoadducts were excised by dual excisions bracketing the lesion similar to the bimodal excision of single strand UV induced lesions in yeast. In contrast, excision induced by a crosslink lesion was shown to initiate with a dual incision on one strand spaced 22-28 base pairs apart, with both incisions occurring 5' to the lesion. The dual incisions result in the generation of a gap (22-28 bp.) immediately 5' of the damaging crosslink. It has been suggested that this gap acts as a recombinogenic signal to initiate crosslink removal.

Mutational capacity of psoralen:

Strains carrying mutant backgrounds of error-free repair (*rad3*, *rad6*, and *rad52* epistasis groups) show increased levels of induced mutations from psoralen

modification (reviewed Haynes and Kunz 1981). Strains carrying mutations in *RAD1*, *RAD6*, *RAD18*, and *RAD52* genes are mutators, showing increased levels of spontaneous G·C → T·A transversions. The mutator phenotype is partially or entirely removed by a mutation in the *REV3* gene (Roche *et al.*, 1995).

A dose dependence for induced mutagenesis has been reported for psoralen modification. Crosslinks were shown to induce higher levels of mutations than monoadducts at the same number of lesions and the level of mutations was highly dependent on the level of crosslinks (Averbeck *et al.*, 1990).

Repair of Psoralen carried on exogenous DNA molecules:

The repair of psoralen crosslinks carried on an exogenous plasmid DNA molecule was shown to depend on both nucleotide excision repair and recombinational repair. Repair of psoralen crosslinks in both centromeric replicating plasmids (Magana-Schwencke and Averbeck 1991) and non-replicating plasmids (Saffran *et al.*, 1992; 1994) involved *RAD1* excision pathway and *RAD52* pathway. *RAD52* function was a requirement for the repair of non-replicating plasmids. The transformation efficiency of *CEN* plasmids damaged with 8-MOP plus UVA in mutants of either *RAD6* or *PSO2* was the same as in wild-type cells (Magana-Schwencke and Averbeck 1991).

In addition to the genotoxic effects of psoralen modification both psoralen crosslinks and monoadducts have been shown to induce mitotic recombination and gene conversion. Intergenic recombination leading to both crossover and non-

crossover products was observed in wild-type diploid strains treated with a variety of psoralen derivatives that produce either monoadducts, crosslinks, or different proportions of both kinds of lesions (Saeki *et al.*, 1983). The frequency of both crossover and non-crossover events exhibited dose dependence for all derivatives used. The level of recombination was decreased in a *pso2* mutant and required *RAD52* function.

We have previously compared induction of recombination due to psoralen modification, UV_{245nm} irradiation, and double strand breaks produced by restriction endonuclease digestion, carried on a non-replicating plasmid substrate (Saffran *et al.*, 1994). In a RAD^+ strain double strand damage (psoralen crosslinks and DSB) produced near identical levels of recombination products overwhelmingly favoring multiple integration of substrate plasmids. Damage affecting only one strand (Psoralen monoadducts and UV photodimers) also exhibited near identical levels of recombination products but showed increased levels of single integration events and non-crossover gene conversions compared to double strand damage. The distribution of recombination products induced from psoralen crosslinks was markedly altered in both *rad1* and *rad3* strains, showing increased levels of non-crossover gene conversions and single integration events. The distribution of recombination products induced from double strand breaks was altered in *rad1* and *rad10* strains showing a significantly larger proportion of gene conversion and single integration events. However, the wild-type distribution of products was observed in *rad3* and *rad4* strains.

We also observed a dose dependence of transformation frequency in *RAD*$^+$ cells for both psoralen crosslinks and monoadducts. At low levels of adducts per plasmid molecule (less than 30 adducts per plasmid) substrates carrying crosslink damage were more recombinogenic, producing higher levels of transformants than substrates carrying an equal number of monoadducts. At adduct per plasmid levels above 30 adducts per plasmid molecule, monoadduct modified substrates yielded higher levels of transformants than substrates carrying an equal number of crosslink adducts.

Model for psoralen repair:

The collective data obtained from the genetic and physical studies of the repair of psoralen lesions evokes separate models for the repair of psoralen interstrand crosslinks and psoralen monoadducts. The model of crosslink repair predicts that repair of a crosslink occurs by a two-step process. Following crosslink formation the nucleotide excision repair pathway recognizes changes in the continuity of the DNA molecule which induces excision of the damage, resulting in a double strand break. The double strand break, in turn, induces the recombinational pathway prompting homologous recombination at the site of the break. Repair of a psoralen monoadduct in contrast, occurs by nucleotide excision repair followed by template directed repair synthesis using the undamaged strand to direct proper base insertion. A single monoadduct should be non-recombinogenic.

There are certain aspects of psoralen crosslink and monoadduct repair, discussed above, that support this model; the repair of psoralen crosslinks occurs through intermediates that accumulate double strand breaks, and psoralen crosslink modification induces recombination. The repair of gaps produced by psoralen monoadducts occurs at wild-type levels in a mutant strains of *rad51*, which is defective in recombination. At high levels of monoadduct formation double strand breaks have been observed in recipient DNA molecules (Dardalhon and Averbeck, 1995). However, this is probably due to the overlap of gaps produced by the excision of close adducts on opposite strands. Recombination induced by high doses of monoadduct modification has been observed (Saffran *et al.*, 1994). Together, these data suggest that recombination induced by monoadduct damage is due to the formation of double strand breaks at high doses.

It is generally believed that the damage tolerance systems engage when the error-free repair systems are inundated due to excessive DNA damage. A single lesion from either form of psoralen adduct (crosslink or monoadduct) should be non-mutagenic. However, assessment of what constitutes "excessive" DNA damage with respect to psoralen modification is unknown and the induction of the damage tolerance pathways may indeed occur from a single lesion.

The model for crosslink repair predicts that the induced recombination is due to the repair intermediate of NER, a DNA molecule containing a double strand break. Repair of a substrate carrying a single psoralen crosslink should result in products exhibiting recombination frequencies and gene conversion patterns that

are similar to the recombination frequencies and gene conversion patterns induced by substrates carrying a single double strand break at the same site.

Previous studies of psoralen induced recombination and gene conversion cannot be compared, on a molecular level, to recombination and gene conversion induced by a double strand break. The techniques used to introduce psoralen damage, in both in vivo and in vitro systems, produce lesions at random sites on the damage-intended molecule. The number of lesions in both the local sequences analyzed for gene conversion and throughout the entire genome differs from cell to cell or plasmid to plasmid in the study population and, the monoadduct/crosslink ratios are produced at different levels at random positions during irradiation procedures. Since monoadducts and crosslinks exhibit different repair inducing abilities the direct comparison of psoralen induced repair of either adduct to double strand break induced repair, where the damage is uniform throughout the population of damaged substrates, has not been accomplished on the molecular level.

MATERIALS AND METHODS

All cloning techniques including restriction fragment electro-elution, plasmid constructions, *E.coli* transformations, plasmid isolation and purification, followed the protocols of Maniatis *et al* (1982) except where indicated. Restriction endonuclease digestions were carried out as per directions from the manufacturer. Medium recipes and growth conditions for *S. cerevisiae* were as indicated in Guthrie and Fink (1991).

Genomic DNA for Southern hybridization analysis was prepared by the method of Sherman *et al* (1984). Biotinylated probes were synthesized from CsCl purified pUC18- *HIS3* plasmids using BIO NICK™ labeling system purchased from Gibco BRL. Southern blots were prepared by the method of Chomczynski and Qasba (1984) using BLU GENE® non-radioactive nucleic acid detection kit purchased from Gibco BRL. Nytran nylon-cellulose filters purchased from Schleicher and Schuell, were used in all blotting experiments.

Plasmids:

The plasmids constructed and/or used in this study are shown in table 2. Frameshift mutations were introduced at specific sites within the coding sequence of the *HIS3* gene in pUC18-*HIS3*. The *Xba*I site of pUC18-*HIS3* was eliminated by *Xba*I digestion. Cohesive ends were made blunt by treatment with Klenow fragment and the plasmid was re-circularized with T4 ligase. To introduce frameshift mutations the plasmid was opened within the *HIS3* coding sequence by partial or complete digestion with *Hind*III, *Kpn*I, *Msc*I, or *Rsa*I. Digests were

TABLE 2.

Plasmid used or constructed

Plasmid	Reference:
pUC18	
YRP-HUT	Han and Saffran 1992
pUC18:URA3:*his3-75X*	This study
pUC18:URA3:*his3-207X*	This study
pUC18:URA3:*his3-304X*	This study
pUC18:URA3:*his3-622X*	This study
p*his3-75X*	This study
p*his3-622X*	This study

treated with Klenow fragment or T4 DNA polymerase to remove cohesive ends. An 8 base *Xba*I linker was ligated to the blunt ends. Full-length linear DNA was extracted from agarose gels and the plasmid was re-circularized by treatment with T4 DNA ligase.

Four different *his3X* alleles were constructed, each carrying an *Xba*I linker insertion at a different position within the *HIS3* coding region. Partial digestion with *Rsa*I or *Hind*III opens the *HIS3* gene at position 75 and 304 respectively. Complete digestion with *Msc*I or *Kpn*I opens the *HIS3* gene at positions 207 and 622 respectively. Ligation of an 8 base *Xba*I linker at these positions results in a frameshift mutation, creating the series of *his3X* alleles used for both substrate and strain construction. The linker also provides the markers used to measure damage induced gene conversion. The position of the *Xba*I linker in each allele was verified by restriction mapping.

The vector pIBI25, a pUC derived vector containing the *E.coli* origin of replication, Amp^r gene, *LacZ*, and the phage replication element *f1IG*, was chosen for its ability to replicate as double stranded plasmid in *E. coli* or as single stranded phagemid from *E. coli* infected with the helper phage M13K07. The *TRP1:ARS1* fragment was cloned into the *Eco*RI site of the plasmid to enable extrachromosomal replication of the plasmid in *S. cerevisiae,* and allow phenotypic expression of *TRP1* used to identify strains containing repaired plasmids. The *his3-75X* and *his3-622X* alleles were separately cloned into the

*BamH*I site of the vector to produce plasmids p*his3-75X* and p*his3-622X*, which were used for substrate synthesis.

To make the pUC18-*URA3-his3X* plasmids, the gel purified 1.8 kb *BamH*I restriction fragments containing the mutated *his3X* alleles were ligated into the pUC18-*URA3* plasmid

Phagemid-template purification:

Single stranded phagemid preparations of p*his3-75X* and p*his3-622X* were cultured and purified by the method of Maniatis *et al.* 10 mL cultures of 2YT broth (0.25mg/ml ampicillin) were inoculated with 10 small colonies of an *E.coli* strain carrying the respective plasmids. Cultures were grown 4 hours at 37 °C to an $O.D._{600} = 0.20$. 2 ml of each culture was used to inoculate 100 ml of 2YT broth (0.25 mg/ml ampicillin). Cultures were grown at 37 °C for 30 minutes. The $O.D._{600}$ was measured (0.034) and the cell density was calculated as the $O.D._{600}$ x $8x10^8$ cells. Using a multiplicity of infection of 20 phage/cell with a 100 ml culture, the number of plaque forming units (pfu) was determined from the cell density (# pfu = cell density x culture volume x multiplicity of infection). The stock M13K07 helper phage was titered to 2-4 x 10^{11} phage/ml. Using the pfu and the phage titer, 0.181 ml of the phage stock was added to each culture. Following the addition of the phage, cells were grown for 30 minutes at 37 °C and kanamycin was added to a final concentration of 7.0μg/ml. Cultures were grown overnight at 37 °C.

E. coli cells were pelleted by centrifugation and removed from the culture. 20% PEG6000 in 3.5M sodium acetate was added to the supernatant to a final concentration of 3.33% PEG. Phage was precipitated on ice and repetitive phenol, phenol/chloroform, and chloroform extractions were performed, using equal volumes, to purify phagemids. DNA was precipitated by the addition of 0.5 volumes of 10M sodium acetate and 2.0 volumes of 100% ethanol. Pellets were washed in 1 ml of 70% ethanol and resuspended in 100 µl of TE buffer. Samples were run on 1% agarose TAE gels against double stranded plasmid controls. The $A_{260/280}$ of each preparation was measured and the concentrations were calculated from the A_{260} absorbance. Yields ranging from 1.4 mg/ml to 3.8 mg/ml of single stranded phagemid DNA were obtained from this procedure.

***S.cerevisiae* strain construction:**

The *S. cerevisiae* strains used in this study are shown in table 3. Alleles carrying an *Xba*I frameshift mutation in the coding sequence of the *HIS3* gene were introduced into WS100 at the *HIS3* locus of chromosome XV by two-step gene replacement using pUC18-*URA3-his3X* plasmids. For WS104 construction, the plasmid pUC18-*URA3-his3-622X* was digested with *Msc*I (position 207) and was introduced into WS100 by spheroplast transformation (Beggs 1978). Ura^+ transformants were selected on uracil omission media and streaked onto 5-FOA plates to select for spontaneous loss of the *URA3* gene. Colonies resistant to 5-

TABLE 3.

Strains used or constructed

Strain	Reference:
W303 *MAT a ura3-1 leu2-1 his3-11,15 can1 ade2-1 trp1-1*	Rothstein 1983
WS100 as W303 *HIS3*	This study
WS101 as W303 *his3-75X*	This study
WS102 as W303 *his3-207X*	This study
WS103 as W303 *his3-304X*	This study
WS104 as W303 *his3-622X*	This study

FOA were transferred to YPD plates and replica-plated onto histidine omission and uracil omission media to identify possible mutants containing the frameshift allele in single copy at the *HIS3* locus. His$^-$Ura$^-$ colonies were chosen for Southern hybridization analysis. Genomic blots of *Xba*I digests were prepared and hybridized with pUC18-*HIS3* probe to identify the presence and verify the position of the frameshift mutation. All other WS strains were prepared in the same manner.

Synthesis of site specifically damaged repair substrates:

Site specifically damaged substrates were synthesized by using a single strand oligonucleotide modified in vitro with psoralen. The oligo was used to prime second strand synthesis using single strand phagemid carrying the *his3X* frameshift alleles as template.

Oligonucleotide primer sequence and modification with Psoralen:

The oligonucleotide primer used for psoralen modification was purchased from Midland Certified Reagents. The unmodified primer sequence was 14 bases long with a double stranded region of 8 bases. The 14-mer constitutes the sequence of the sense (+) strand of the *HIS3* coding region encompassing the unique *BsiW*I restriction site at position 416 of the gene. The sequence of the oligo is shown in figure 5. Psoralen modification was performed by Marie Alberti and John Hearst, UC Berkeley. HMT crosslinks at the juxtaposed thymine

5'-CAGGC*CGTACG*CAG-3'
3'-G*GCATGC*G-5'

Figure 5. Sequence of oligonucleotide used for psoralen modification. Top strand of the duplex is the sense (+) strand. MAF modified strands were purified by HPLC after photo-reaction and used as primer for second strand synthesis. The *BsiW*I restriction site is indicated by lines above and below the sequence and the thymine bases modified by photocycloaddition with psoralen are indicated in bold type.

5'-TpA residues were produced by irradiation with a laser, followed by photoreversal to obtain a mixed population of furan ended monoadducts (MAF) and pyrone ended monoadducts (MAP) on both strands of the oligo. Under denaturing conditions, HPLC chromatography was used to separate and isolate 14-mer MAF and unmodified 14-mer single strand primer to use in the synthesis of substrate plasmids. Primer prepared in this manner produced yields of 2.14μmol (unmodified), and 1.40μmol (MAF modified primer).

Synthesis of psoralen modified and unmodified Plasmid Substrates:

Plasmid substrates containing a site specifically placed psoralen crosslink, or psoralen monoadduct, as well as unmodified substrate were prepared using either furan-end modified oligonucleotide or unmodified oligonucleotide and single strand phagemid DNA.

Kinase reaction of oligonucleotide primers:

Both the 14-mer MAF primer and the unmodified primer were treated with T4 polynucleotide kinase (Boehringer Mannheim) to ensure efficient ligation after the second strand synthesis reaction. Kinase reactions were run in a total volume of 50 μl containing 100 EU of T4 polynucleotide kinase, 1X supplied buffer, 4 mM ATP (Pharmacia) and either 966 pmol of MAF primer (161 pmol for each of 6 annealing reactions) or 1826 pmol of unmodified primer (161 pmol for each of 12 annealing reactions). Following the kinase reaction the enzyme was heat inactivated and the samples were washed and concentrated to a volume of 480 μl

and 960 µl respectively by centrifugal filtration using Centricon-3 ™ filters (Amicon) and 0.1X TEN 7.4 buffer (10 mM NaCl, 1mM Tris, 0.1 mM EDTA).

Prior to large-scale synthesis of double stranded plasmid substrates, the efficiency of the synthesis reaction and the possibility of random RNA priming during the synthesis reaction was tested for each phagemid preperation. Agarose gel electrophoresis of small-scale synthesis reactions confirmed that both p*his3-75X* and p*his3-622X* phagemid preparations efficiently directed second strand synthesis and did not show random priming in the absence of the 14-mer primer. These preparations were used in large-scale second strand synthesis reactions.

Large Scale Second Strand Synthesis Reaction:

1) Annealing reaction:

161 pmol of phosphorylated MAF primer or unmodified primer was combined with 5 pmol of single strand phagemid-template and annealing buffer (20 mM Tris7.4, 2mM $MgCl_2$, 50 mM NaCl). The annealing reactions were carried out in a total volume of 500 µl. Primer/template mixtures were placed in a heating block at 73°C for 1 minute. The block was then turned off and the samples were allowed to slow cool to 34°C to effect annealing. Samples were then placed on ice for 10 minutes and then spun down in the micro-centrifuge to return condensed solvent to the reaction mixture.

Six annealing reactions were run simultaneously for each primer with p*his3-622X* phagemid. For p*his3-75X* phagemid sixteen annealing reactions were run using only the MAF primer. Eight reactions were pooled for photoreaction to produce crosslinks. The remaining eight samples were pooled and used in second strand synthesis to produce monoadduct containing plasmids.

Synthesis reactions to produce both the psoralen monoadducted plasmid substrate and the unmodified plasmid substrate used for double strand break damage (produced by enzymatic digestion) were performed immediately following the primer/template annealing reaction. For psoralen crosslinked substrates, the primer/template product of the annealing reaction was used for photo-reaction to convert the psoralen monoadduct on the primer to a crosslink.

2) Photoreaction for crosslink formation:

MAF primer-template annealing reactions were pooled and placed onto parafilm in a large petri dish in 500µl aliquots. Crosslinks were formed by irradiation with a Schleicher and Schuell 365nm RAD-FREE® long wave UV lamp with a BLE-760B Spectronics Corp. bulb positioned 5.0 cm from the surface of the plate. Irradiation was carried out for 45 minutes delivering 130 $kJ \bullet m^{-2}$. Photo-reacted samples were pooled, transferred to Centricon-30™ filtration units, washed with 0.1X TEN and concentrated to 100µl. 135mg of urea was added to denature non-crosslinked primers from the template. The sample was applied to a Sepharose 4B column and eluted through the column with 0.1X TEN. 50, two-

drop fractions (≅ 100μl), were collected off the column. 2μl of fractions 1-40 were run on 1% agarose TAE gels. Phagemid DNA (with crosslinked primer) eluted from the column in fractions 14-20. Fractions 15-18 were pooled (≅400μl) and used for second strand synthesis reactions.

3) Second strand synthesis reaction:

10X synthesis buffer (200 mM Tris pH 7.4, 20 mM $MgCl_2$, 500 mM NaCl), Glycerol, T4 ligase, and T4 polymerase was added to each annealed primer/template reaction for both the unmodified and monoadduct primers. For crosslinked samples, pooled column fractions of primer/template were split into six aliquots, 66μl each. 10X annealing buffer and water was added to restore the concentrations of reagents in the annealing reactions. 10X synthesis buffer, glycerol, T4 ligase, and T4 polymerase was added to the same concentrations as with the monoadduct and unmodified samples. Ail reactions were carried out in a final volume of 650 μl with 150 units of T4 ligase (Boehringer Mannheim), 50 units T4 polymerase, glycerol 3%, 10 mM Tris, 1.0 mM ATP, 2.0 mM DTT, 5.0 mM $MgCl_2$, and 0.5 mM each dNTP. Reactions were incubated at room temperature for 5 minutes and then transferred to 37 °C for 90 minutes. EDTA was added to a final concentration of 20 mM to quench the reaction. Second strand synthesis was confirmed by 1% agarose TAE electrophoresis against single strand phagemid DNA controls. All samples showed the conversion of single strand phagemid to double strand plasmids.

The samples were pooled and extracted with an equal volume of phenol/chloroform. For unmodified and monoadduct primer reactions, urea was added to a concentration of 1.0 g/ml to remove non-extended primers. These samples were applied to centricon-30™ units, washed with 8.0 M urea in 1X TEN (0.1 M NaCl, 10 mM Tris, 1 mM EDTA) followed by consecutive washes with 1X TEN, and were concentrated to a volume of ≅ 500 µl. Crosslinked samples were applied to Centricon-30™ units and washed with 1X TEN to remove reagents from the synthesis reaction.

All second strand synthesis products were applied to continuous CsCl gradients for centrifugation (Maniatis *et al.*) to separate closed circular plasmids from open circular plasmids due to insufficient ligation. The sample volumes were adjusted to 7.0 ml by addition of 1X TEN. CsCl and 10 mg/ml ethidium bromide were added to the solution at concentrations of 1.0 g/ml and 0.4ml/10ml respectively. Solutions were transferred to Beckman sealing tubes, balanced with additional TEN:CsCl:EtBr solution, sealed and centrifuged at 40,000 rpm at 20 °C for 72 hours. Sealing tubes were removed and 22 gauge hypodermic needles were inserted into both ends of the tubes. 90, 4-drop fractions were collected from each tube and run on 1% agarose TAE gels to identify fractions containing closed and open plasmids.

Respective fractions were pooled and extracted with H_2O saturated 1-butanol to remove ethidium bromide. CsCl was removed by centricon-30™

washes with 1X TEN. Final volumes of 400 – 500 µl were obtained. 2 µl of each preparation was run on 1% agarose TAE gel to check purity and yield of each sample.

Verification of psoralen modification:

Two tests were performed on the plasmid substrates to confirm the presence of both monoadduct and crosslink modification at the *BsiW*I site within the *his3X* allele. First, plasmids were digested with *BsiW*I. Psoralen modification at this site will prevent digestion by the restriction enzyme. The *BsiW*I restriction site occurs only at one site on the plasmid, position 416 of the *his3X* allele coding sequence. Unmodified plasmid was completely linearized by *BsiW*I digestion (figure 6a lane 5). Crosslinked plasmids were fully resistant to *BsiW*I digestion and remained as closed circular DNA (figure 6a lane 7). Monoadducted plasmids were partially resistant to *BsiW*I digestion (figure 6a lane 6). Digestion was confirmed by agarose gel electrophoresis.

The results of the *BsiW*I digestion confirm that both the crosslink and monoadduct substrates contain modification at the *BsiW*I site. However, the results do not verify, or distinguish between, the presence of either a psoralen crosslink or a psoralen monoadduct as the cause of resistance to enzymatic digestion. The physical presence of either a psoralen crosslink or monoadduct within the *his3X* allele has been verified by subjecting the plasmids to denaturing conditions.

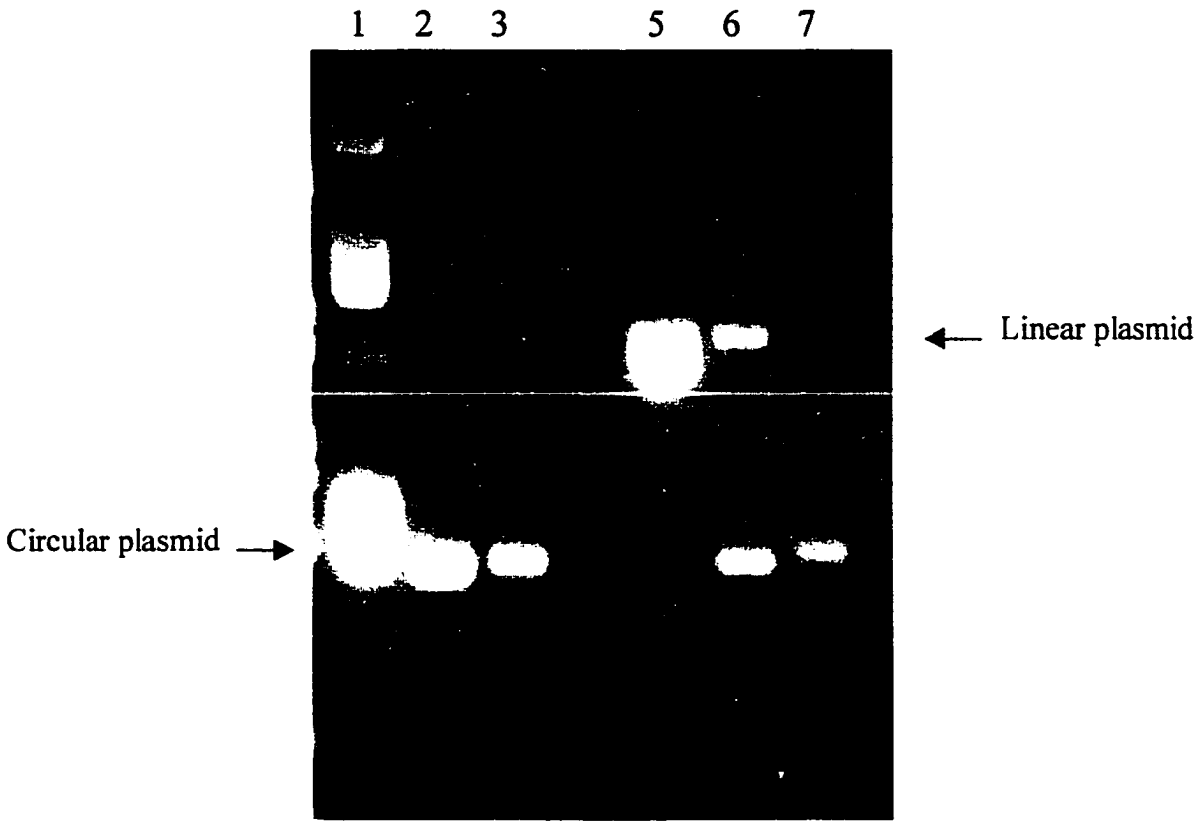

Figure 6A. BsiWI digestion of plasmid substrates: Electrophoresis gel of native and *BsiWI* digests of unmodified, monoadduct, and crosslink modified plasmids. Lanes 1,2, and 3: Native DNA preps of unmodified, monoadduct, and crosslink plasmids. Lanes 5,6, and 7: *BsiWI* digested plasmids. Unmodified plasmid (lane 5) is fully susceptible to digestion. Monoadduct plasmid (lane 6) is partially digested by *BsiWI*, and crosslink plasmid (lane 7) is fully resistant to *BsiWI* digestion.

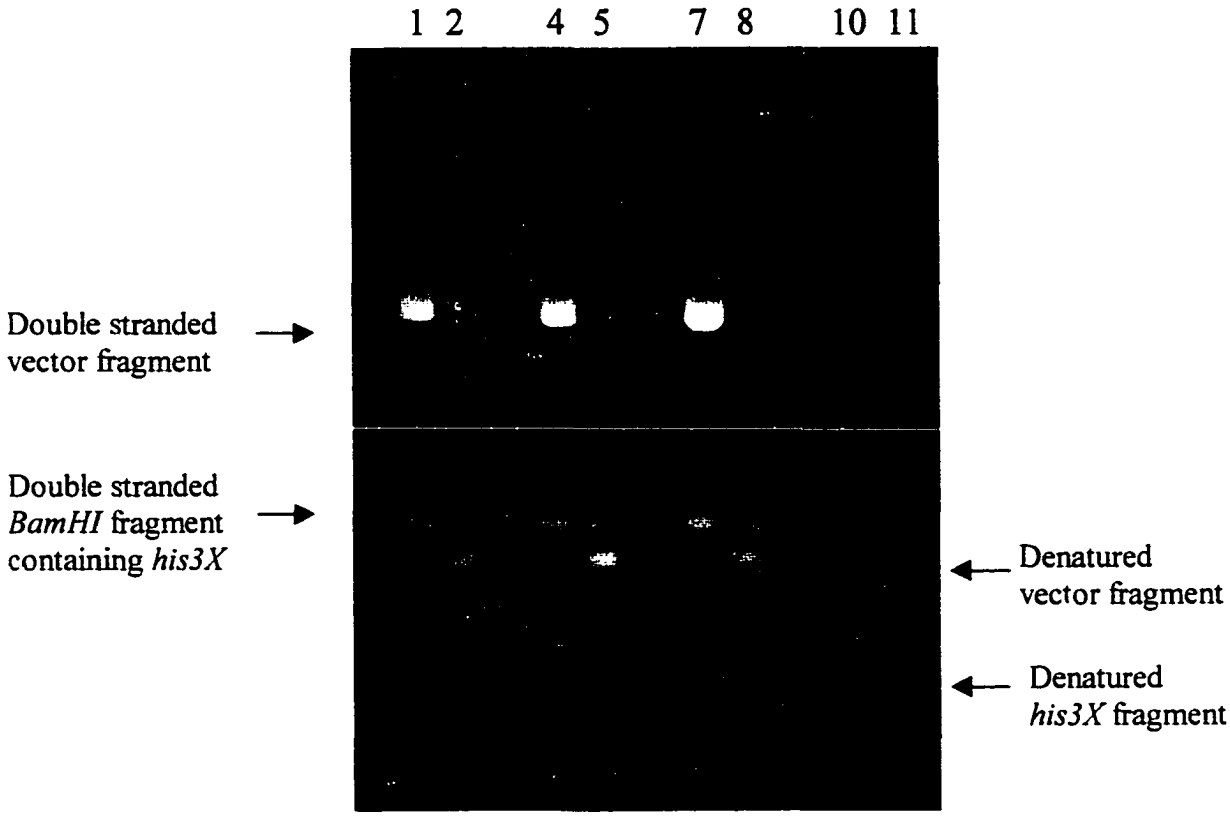

Figure 6B. Quick renaturing TAE gel of native and NaOH-denatured plasmid substrates. Native, unmodified plasmid is cut into two fragments (lane 1). The smaller fragment (1.8 kb.) contains the *his3X* allele. After treatment with NaOH, both fragments denature (lane 2). Native, monoadduct plasmid digested with *BamHI* before (lane 4) and after (lane 5) NaOH treatment. Both fragments denature after NaOH treatment. Native monoadduct plasmid digested with *BamHI* after 15 min. photo-irradiation (365 nm)(lane 7). NaOH treatment denatures the vector fragment but the *his3X* fragment runs as double strand DNA due to conversion of the monoadduct to a crosslink by the photo-irradiation (lane 8). Native (lane 10), and NaOH-denatured (lane 11) crosslink-modified plasmid. The *his3X* allele runs as double stranded DNA due to the presence of the crosslink.

1) Crosslink verification:

20 µl of closed circular crosslinked plasmids preps (about 3µg each) were digested with *BamHI* releasing the 1.8-kb. *his3X* fragment from the vector. 5 µl of unmodified plasmid was digested as a control. Digests were halved and 4µl of 1M NaOH was added to one set of the crosslinked and unmodified digests to denature the plasmids. Native and denatured samples were run on a 1% agarose gel in TAE buffer.

The 1.8-kb. *his3X* fragment from the crosslink sample ran as double strand DNA due to the presence of the crosslink, which holds the strands in proximity allowing them to successfully renature (figure 6b lane 11). The vector fragment however, did not renature and ran as single strand DNA. The unmodified plasmid was susceptible to NaOH denaturation, and both the vector fragment and *his3X* fragment ran as single strand DNA (figure 6b lane 2).

2) Monoadduct verification:

12 µg of monoadducted plasmid was digested with *BamHI* in a volume of 100 µl. 50 µl of the digest was irradiated for 15 minutes, to convert the monoadduct to a crosslink. Irradiated and non-irradiated aliquots were halved for NaOH denaturation. NaOH treated samples were applied to a 1% agarose TAE quick renaturation gel.

Both the vector fragment and *his3X* fragment of the non-irradiated sample were susceptible to full denaturation and ran as single strand DNA (figure 6b lane

5). The *his3X* fragment of the irradiated sample ran as double strand DNA, which resulted from the conversion of the monoadduct to a crosslink during the photo-irradiation (figure 6b lane 8). These results verify the presence of a crosslinkable monoadduct within the *his3X* allele.

Transformation of plasmids into *S. cerevisiae* strains; repair growth and genetic analysis:

Unmodified plasmids were digested with *BsiW*I to produce the double strand break damaged substrates. Plasmids carrying a crosslink, a monoadduct, or a double strand break, or undamaged plasmid was separately transformed into the WS 101-WS 104 strains for repair.

YPD cultures of the WS *his3X* strains were grown to an A_{600} between 0.5 and 1.0. From each culture 0.1, 0.2, and 0.4 ml aliquots were used to separately inoculate 100 ml YPD cultures. Cells were grown overnight to mid-log phase (A_{600} between 0.25 and 0.60 for 10X diluted culture). Cells were spun down in 50 ml centrifuge tubes at 2000 rpm for 5.0 minutes. Pellets were washed in water, centrifuged, and resuspended in 10 ml of 1.0 M sorbitol, 20 mM EDTA pH 8.0. 10 µl of 2-mercaptoethanol was added and cells were incubated at 30°C for 10 minutes. Cells were then centrifuged, washed 2X with 1.0 M sorbitol and resuspended in 10.0 ml of sorbitol-citrate-EDTA. 100 µl of Glusulase (DuPont) was added and cell were incubated at 30°C in a shaker bath until spheroplasting was verified by a turbidity test of 50 µl cells mixed with 100 µl of 5% SDS/0.5 M

sorbitol solution. Spheroplasts were pelleted by centrifugation at 1500 rpm for 5.0 minutes, washed 3 consecutive times with 10.0 ml of 1.0 M sorbitol, and finally resuspended in 2.0 ml of 1.0 M sorbitol. The volume of the cells was measured and 0.1M Tris- 0.1 M $CaCl_2$ was added (1/10 of the cell volume). Cells were stored on ice while 5.0 µl of plasmid DNA was transferred to 14.0 ml culture tubes. 200 µl of the cell solution was added to each DNA tube. Cells were mixed and stored at room temperature for 15.0 minutes. 2.0 ml of 20% PEG- 10mM $CaCl_2$ –10 mM Tris was added and cells were incubated for 20.0 minutes at room temperature. Cells were pelleted and resuspended in 400 µl of SOS medium. 200 µl of each transformation was added to 8.0 ml of melted SD-Trp top agar and plated on SD+sorbitol-Trp plates.

Plates were incubated at 30 °C for four days and were scored for the number of Trp^+ colonies. Colonies were chosen at random and transferred to SD-Trp plates. To screen for gene conversion of the his3X alleles, colonies were replica-plated on to SD-His plates. Colonies were also replica-plated to YPD for 3 rounds of non-selective growth followed by return to selective media (both SD-Trp and SD-His) to determine the stability of the Trp and His phenotypes.

Between 66 and 224 colonies of each combination were analyzed by genetic techniques. Trp and His phenotype and stability were determined for each colony and the data were compiled to construct the genetic analysis. In addition, determination of phenotype and stability associated with each colony served as an

indicator for the method required to isolate the products in order to study each repair product by physical analysis techniques.

Physical analysis:

Determination of the stability of the Trp phenotype allowed repair events to be classified as crossover or non-crossover. If repair resulted in a non-crossover product the plasmid remains extra-chromosomal. The resulting Trp^+ phenotype will be unstable, as the *TRP1* gene is plasmid borne. Extra-chromosomal repair products identified by Trp^+ instability were isolated by plasmid rescue techniques to physically analyze the gene conversion events that may have occurred during recombination.

Repair events resulting in crossover recombination integrate the plasmid into the yeast genome. Incorporation of the *TRP1* gene at the site of integration (the *HIS3* locus) produces a stable Trp^+ phenotype. Stable Trp^+ colonies were identified by the genetic analysis, and were analyzed by Southern hybridization of genomic DNA to physically categorize the gene conversion events associated with crossover recombination.

Plasmid rescue:

Extra-chromosomal repair products carry the *E. coli* origin of replication (*ori*). Only the extra-chromosomal plasmid will replicate when total yeast DNA purified from strain carrying plasmids is transformed into *E. coli*.

Overnight cultures of yeast strains were pelleted and resuspended in 100 µl of lysis buffer (2.5 M LiCl, 50 mM Tris pH 8.0, 20 mM EDTA pH 8.0, 4% Triton-X 100). 100-µl of phenol/chloroform and 60 µl glass beads (Crown Corning Braun 0.45-0.50 mm) was added and cells were vortexed at maximum speed by hand for 3 minutes. Cells were then placed in a vortexing rack and vortexed for an additional 10.0 minutes at maximum speed. Tubes were incubated at 65°C for 5.0 minutes, spun in the micro-centrifuge, and the aqueous phase was extracted. The phenol/chloroform extraction was repeated and the aqueous phases were pooled. 0.50 ml of Wizard™ DNA binding resin (Promega) was added to each tube. After mixing, solutions were transferred to 3-ml syringes fitted with Wizard™ mini-columns, placed on a vacuum rack. The resin was drawn into the columns and packed by vacuum. A total of 3.0 ml of column wash buffer (55% ethanol, 200 mM NaCl, 20 mM Trip pH 7.5, 5 mM EDTA) was drawn through the columns in 1.0 ml aliquots. Columns were dried on the vacuum for an additional 3 minutes and spun in the micro-centrifuge to remove residual wash. Total yeast DNA was eluted by addition of 50 µl of TE (65°C) to each column followed by cenrifugation after 1.0 minutes. 2µl of DNA was transformed into ultra-competent *E.coli* DH5α by heat-shock (Maniatis et al). Transformed cells were plated on LB+Amp plates.

Two colonies from each transformation were streaked onto fresh plates and used to prepare E.coli plasmid mini-preps by alkaline lysis (Maniatis et. al.). Plasmids were digested with *XbaI* restriction endonuclease and run on agarose

electrophoresis gels to determine the presence and position(s) of the *Xba*I marker(s) within the *HIS3* gene. Plasmids were also digested with *BsiW*I restriction endonuclease to determine the integrity of the *BsiW*I site (the site of the original damage) within the *HIS3* gene.

Southern analysis:

Genomic DNA from Trp^+ stable colonies was prepared from overnight 10 ml YPD cultures. Cells were pelleted and resuspended in 1 M sorbitol, 0.1 M EDTA pH 7.5. 20 µl of zymolyase (2.5 mg/ml) was added to strip the cell wall. Cells were incubated at 37°C for 1 hour, pelleted, and resuspended in 0.5 ml 50 mM Tris pH7.4, 20 mM EDTA. 50µl of 10% SDS was added to strip cell membranes. Cells were incubated at 65°C for 30 minutes. To precipitate cell membranes and proteins, 200 µl of 5.0 M potassium acetate was added. Tubes were placed on ice for 60 minutes, spun in micro-centrifuge, and the supernatant containing the DNA was transferred to fresh tubes. DNA was precipitated with an equal volume of isopropanol, resuspended in 0.3 ml TE, and re-precipitated with 200 µl of isopropanol after the addition of 30 µl of 3 M sodium acetate.

DNA preps were split in half and digested with either *Xba*I or *EcoR*I to determine the *Xba*I linker positions at the *HIS3* locus (*Xba*I digests) and to distinguish multiple and single integration events (*EcoR*I digests). Digests were run on 1% agarose electrophoresis gels, and the DNA was transferred to Nytran™ nylon filters by alkaline blotting solution (0.4 N NaOH, 0.6 N NaCl). Filters were

hybridized with heat denatured biotinylated pUC 18-*HIS3* probe in hybridization buffer (2 % dextran sulfate, 1% SDS, 1M NaCl). Salmon sperm DNA was added to block non-specific binding to the filter. Hybridization was carried out at 65°C for 24 hours.

Filters were washed twice in 250 ml of 2X SSC, followed by two washes with 250 ml of 2X SSC,1% SDS and two washes with 250 ml of 0.1X SSC. Blots were then washed in buffer 1 (0.1 M Tris-HCl pH7.5, 0.15 M NaCl) followed by incubation in buffer 1, 3% BSA for 1 hour at 65°C. Blots were drained and strepdavidin-alkaline phosphatase complex (in 10 ml of buffer 1) was passed over the surface of the filters for 10 minutes. Filters were washed twice in 500 ml of buffer 1, followed by a wash in 0.1 M Tris-HCl pH 9.5, 0.1 M NaCl, 50 mM $MgCl_2$. Color development solutions (NBT and BCIP) from the BLU GENE® (Gibco BRL) non-radioactive nucleic acid detection kit was added to visualize hybridized fragments.

RESULTS

Experimental Strategy:

Repair, recombination, and gene conversion induced by a single, site-specifically placed psoralen crosslink, psoralen monoadduct, or double strand break were compared by analyzing the repair products obtained from in vivo repair of plasmid substrates carrying each form of damage. The plasmid substrates used for repair studies were synthesized containing either a psoralen crosslink or psoralen monoadduct at position 416 (the *BsiW*I site) in a frameshift allele of the *HIS3* gene sub-cloned into the plasmid. To create the double strand break substrate unmodified plasmid was subjected to restriction endonuclease digestion with *BsiW*I.

The *his3* frameshift alleles were created by insertion of an 8 base *Xba*I linker into the *HIS3* gene at either position 75 or 622 within the coding region of the gene. The plasmids carried an autonomous replication sequence to enable episomal replication, but lacked a *CEN* sequence, to allow survival of cells that incorporate the plasmid into the genome by crossover recombination. The *TRP1* gene was included on the plasmid to enable tryptophan prototroph selection, used to identify repaired substrates. *Amp*^{r} and *ori* were included for selection and replication in *E. coli* and a f1IG element was included for single strand phagemid replication. A general diagram of the plasmid substrate is shown in fig 7.

The phenotype of yeast cells carrying the mutated *his3* gene is sensitive to

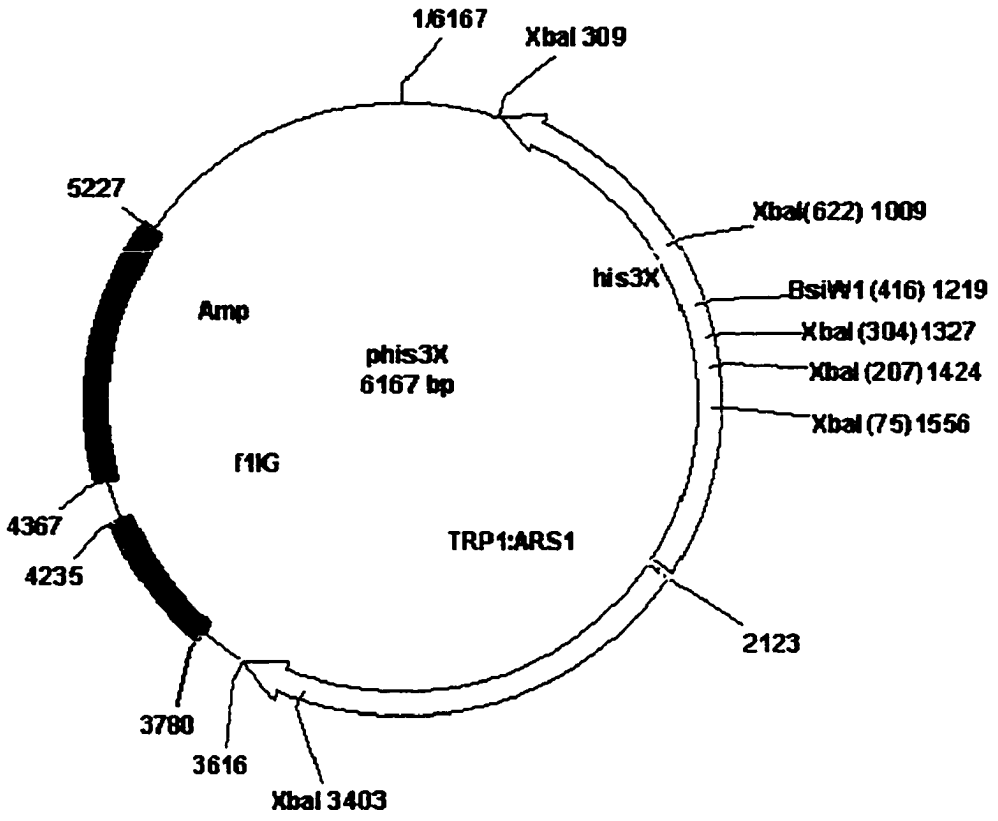

Figure 7. **Map of plasmid substrate constructed for repair studies.** The location of the *Xba*I and *BsiW*I sites within the *HIS3* gene are shown as base pair numbering of the *HIS3* coding sequence (in parentheses) in addition to the location defined by plasmid numbering.

the position of the frameshift. Frameshifts at positions 75, 207, and 304 all produce a null mutation when the allele is plasmid borne. The frameshift at position 622 resides in the C-terminus of the protein and produces a slow growth phenotype in histidine omission medium when the allele is plasmid borne, and therefore present in high copy number. We have called this slow growth phenotype $His^{+/-}$. The $His^{+/-}$ phenotype has facilitated the genetic analysis of the *his3-622X* substrate as it allows phenotypic identification of gene conversions at the *his3* allele that produces both His^{+} and His^{-} colonies.

A series of repair proficient yeast strains carrying homologous frameshift alleles of the *HIS3* gene was constructed by two-step gene replacement of the wildtype *HIS3* gene with an allele carrying an *Xba*I 8-base linker insertion. The frameshift within the chromosomal *his3* allele was located at either position 75, 207, 304, or 622 in the coding sequence of the gene. All chromosomal frameshift alleles, including the *his3-622X* allele, were phenotypically His^{-}.

Strains were grown to mid-log phase and plasmid substrates carrying the different forms of damage were transformed into each strain for in vivo repair. Colonies carrying repaired plasmids were selected by growth on tryptophan omission medium. After plates were scored, random colonies were transferred to fresh Trp omission plates and screened for His prototrophy to determine gene conversion events. Colonies were subjected to serial replica plating on complete medium, and then returned to growth on both tryptophan and histidine omission media, to determine the stability of each phenotype. After Trp and His phenotypes

were assigned to each colony the repair products were isolated and physically analyzed to determine the gene conversion pattern. Non-crossover products were isolated by plasmid rescue and analyzed by restriction mapping. Crossover products were analyzed by Southern hybridization. Gene conversion profiles were constructed by combining the results of the genetic and physical analysis.

The substrates and strains in the combinations used in this study create 3 marker orientations with respect to the damage site (fig 8). We call these arrangements Types I, II, and III. In the Type I arrangement the *Xba*I markers flank the damage site, with the chromosomal marker upstream and the plasmid marker downstream, relative to the damage site. In the Type II arrangement, the plasmid marker is upstream and the chromosomal marker is downstream of the damage site. This marker orientation is the reverse of the Type I arrangement. We have distinguished Type I and Type II arrangements from each other as we have found differences in the gene conversion patterns associated with these arrangements (discussed below). Finally, in the Type III arrangement, both plasmid and chromosomal markers are on the same side, upstream of the damage site, with the chromosomal marker between the damage site and the plasmid marker. These combinations have enabled us to measure the repair efficiency of each form of damage as well as various aspects of recombination and gene conversion induced by each form of damage. Through genetic and physical analysis of the repair products we have been able to quantitatively measure levels of crossover recombination, polarity of gene conversion, conversion tract length

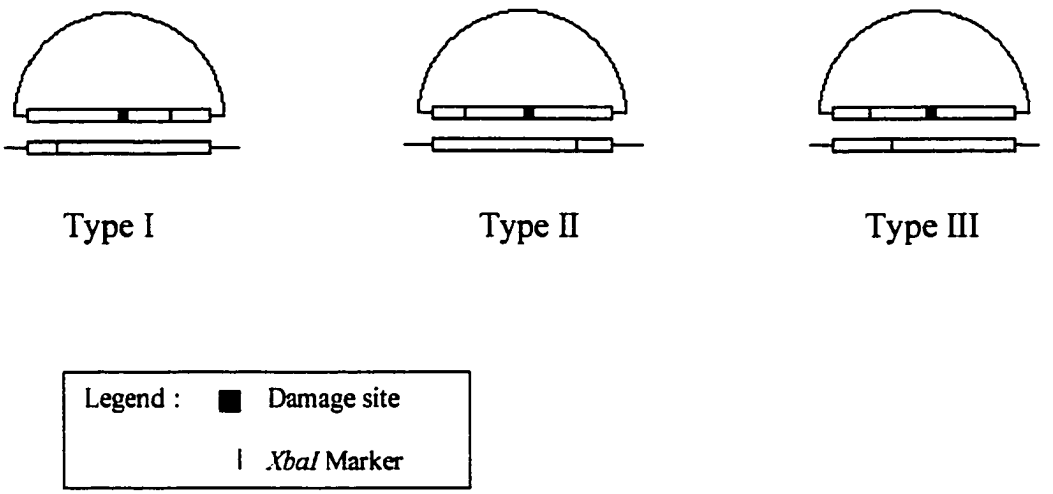

Figure 8. **Classes of marker arrangements used in repair experiments.** *Type I:* markers flank the damage site with the plasmid marker downstream of the damage site. *Type II*: markers flank the damage site with the plasmid marker upstream of the damage site. *Type III*: both plasmid and chromosomal markers upstream of the damage site with the chromosomal marker proximal to the damage site.

and direction, and levels of mutagenesis induced from each form of damage on the molecular level. Comparison of the trends and physical characteristics of the repair products has enabled us to test the general model for psoralen crosslink repair. Differences observed in the trends of recombination and gene conversion provide evidence of either physical difference between the repair intermediates formed during psoralen crosslink and double strand break repair or mechanistic differences in the processing of the repair intermediates during recombination.

Genetic analysis:

By measuring the levels of Trp and His phenotype, and the trends and patterns therein, we have been able to compare repair, recombination and gene conversion induced from a single psoralen crosslink, monoadduct, or double strand break by genetic techniques. Some of the properties and trends that we have measured indicate similarities between crosslink and double strand break repair while showing distinctions for monoadduct repair. These results support the models for psoralen crosslink and monoadduct repair. However, we have detected certain properties of crosslink and double strand break induced repair that are different, which suggest distinctions between repair and recombination induced from a single crosslink and a double strand break. These differences merit reconsideration of the model for psoralen crosslink repair.

Toxicity of a single damaging lesion:

The toxicity of a single damaging lesion for each form of damage (monoadduct, crosslink, and double strand break) has been determined by measuring the levels of tryptophan prototrophy arising from repair of the damaged substrates. The damage carried within the plasmid borne *his3* allele inhibits plasmid replication. In order for a cell to replicate the plasmid and express the *TRP1* gene, repair of the damage must occur. The level of tryptophan prototrophy generated from each form of damage compared to the level of tryptophan prototrophy arising from cells transformed with unmodified plasmid represents the efficiency at which each form of damage is repaired and reflects the level of toxicity that a single damaging lesion imposes.

Strains were transformed with equimolar amounts of substrate carrying each form of damage for in vivo repair. Transformants were plated on tryptophan omission plates and the Trp^+ colonies were counted and compared to the number of Trp^+ colonies obtained from strains transformed with unmodified plasmid. The repair efficiency was calculated as the percent of Trp^+ prototrophs generated from each damaged substrate against the number of prototrophs generated from transformation with equimolar amounts of unmodified plasmid. The repair efficiencies for the *his3-75X* substrates are shown in figure 9.

A single double strand break and a single monoadduct induce different levels of repair. Strains transformed with double strand break damaged plasmids

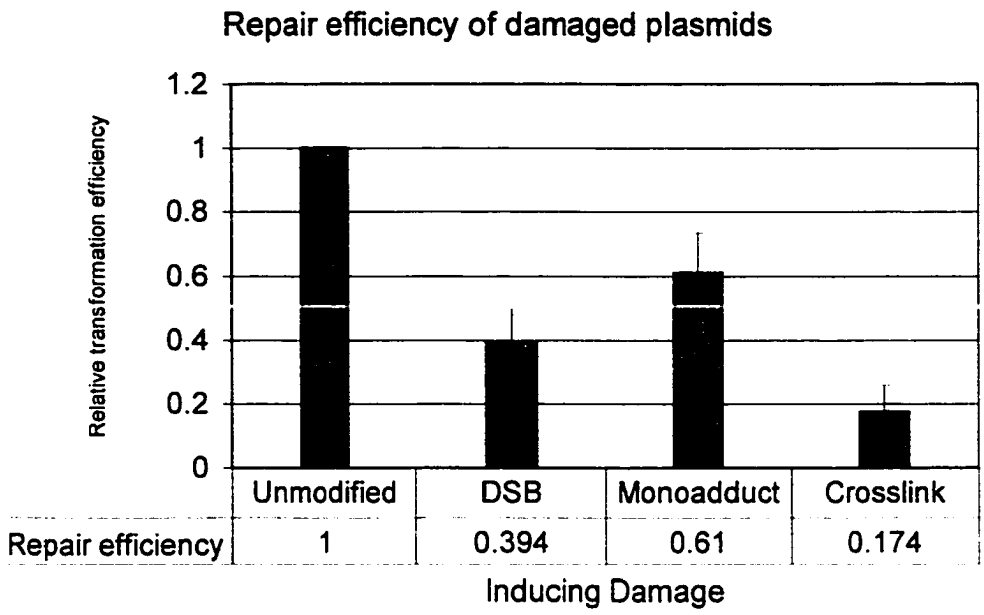

Figure 9. **Repair of damaged plasmid DNA in yeast cells.** The number of Trp^+ transformants was normalized to the number of Trp^+ colonies resulting from transformation by undamaged plasmid. The reported values are the means and standard deviations of duplicate transformations from 6 determinations for each form of damage. Each transformation yielded from 100 to1500 colonies. The repair efficiency of psoralen crosslinks is significantly lower than double strand breaks ($P < 0.01$, $t = 4.02$) and psoralen monoadducts ($P < 0.001$, $t = 7.10$)

and psoralen monoadduct damaged plasmids resulted in levels of 39.4% and 61.0% respectively ($P < 0.01$, $t = 3.24$) of the number of Tpr^+ colonies arising from transformation with unmodified plasmid. The different levels of repair between a single monoadduct and a double strand break indicate that the toxicity of these forms of damage is different. The level of Trp^+ colonies arising from cells transformed with plasmids carrying a single psoralen crosslink was only 17.4% of the level of Trp^+ colonies from cells transformed with undamaged plasmid. This is 2 to 3 times lower than the repair efficiency of either a double strand break or a psoralen monoadduct. The single crosslink lesion exhibits a lower efficiency of repair and is therefore more toxic that either a psoralen monoadduct or a double strand break.

Crossover recombination levels for crosslink and double strand break damage are similar but monoadduct damage is non-recombinogenic:

Repair mediated by the recombinational pathway can result in either crossover or non-crossover products. Our system has been designed to distinguish crossover and non-crossover products by genetic analysis of tryptophan prototrophy. Repaired plasmids express the *TRP1* gene whether repair results in a crossover or non-crossover product. If tryptophan prototrophy results from a non-crossover repair event the phenotype is expressed from a plasmid borne *TRP1* gene and will be unstable. When grown on non-selective medium unequal segregation of the plasmid occurs during replication due to the lack of a plasmid borne *CEN* sequence. This results in progeny that lose the plasmid. After

successive rounds of growth on non-selective medium, cells lacking the plasmid will over-take the colony. Upon return to the selective growth condition tryptophan prototrophy will be lost. The loss of tryptophan prototrophy after non-selective growth conditions has been used to identify cells that have repaired the damaged plasmid through non-crossover repair events

If tryptophan prototrophy results from a crossover repair event the *TRP1* gene will be integrated into the chromosome. After successive rounds of growth on non-selective medium the *TRP1* gene will be present in all cells due to its inclusion into the genome. Tryptophan prototrophy will be stable. Retention of tryptophan prototrophy after non-selective growth conditions has been used to identify cells that have repaired the damaged plasmid through crossover repair events.

Trp^+ transformants were transferred to fresh tryptophan omission medium and serially replica-plated onto non-selective medium (YPD). Colonies were then returned to tryptophan omission medium and plates were scored after incubation for 16 hours to determine the stability of the Trp^+ phenotype. Colonies expressing *TRP1* were considered to contain crossover repair products. The percent of Trp^+ stable transformants, representing crossover recombination levels, is shown in figure 10. Both crosslink damage and double strand break damage result in similar levels of crossover recombination. A single monoadduct at the same position does not effectively induce crossover recombination.

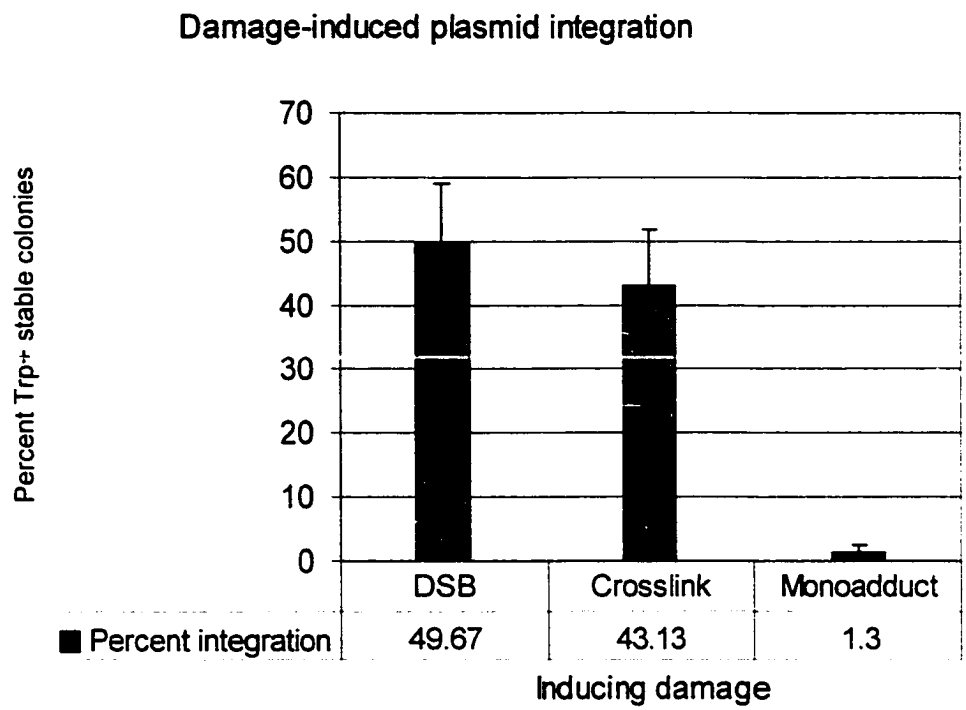

Figure 10. **Damage-induced plasmid integration.** The number of stable Trp^+ colonies was determined by serial replicaplating and percent Trp^+ stable was calculated out of the total Trp^+ colonies. The reported values are the means and standard deviations of 6 independent samples for both double strand break and crosslink damaged plasmids and 3 independent samples for monoadduct damaged plasmids. Each sample ranged from 96 to 200 colonies. The levels of induced plasmid integration between crosslink and double strand break damage was similar ($P > 0.05$, $t = 1.25$). The level of induced plasmid integration by monoadduct damage was significantly lower than that of crosslinks (and double strand breaks) ($P < 0.001$, $t = 8.0$)

In previous studies, plasmid substrates capable of autonomous replication that carried either a double strand break or a double strand gap have been shown to stimulate similar levels of crossover and non-crossover recombination repair products (Orr- Weaver and Szoztak 1983). For psoralen damage, the ratio of crossover versus non-crossover recombination induced by both psoralen monoadducts and psoralen crosslinks has been shown to exhibit a dose-dependency (Saeki et.al. 1983). At lower doses of 8-MOP, AMT, or psoralen, crossover events occur at a higher frequency than non-crossover events. As the dose increased the proportion was observed to shift to favor non-crossover events. Crossover events initiated by the mono-functional 3-carbethoxypsoralen derivative exhibited a similar dose dependency.

The similarity of the levels of the crossover and non-crossover recombination induced by a single double strand break and a single psoralen crosslink suggest that the recombinational repair machinery acts on the repair intermediates of these forms of damage in a similar fashion. In turn, these results suggest a physical similarity exists between the recombination intermediates of a double strand break and a crosslink damaged substrate, as predicted by the model of psoralen crosslink repair

While monoadduct lesions, in high quantity, produce intermediates that effectively enter the recombinational repair pathway, on the molecular level the repair intermediate produced by a single psoralen monoadduct is a poor substrate of recombination, and is shown here to enter this pathway infrequently. These

results indicate that a physical distinction between the repair intermediate of monoadduct damage exists, compared to the repair intermediates of both crosslink and double strand break damage when the intermediate is produced from a single lesion. The model of psoralen monoadduct repair predicts these results.

Gene Conversion of the *his3* allele(s):

The induction of the homologous recombinational repair pathway by crosslink and double strand break damage may result in gene conversion of the marker(s) within the *his3* alleles carried by the plasmid and/or in the genome. Some of these changes in sequence result in phenotypic changes, which we have characterized by genetic analysis of the colonies carrying repaired plasmids. We have compared the trends and properties of gene conversion induced by double strand breaks and psoralen crosslinks and have found evidence that supports the model of crosslink repair, but have also found evidence that necessitates reconsideration of the model.

his3-622X substrate.

The *his3-622X* substrate is shown in figure 11a, along with a homologous chromosomal sequence showing the possible positions of the frameshift mutation carried by this allele. The plasmid marker at position 622 is downstream of the damage site. When the chromosomal *his3* allele carries the *Xba*I marker at one of the positions indicated in the diagram the combination of this allele with the *his3-622X* substrate creates the series of Type I marker arrangements. This arrangement occurs for the *his3-622X* substrate in combination with the *his3-75X*, *his3-207X*,

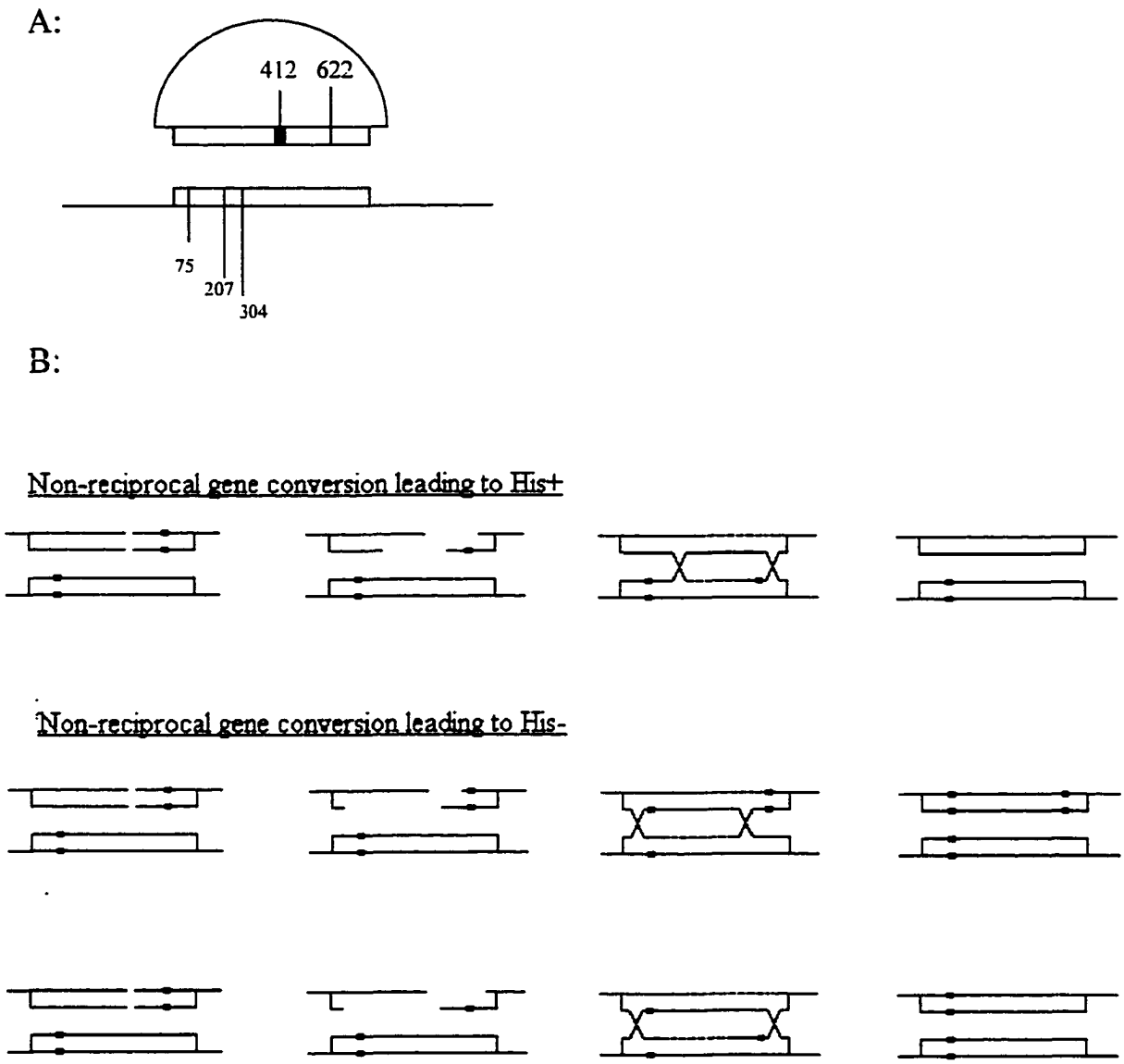

Figure 11. **The *his3-622X* substrate and possible non-crossover gene conversion events for the Type I arrangements of the *his3-622X* substrate.**
A: *his3*(622X) substrate and homologous chromosome. *Xba*I linker at the positions indicated create the Type I combinations.
B: Possible chromosome-to-plasmid gene conversion events and phenotype outcome for non-crossover recombination of the Type I combinations. In each combination shown the allele on the top represents the plasmid borne *his3* allele. Conversion to His^+ (top) occurs from a gene conversion tract extending downstream from the damage site (shown as a break). Conversion to His^- occurs from either a unidirectional gene conversion tract extending upstream from the damage site, or by a bi-directional conversion tract extending in both directions.

and *his3-304X* strains.

The phenotype of strains carrying the *his3-622X* substrate, prior to gene conversion, is $His^{+/-}$. This atypical phenotype is ideal for genetic analysis studies, since a change of the $His^{+/-}$ phenotype indicates a gene conversion event. Both His^{+} and His^{-} arise from gene conversion, which depends on conversion tract length and direction (fig 11b). We have quantitatively measured the changes in the $His^{+/-}$ phenotype, to compare by genetic techniques, the overall levels of gene conversion induced by psoralen crosslink damage and double strand break damage in the Type I series.

Gene conversion levels of *his3*, in the non-crossover products, are higher from double strand break induced repair than from crosslink induced repair:

The overall levels of phenotypic change associated with non-crossover events during repair of the *his3-622X* substrate are shown in figure 12. Double strand break induced repair resulted in a higher level of colonies exhibiting a change of the $His^{+/-}$ phenotype compared to crosslink induced repair. A single psoralen monoadduct lesion did not induce a change of the $His^{+/-}$ phenotype in any of the strains.

Differences in gene conversion levels indicate that either one substrate enters the recombinational repair pathway more efficiently over the other, since gene conversion is a consequence of recombination, or that one substrate imposes a limitation of hDNA formation which creates a bias against gene conversion. We

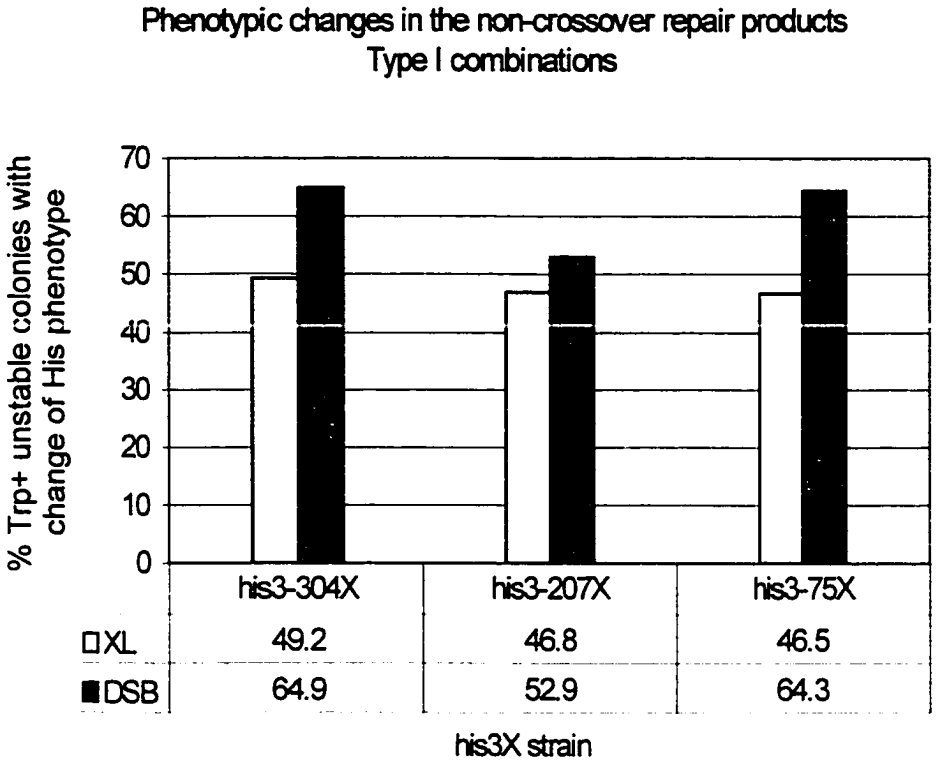

Figure 12. **Phenotypic change for non-crossover repair products of Type I combinations.** The number of colonies carrying repaired plasmids (non-crossover products) with a changed His phenotype was determined by replicaplating. Phenotypic changes resulting in both His^+ and His^- colonies were totaled for each form of damage in each combination. The percentage was calculated out of the total non-crossover products (Trp^+ unstable). Sample sizes ranged from 85 to 98 colonies for double strand break (DSB) damage, and 32 to 71 colonies for crosslink (XL) damage. The reported value is for 1 determination for each form of damage in each strain.

have shown that psoralen crosslinks induce the mutagenic repair pathway (discussed below). Substrates entering this pathway lower the possible frequency of gene conversion by removing available substrate for the recombination pathway. The detection and measurement of substrates entering the mutagenic pathway will be discussed in detail in the physical analysis section.

A distance-dependent gradient of gene conversion levels is an indication that the formation of hDNA is limiting (Sweetser et al., 1994). To determine if the difference in gene conversion levels that we have observed between crosslink and DBS induced recombination is the result of hDNA limitation imposed by crosslink damage, we have compared the levels of gene conversion within the Type I series.

The marker arrangement for the different combinations of the Type I series are in the same orientation. However, the different combinations of the series differ from each other with respect to the distance of the chromosomal marker to the damage site on the plasmid. In the series, the chromosomal markers are positioned at approximately 100 base intervals upstream from the damage site. We have compared the levels of gene conversion between the different combinations of the series to determine if gene conversion tracts exhibit a distance limitation. If conversion tract length is limiting over the 300 base stretch encompassing the chromosomal markers, a decline in the level of gene conversion at the marker(s) further from the damage site is expected. We have also compared tract lengths induced from psoralen crosslinks to double strand breaks to determine if the specific form of damage affects conversion tract structure.

Conversion tract length (and hDNA formation) is not limiting over an identical homology stretch of 300 bp:

By comparing the levels of gene conversion within the Type I series, gene conversion at approximately 100 bp. intervals from the damage site can be compared. Evidence of a distance-dependent gradient of gene conversion levels was not detected over the 300 bp. span of identical sequence homology for either psoralen crosslink or a double strand break induced recombination (figure 13). Conversion levels generating His^- decrease only marginally as the distance of the marker from the damage site increases. Conversion of the *his3-622X* substrate in the *his3-304X* strain requires a minimum tract length of 112 bp upstream to produce His^- colonies. In the combinations involving the other *his3X* strains, the tract length required to produce His^- is longer (209 bp in *his3-207X* and 341 bp in *his3-75X*). The marginal change in the levels of conversion to His^- suggests that for distances in the range of 100 to 300 base pairs, gene conversion tracts (and hDNA formation) do not exhibit a length-limitation when progressing through a stretch of identical sequence homology.

A conversion tract of at least 206 base pairs, extending downstream of the damage site, in all of the Type I combinations will produce the His^+ phenotype. However, if bi-directional conversion results in co-conversion of the upstream marker, the chromosomal marker will transfer to the plasmid producing a His^- phenotype. If hDNA formation exhibit a distance limitation, conversion to His^+ should be substantially highest in the *his3-75X* strain as this marker is furthest

from the damage site and will be excluded from co-conversion. Figure 13 shows the level of conversion to His^+ for the Type I combinations. As with conversion to His^-, there is only a marginal difference in the levels of conversion to His^+ between the combinations of the series, indicating little or no hDNA formation limitation in the 100 to 300 base pair range.

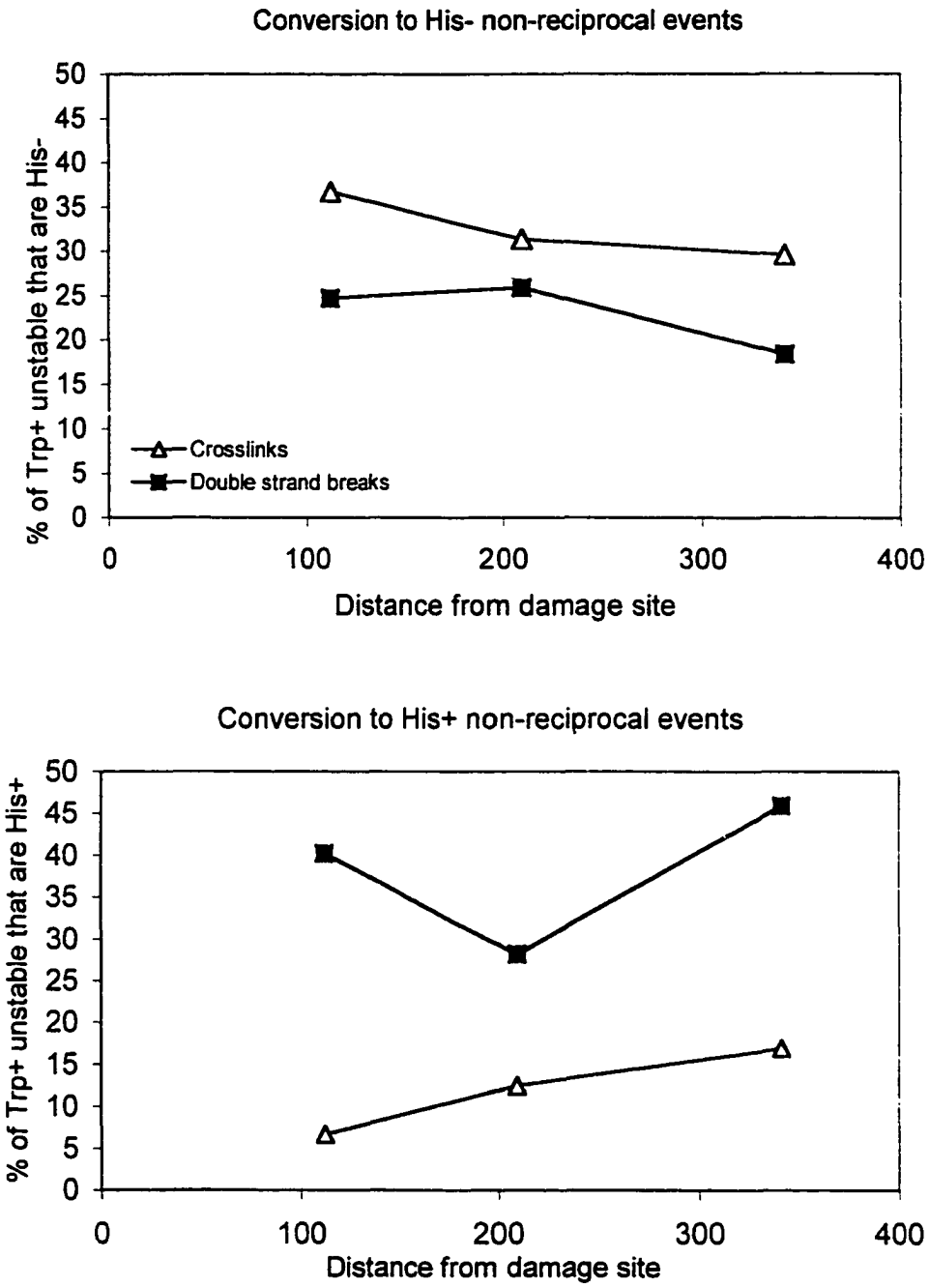

Figure 13. **Gene conversion of *his3X* as a function of distance from the damage site.** Colonies reported in figure 12 were separated into His^+ and His^-. Marker conversion levels leading to His^- (top) and marker conversion levels to His^+ (bottom) are shown versus the distance of the chromosomal marker from the plasmid borne damage site. The sequences between the damage site and the marker share identical homology.

In the Type I combinations, psoralen crosslinks preferentially induce gene conversion yielding His^- products while double strand breaks preferentially induce His^+ products:

When the products of damage-induced repair and recombination are compared for gene conversion outcome, a trend in the pattern of His phenotype generation is observed. For Type I combinations, crosslink damaged substrates result in the preferential generation of His^- products while double strand break damage preferentially induce His^+ colonies. The level of gene conversion generating His^- is significantly higher during repair of crosslink damaged substrates than the level of gene conversion generating His^- during repair of double strand break damaged substrates. This trend was observed in both the crossover and non-crossover products for all of the Type I combinations (fig 14).

The level of gene conversion generating His^+ colonies during the repair of double strand break damaged substrates is significantly higher than the level of gene conversion generating His^+ colonies during repair of crosslink damaged substrates (fig15). This trend was also observed in both the crossover and non-crossover products for all of the Type I combinations.

The difference in phenotype generation induced by crosslinks and double strand breaks, and the specificity of tract direction dictated by the marker arrangement in Type I combinations to produce His^+ and His^- imply that conversion tracts exhibit a directional polarity that is a function of the inducing form of damage. The results suggest that conversion tracts preferentially extend

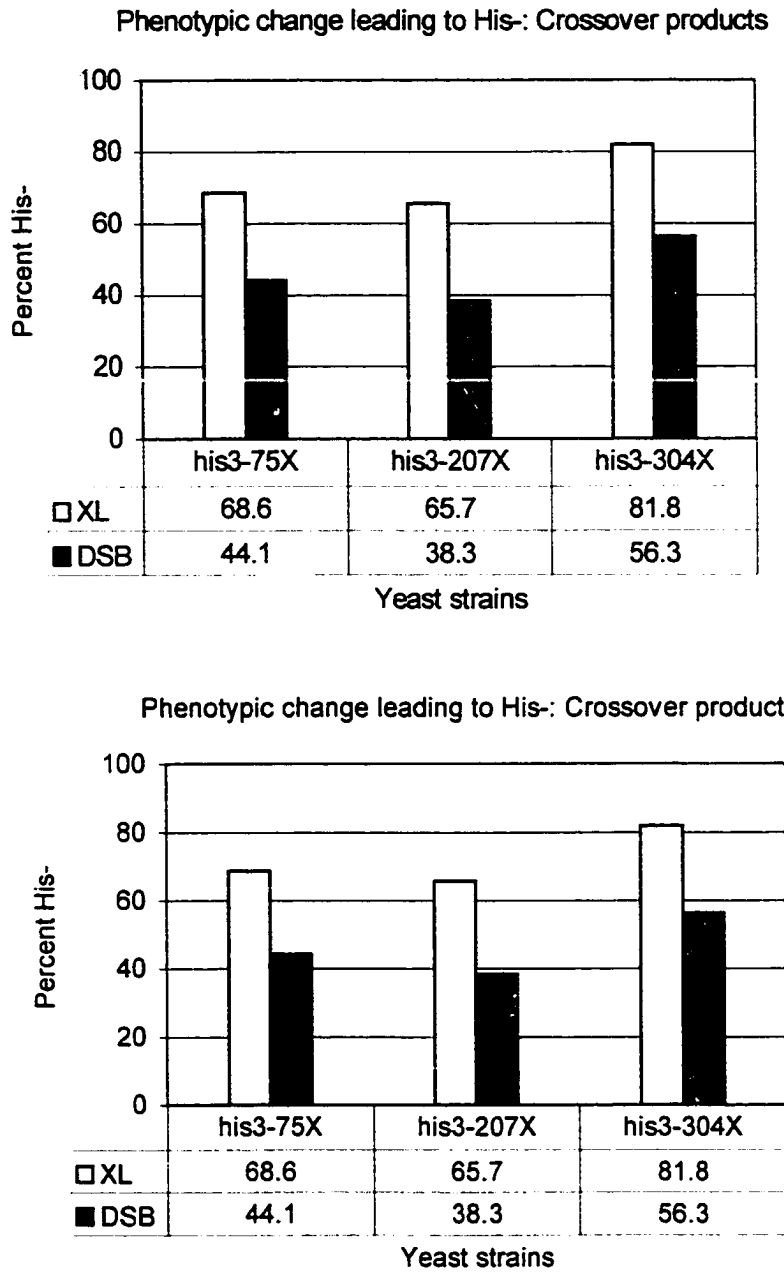

Figure 14. **Preferential His$^-$ phenotype generation by psoralen crosslinks during gene conversion of Type I combinations.** Percent of repair products (Trp$^+$) exhibiting the His$^-$ phenotype for non-crossover (top) and crossover (bottom) products from Type I arrangements. Trp$^+$ colonies were screened for His phenotype and Trp and His stability by replicaplating. Percentage of His$^-$ colonies from the total colonies analyzed is shown for substrates carrying a psoralen crosslink (open bars) or a double strand break (closed bars) in each strain. Sample sizes ranged from 66 to 200 colonies.

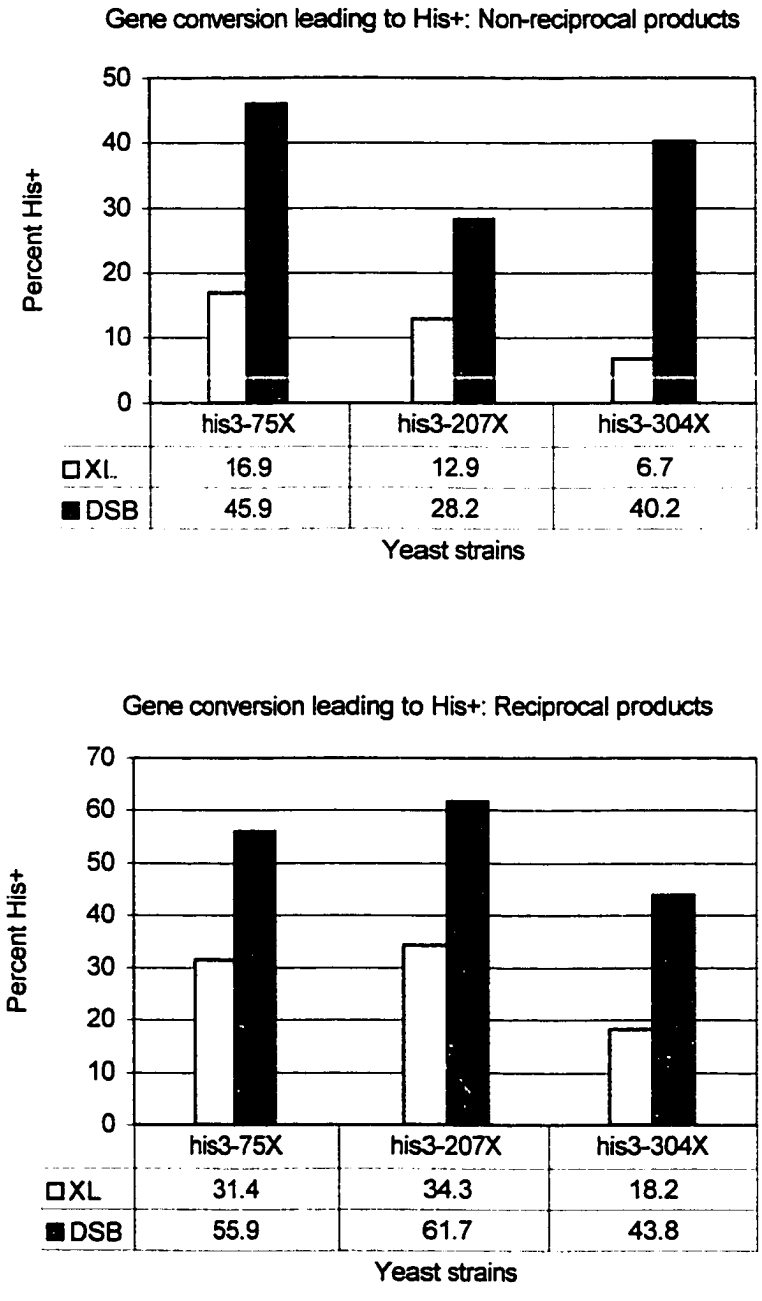

Figure 15. **Preferential His$^+$ phenotype generation by double strand breaks during gene conversion of Type I combinations.** Percent of repair products (Trp$^+$) exhibiting the His$^+$ phenotype for non-crossover (top) and crossover (bottom) products from Type I arrangements. Trp$^+$ colonies were screened for His phenotype and Trp and His stability by replica plating. Percentage of His$^+$ colonies from the total colonies analyzed is shown for substrates carrying a psoralen crosslink (open bars) or a double strand break (closed bars) in each strain. Sample sizes ranged from 66 to 200 colonies.

upstream from the damage site when induced by a psoralen crosslink and downstream from the damage site when induced by a double strand break.

Phenotype generation pattern is reversed in the Type II combination:

The Type II marker arrangement occurs when the *his3-75X* substrate is in combination with the *his3-622X* strain (fig 16). In this combination the plasmid borne marker is upstream of the damage site and the chromosomal marker is downstream of the damage site. This orientation is the reverse of Type I with respect to the position of the markers relative to the damage site. Reversing the positions of the plasmid and chromosomal marker reverses the outcome phenotype produced from upstream and downstream conversion tracts compared to the Type I arrangements. Conversion tracts extending downstream from the damage site will yield a His^- phenotype and those extending upstream will yield a His^+ phenotype. If conversion tracts exhibit a directional polarity, which is a function of the inducing form of damage, the expectation for the Type II arrangement is that crosslink damage will induce His^+ colonies to a higher degree than double strand break damage.

We have observed a difference in His^+ generation between the products of crosslink and double strand break induced gene conversion that is in agreement with the expectation for Type II arrangement (fig 17). Gene conversion generating His^+ occurs at a higher level when induced from crosslink damage. This trend was observed for both crossover and non-crossover products. Since the original phenotype for this allele is His^-, it was only possible to measure

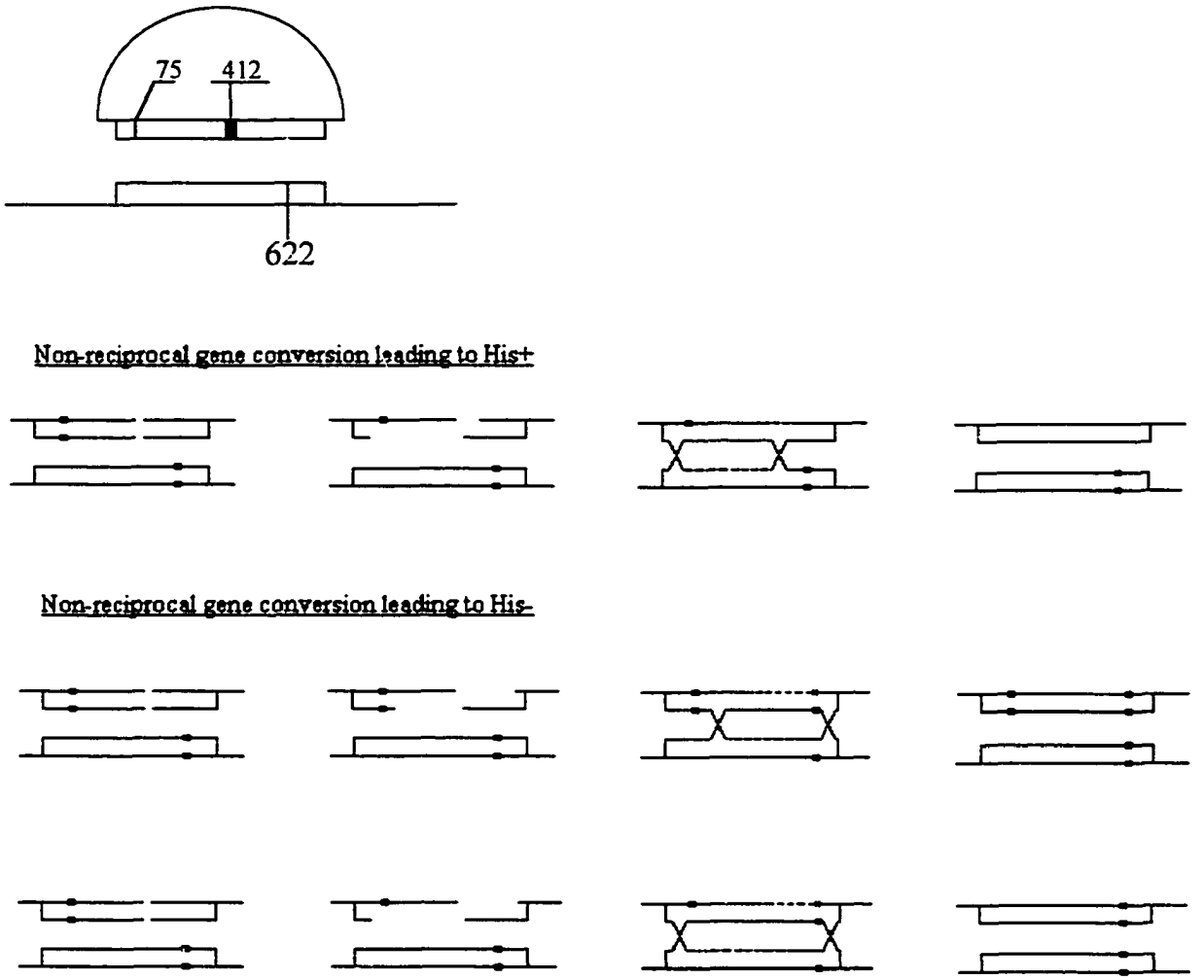

Figure 16. **Gene conversion events for the Type II arrangement of the *his3-75X* substrate.** Possible chromosome-to-plasmid gene conversion events and phenotype outcome for non-crossover recombination of the Type II combination showing the reverse outcome for Type I combinations. His^+ occurs from a gene conversion tract extending upstream from the damage site while His^- occurs from either a unidirectional downstream conversion tract or from a bi-directional conversion tract.

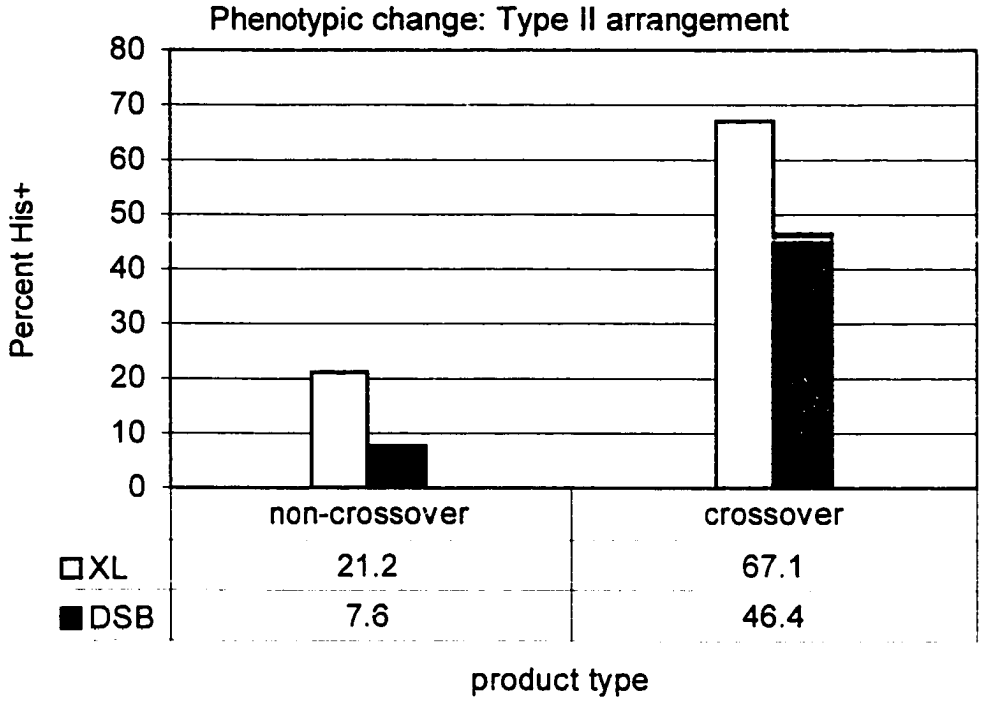

Figure 17. **Preferential His$^+$ phenotype generation by psorslen crosslinks during gene conversion of Type II combinations.** Percent of repair products (Trp$^+$) exhibiting the His$^+$ phenotype for the *his3-622X* strain transformed with the *his3-75X* substrate. Trp$^+$ colonies were screened for His phenotype and Trp and His stability by replica plating. Percentage of His$^+$ colonies from the total colonies analyzed is shown separately for non-crossover and crossover products from substrates carrying a psoralen crosslink (open bars, n = 216) or a double strand break (closed bars, n = 200). Genetic analysis can only detect His$^+$ generation for the Type II arrangement.

conversions resulting in His^+ colonies by genetic techniques.

The preferential conversion to specific phenotypes observed in the Type II arrangement coincides with the preferential conversion to specific phenotypes observed in the Type I combinations. A difference in His phenotype generation for a given marker combination exists that is dependent on the inducing form of damage. When the marker arrangement is inverted, the trend of His phenotype generation for the forms of damage reverses, suggesting that the difference is due to a directional preference of conversion tract formation. Psoralen crosslinks induce more upstream conversion tracts, while double strand breaks induce more downstream conversion tracts. Physical analysis of the repair products (discussed below) supports this trend.

Coincidental Trp^+ and His^+ stability suggest gene conversion occur primarily in the chromosome-to-plasmid direction:

If gene conversion occurs by mismatch of heteroduplex DNA formed by recombination intermediates and homologous sequences, either the damaged or the undamaged DNA molecule can be the donor of genetic information during the event. However, it has been generally observed that the damaged DNA molecule is usually the recipient of genetic information, and the undamaged molecule is the donor of genetic information during gene conversion (reviewed in Nickoloff and Hoekstra 1997). The previous treatment of gene conversion in this system assumes that the damaged plasmid has been the recipient in damage-induced gene

conversion (chromosome-to-plasmid conversion). We have detected, by phenotypic analysis, conversion events in which the undamaged *his3X* allele carried on the chromosome has been the recipient of genetic information. Colonies arising from plasmid-to-chromosome conversion have an extrachromosomal plasmid carrying a *his3* allele and the *TRP1* gene, and a *HIS3* allele on the chromosome. The phenotype and stability of these colonies is Trp^+unstable-His^+stable. In His^+ colonies the location (plasmid or chromosome) of the *HIS3* gene, giving rise to the His^+ phenotype, can be identified by determining the stability of the His^+ phenotype. If the stability of the His^+ and Trp^+ phenotypes coincide (both unstable), both alleles are plasmid borne which is an indication of chromosome-to-plasmid (undamaged-to-damaged) gene conversion. However, if the His^+ phenotype is stable, indicating that the *HIS3* allele resides on the chromosome, and the Trp^+ phenotype is unstable, indicating that the plasmid has remained extra-chromosomal after repair, gene conversion has occurred in the plasmid-to-chromosome direction. Coincidence of the His^+ stability for Trp^+ unstable colonies is shown in figure 18. Most of the His^+ colonies with an unstable Trp^+ phenotype have a coincidental His^+ unstable phenotype indicating that the converted *HIS3* allele resides on the plasmid and conversion occurred in the chromosome-to-plasmid direction. However, a small portion of the damage-induced His^+ colonies, with an unstable Trp^+ phenotype, has a stable His^+ phenotype, indicating plasmid-to-chromosome conversion.

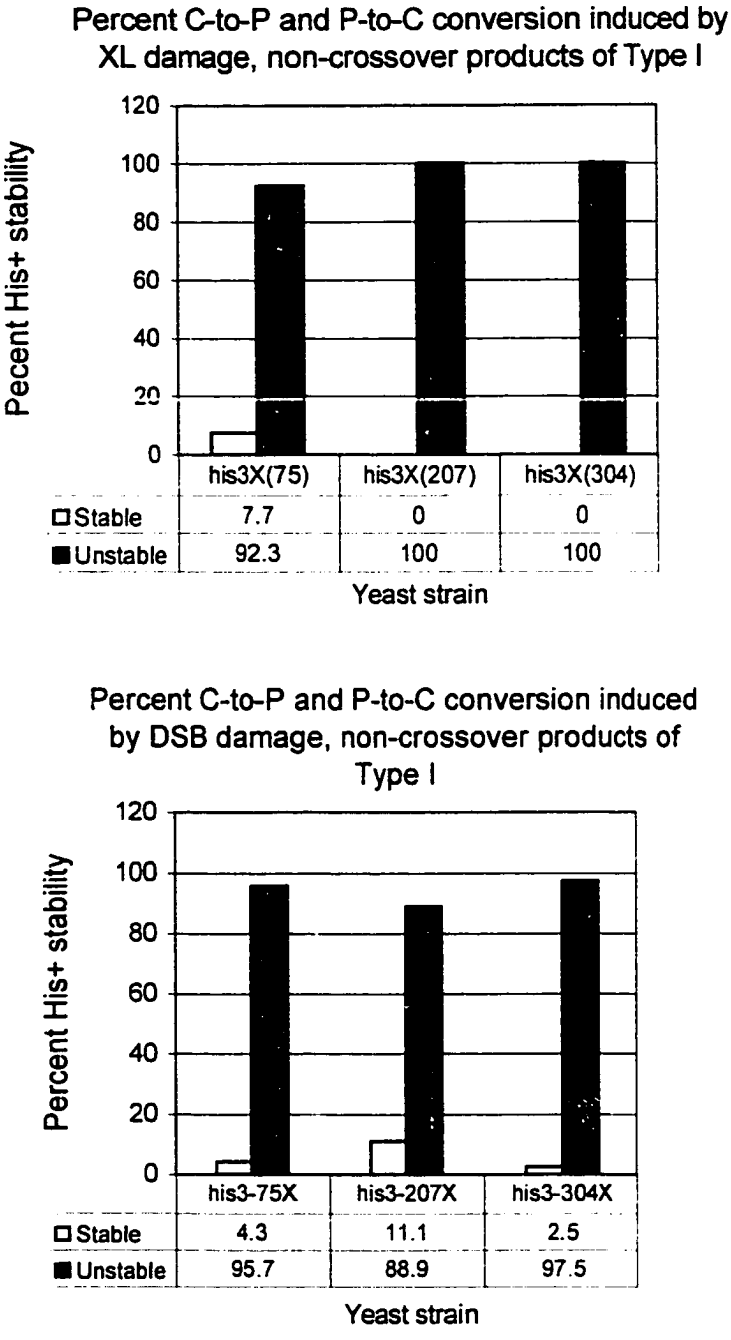

Figure 18. **Percent of chromosome-to-plasmid (C-to-P) and plasmid-to-chromosome (P-to-C) conversion in the non-crossover products of Type I arrangements.** The percent of His^+unstable and His^+ stable for the Trp^+ unstable colonies is shown. XL damage (top): For 12/13(75X), 4/4 (207X), and 4/4 (304X) products conversion occurred in the chromosome-to-plasmid direction. DSB damage (bottom): For 45/47 (75X), 24/27 (207X), and 39/40 (304X) products conversion occurred in the chromosome-to-plasmid direction.

Type III arrangements generate His^+ products by discontinuous gene conversion tracts:

The *his3-75X* substrate in combination with the *his3-207X* and *his3-304X* strains create the Type III arrangements. In these combinations both the plasmid and chromosomal markers are upstream of the damage site with the chromosomal marker proximal to the damage site (fig 19a). If chromosome-to-plasmid conversion is assumed, the His^+ phenotype can only be generated by a discontinuous conversion tract where chromosome-to-plasmid conversion occurs at the plasmid marker site but the chromosomal marker escapes conversion. In accordance with the DSB repair model of recombination (and the variations therein) certain events must occur in order to give rise to a discontinuous conversion tract. The plasmid sequence corresponding to the proximal chromosomal marker, must escape both resection and chromosome-to-plasmid mismatch repair of heteroduplex DNA while the sequence containing the plasmid borne marker must be involved in heteroduplex DNA and induce mismatch repair in the chromosome-to-plasmid direction. One possible model, explaining discontinuous conversion tracts, is shown in figure 19b. Resection, excluding the proximal marker is followed by repair synthesis of the gap. Branch migration then establishes hDNA at the plasmid marker while restoring the chromosomal marker. Mismatch repair in the chromosome-to-plasmid direction converts the plasmid borne marker to the chromosomal sequence.

A:

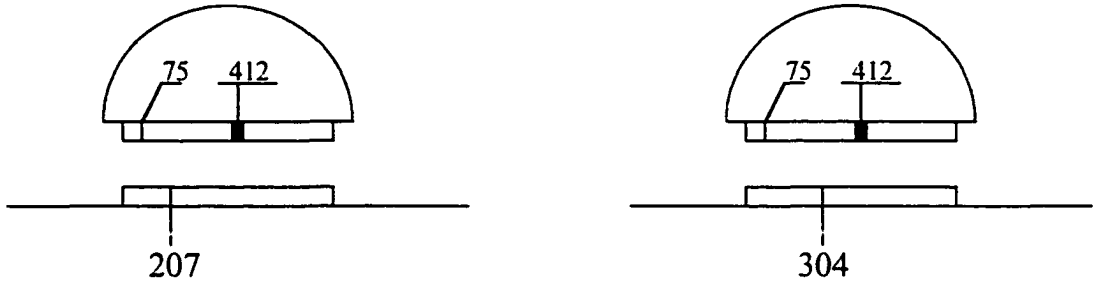

B:

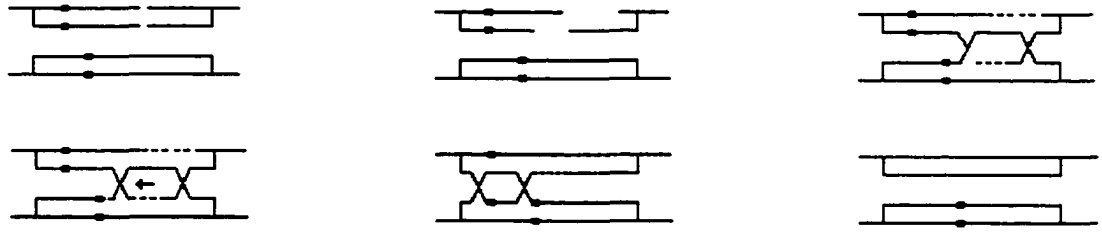

Figure 19. **A: Type III arrangements of the *his3-75X* substrate. B: Discontinuous gene conversion tract resulting in a His^+ plasmid borne allele.** Branch migration of both Holliday junctions restores the marker on the chromosomal allele.

His^+ colonies have been detected in the crossover and non-crossover products of the Type III combinations. Unstable His^+ colonies have been observed in the double strand break repair products of both Type III arrangements and stable His^+ colonies have been observed for both the crosslink and double strand break products of both Type III arrangements. The percent of these events is shown in table 4. The presence of discontinuous conversion tracts is an indication that conversion, in at least these products, occurs by mismatch repair of heteroduplex DNA and possibly involves branch migration of the Holliday junctions after initial repair synthesis is complete.

TABLE 4.

His$^+$ phenotype generated from Type III combinations.

Strain	DSB induced repair		Crosslink induce repair	
	Non-crossover	Crossover	Non-crossover	Crossover
his3-304X	2/80 (2.5)	13/120 (10.8)	0/102 (0.0)	12/109 (11.0)
his3-207X	4/113 (3.5)	23/87 (26.4)	0/111 (0.0)	4/93 (4.3)

His$^+$ colonies detected from genetic analysis of the *his3-75X* plasmid transformed into *his3-304X* and *his3-207X* strains.

Physical analysis of non-crossover products:

The results of the genetic analysis provide evidence that support the models of psoralen crosslink and monoadduct repair: A single crosslink was shown to be more toxic than either a monoadduct or a double strand break. Crosslink and double strand break damage produce similar levels of crossover and non-crossover products while a monoadduct was shown to be non-recombinogenic. Neither crosslink damage nor double strand break damage imposes hDNA limitation in the range of the markers studied. In addition, certain properties of gene conversion induced from a single crosslink and a double strand break have been shown to be similar which is in support of the model of crosslink repair. These properties include the evidence of discontinuous conversion tracts, branch migration, hDNA formation, and the high level of chromosome-to-plasmid gene conversion induced from both forms of damage.

The genetic analysis identified two properties of gene conversion induced from a crosslink and a double strand break that are different. The level of gene conversion in the non-crossover products of double strand break damage-induced repair is higher than the level of gene conversion in the non-crossover products of psoralen crosslink-induced repair. Also, gene conversion induced by crosslink damage in the Type I combinations preferentially produces His^- colonies while double strand break damage preferentially induces gene conversion leading to His^+ for the same combinations of strain and substrate. In the Type II combination, this preference is reversed. On the basis of the marker arrangements and the specific

gene conversion tract required to produce His $^{+}$ and His^{-} colonies, the results suggest that the form of damage initiating the conversion imposes a directionality to the conversion tract, which for these two forms of damage preferentially occurs in opposite directions.

These differences between crosslink and DSB induce gene conversion pose questions to the validity of the model for crosslink repair. To further characterize the similarities and differences between psoralen crosslink and DSB induced repair we have physically analyzed the repair products and compared the physical properties of gene conversion outcome.

Total yeast DNA from Trp^{+} unstable colonies, carrying extra-chromosomal plasmids from the repair of both crosslink and DSB damage was isolated and transformed into ultra-competent *E. coli*. The plasmids carry both the *E. coli* origin of replication (*ori*) and the *Amp^{r}* gene enabling both replication and selection. Plasmid DNA was isolated from ampicilin resistant cells and used for restriction mapping. Changes in the marker arrangement(s) were identified and used along with the results of the genetic analysis to construct gene conversion profiles for each combination of the Type I, II and III arrangements. The profiles for double strand break and crosslink induced gene conversion were compared to identify the unique and common trends of recombination and gene conversion characteristic for each form of damage.

The *Xba*I restriction maps of the original *his3-622X* and *his3-75X* substrates are shown in figure 20. Digestion with *Xba*I cuts the plasmid into 3 fragments.

Restriction maps of his3X substrates:

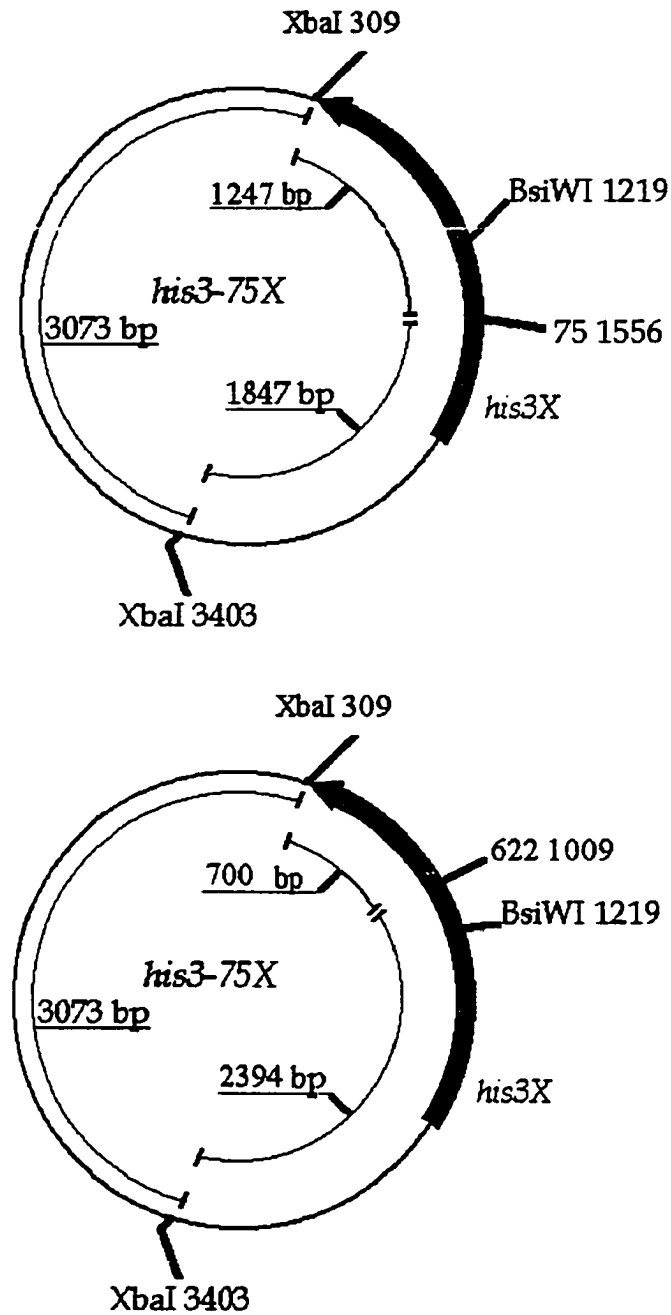

Figure 20. *Xba*I restriction map of original plasmid substrates.

The largest fragment is 3073 base pairs and is generated from the two *Xba*I sites that are outside the *his3*X allele. The length of this fragment is fixed and is unaffected by gene conversion occurring within the *his3X* allele. The position(s) of the *Xba*I marker(s) within the *his3X* allele dictates the length of the other restriction fragments. Changes in the position(s) of the *Xba*I markers due to gene conversion will alter the lengths of these variable restriction fragments. The lengths of the restriction fragments from *Xba*I digests of each repair product have been measured by gel electrophoresis and used to reconstruct the positions of the markers in the *his3* gene. Gene conversion events that account for the marker patterns have been deduced. The products were categorized by the gene conversion event leading to the marker arrangement and the percent occurrence of each category was calculated and combined with the results of the genetic analysis to construct the gene conversion profile. Gene conversion profiles were constructed for crosslink and double strand break repair products for each of the Type I, II, and III combinations. The profiles were then compared to detect the similarities and differences for the trends of gene conversion induced by crosslinks and double strand breaks. The gene conversion profiles for Type I and Type II combinations are shown in figures 21a - d.

Gene conversion products identified by restriction mapping of rescued products:

*Xba*I and *BsiWI* restriction mapping was used to analyze the non-crossover products that were isolated. The products can be classified into 5 groups on the

his3-622X in *his3-75X*: non-reciprocal products

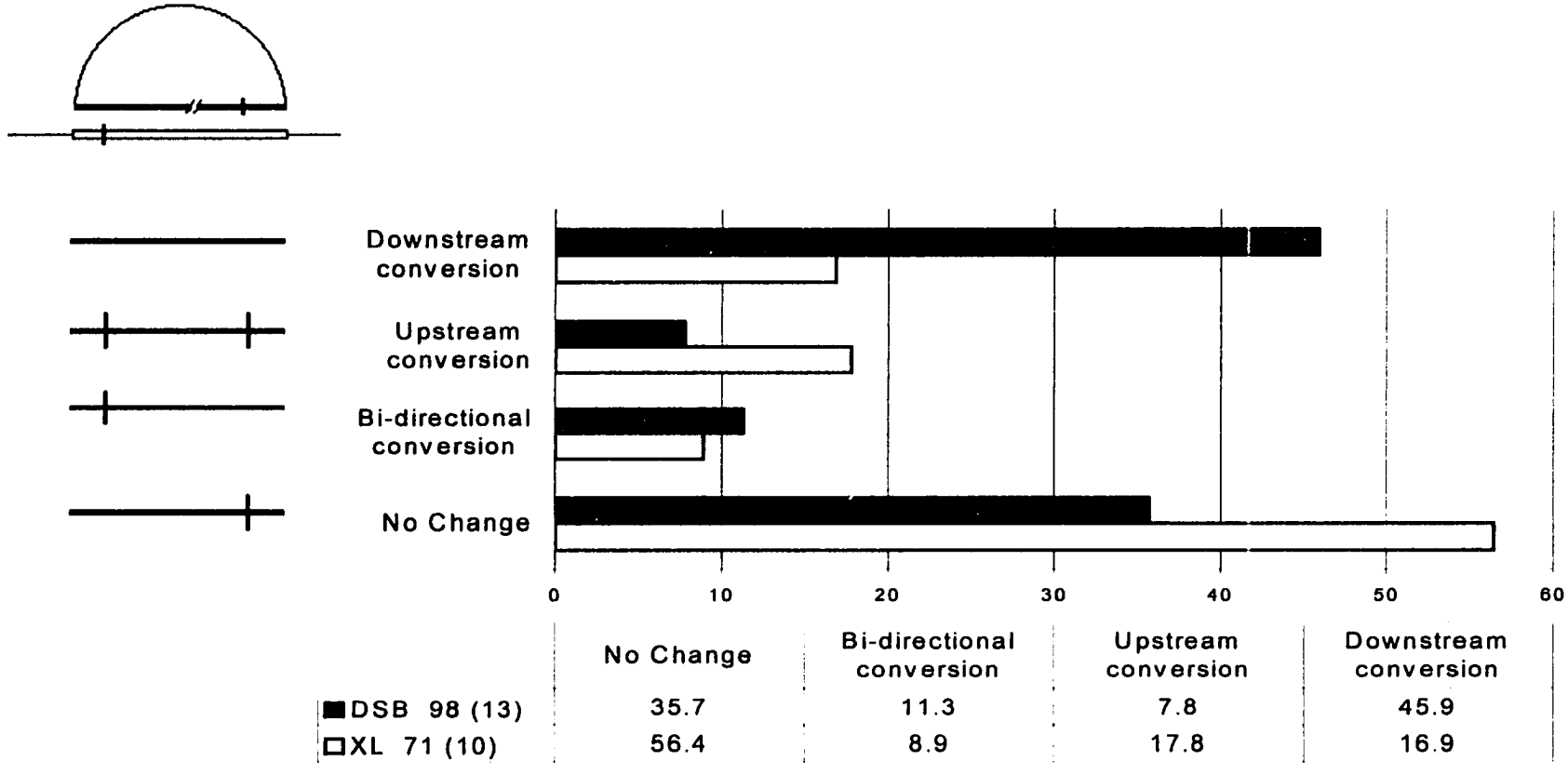

	No Change	Bi-directional conversion	Upstream conversion	Downstream conversion
DSB 98 (13)	35.7	11.3	7.8	45.9
XL 71 (10)	56.4	8.9	17.8	16.9

his3-622X in *his3-207X*: non-reciprocal products

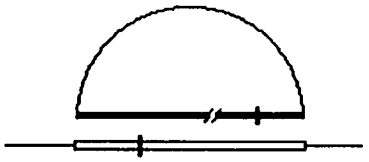

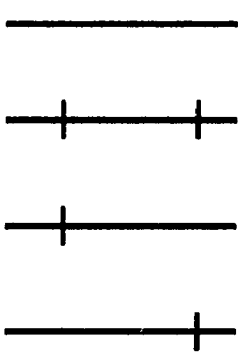

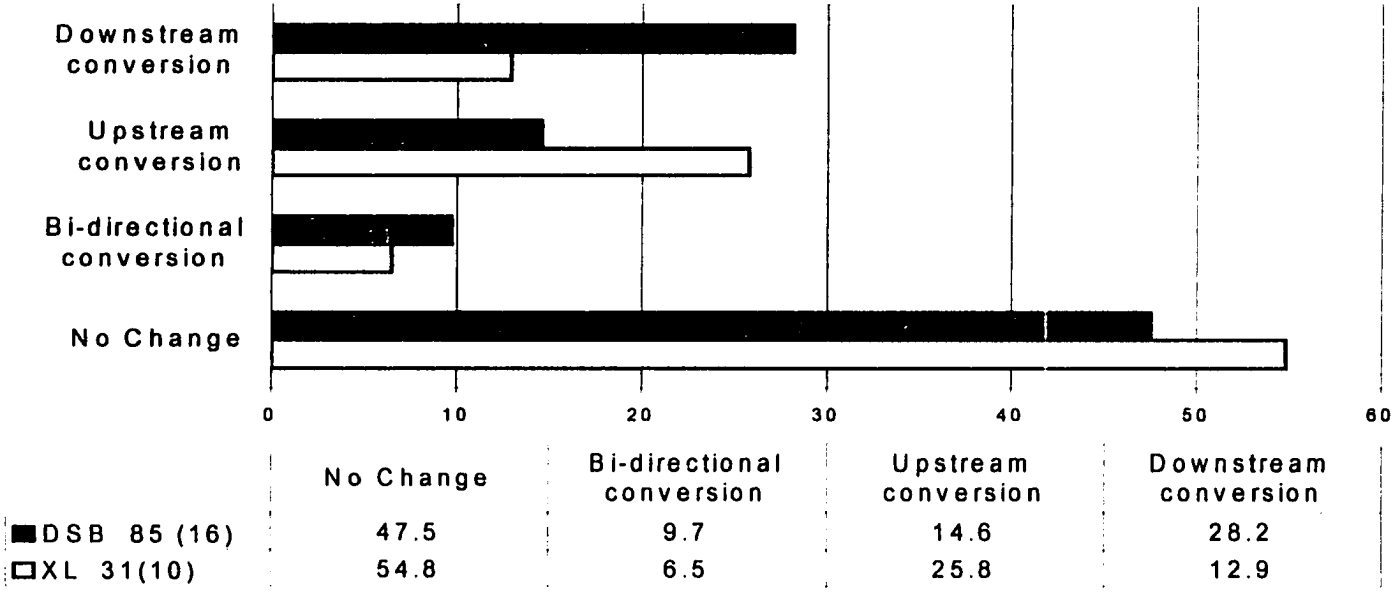

	No Change	Bi-directional conversion	Upstream conversion	Downstream conversion
DSB 85 (16)	47.5	9.7	14.6	28.2
XL 31(10)	54.8	6.5	25.8	12.9

his3-622X in *his3-304X*: non-reciprocal products

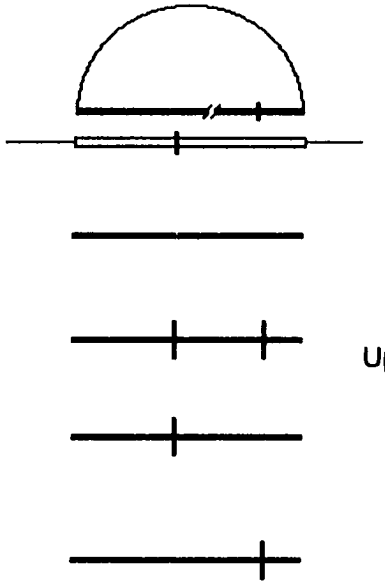

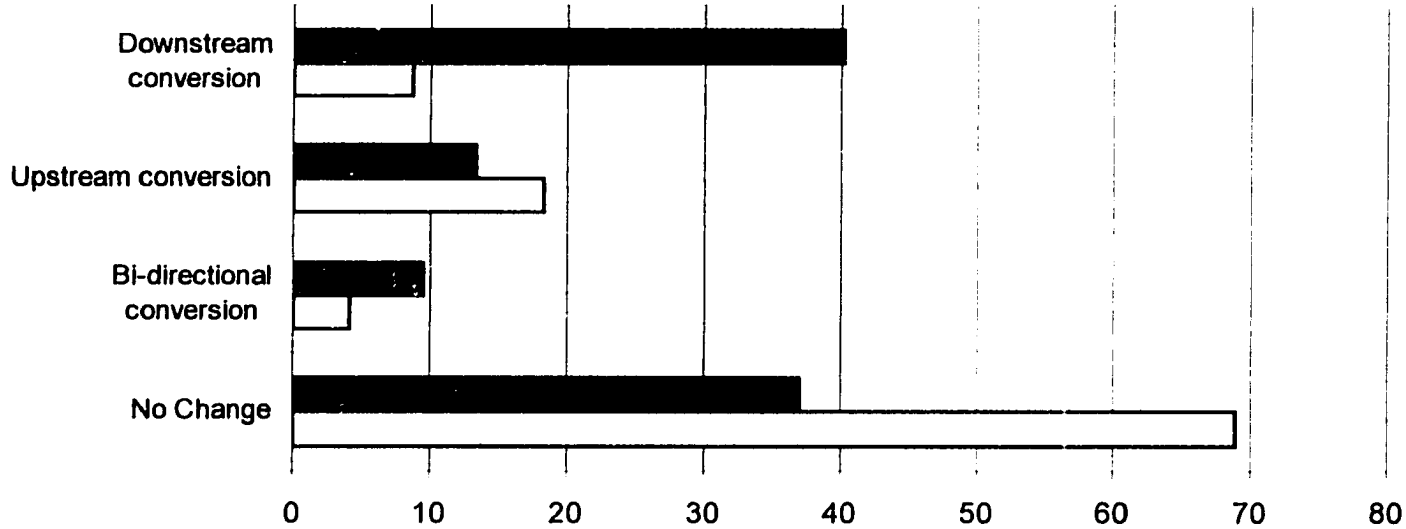

	No Change	Bi-directional conversion	Upstream conversion	Downstream conversion
■DSB 97 (13)	37	9.5	13.3	40.2
□XL 60 (18)	68.9	4.1	18.3	8.7

his3-75X in *his3-622X*: non-reciprocal products

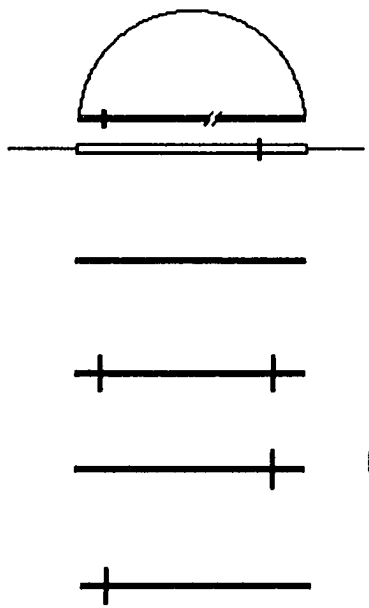

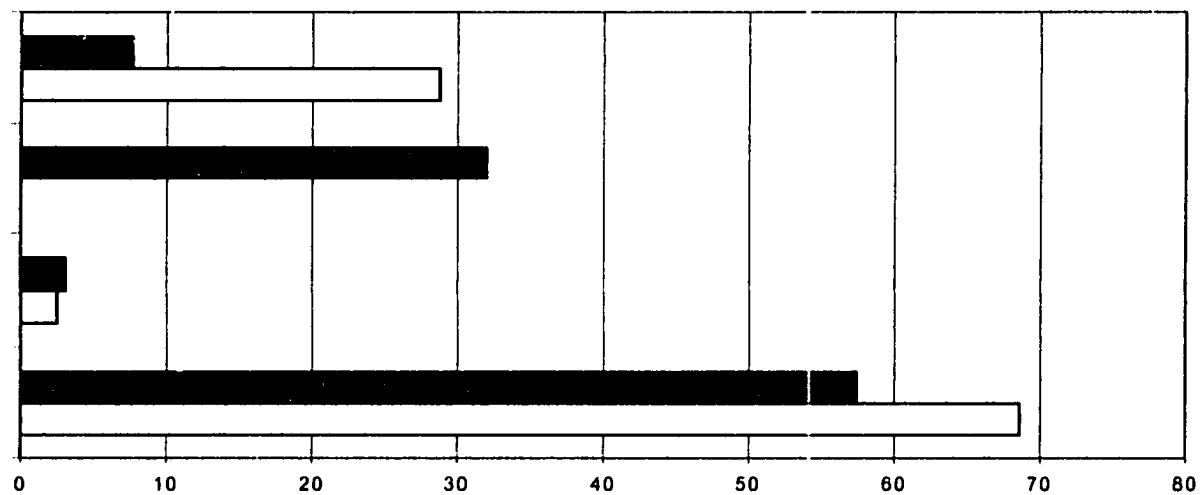

	No Change	Bi-directional conversion	Downstream conversion	Upstream conversion
■DSB 131 (29)	57.4	3.1	31.9	7.6
□XL 146 (31)	68.6	2.5	0	28.8

Figure 21a-d. Gene conversion profiles for the non-crossover products of the Type I (a-c) and Type II (d) combinations. Left (top): Original plasmid and chromosomal marker locations. Left (bottom): Marker location(s) of XbaI marker(s) in the plasmid borne allele of non-crossover products isolated by plasmid rescue. Right: Percent of each product category and gene conversion event determined from genetic and physical analysis. The number of colonies used for the genetic analysis and physical analysis (in parenthesis) are included in the data tables.

basis of marker arrangement or BsiWI sequence. 3 of the 5 product groups arise from different gene conversion events. These product classifications are: 1) Plasmids that have lost the *Xba*I marker, 2) Plasmids that have gained the chromosomal *Xba*I marker, 3) Plasmids that have gained the chromosomal *Xba*I marker and have lost the original plasmid borne *Xba*I marker. Examples of these products are shown in figures 22 and 23. The fourth group consists of plasmids that have been repaired without conversion of either marker and the fifth group consists of plasmid that have been processed by the error-prone pathways and carry a mutation at the *BsiW*I site within the *his3* coding sequence.

Conversion tracts induced from crosslinks and double strand breaks exhibit a polarity in opposite directions:

The gene conversion profiles of the non-crossover products show that conversion tracts induced from psoralen crosslinks and double strand breaks exhibit polarity in opposite directions. In both Type I and Type II combinations, the levels of downstream conversion tracts are 2-to-4 times higher when conversion is induced from double strand breaks and the levels of upstream conversion tracts is 2-to-3 times higher when conversion is induced by psoralen crosslink damage. This trend in conversion tract polarity is consistent with the observations of the genetic analysis and accounts for the preference of His phenotype generation from both crosslink and double strand break damage. The gene conversion profiles provide physical evidence that damage induced conversion tracts exhibit a directional polarity, the direction of which is dependent

Possible products of non-crossover gene conversion:

his3-75X plasmid transformed into *his3-207X* strain

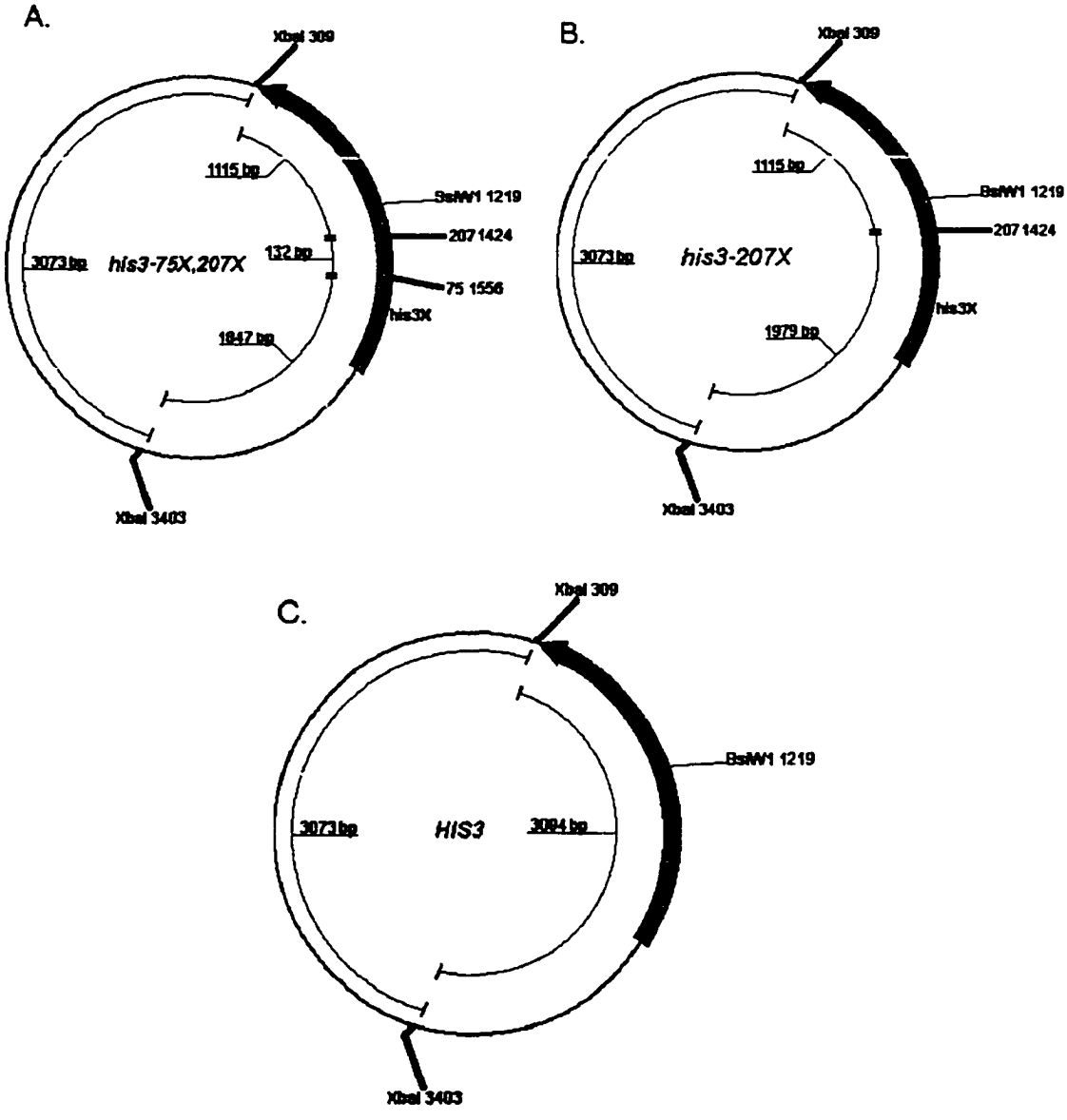

Figure 22. Non-crossover products arising from different gene conversion events.
A. Conversion to the chromosomal marker (partial conversion).
B. Conversion to the chromosomal allele (full conversion)
C. Conversion of the plasmid marker (wildtype allele)

Possible products of non-crossover gene conversion:

his3-622X plasmid transformed into *his3-304X* strain

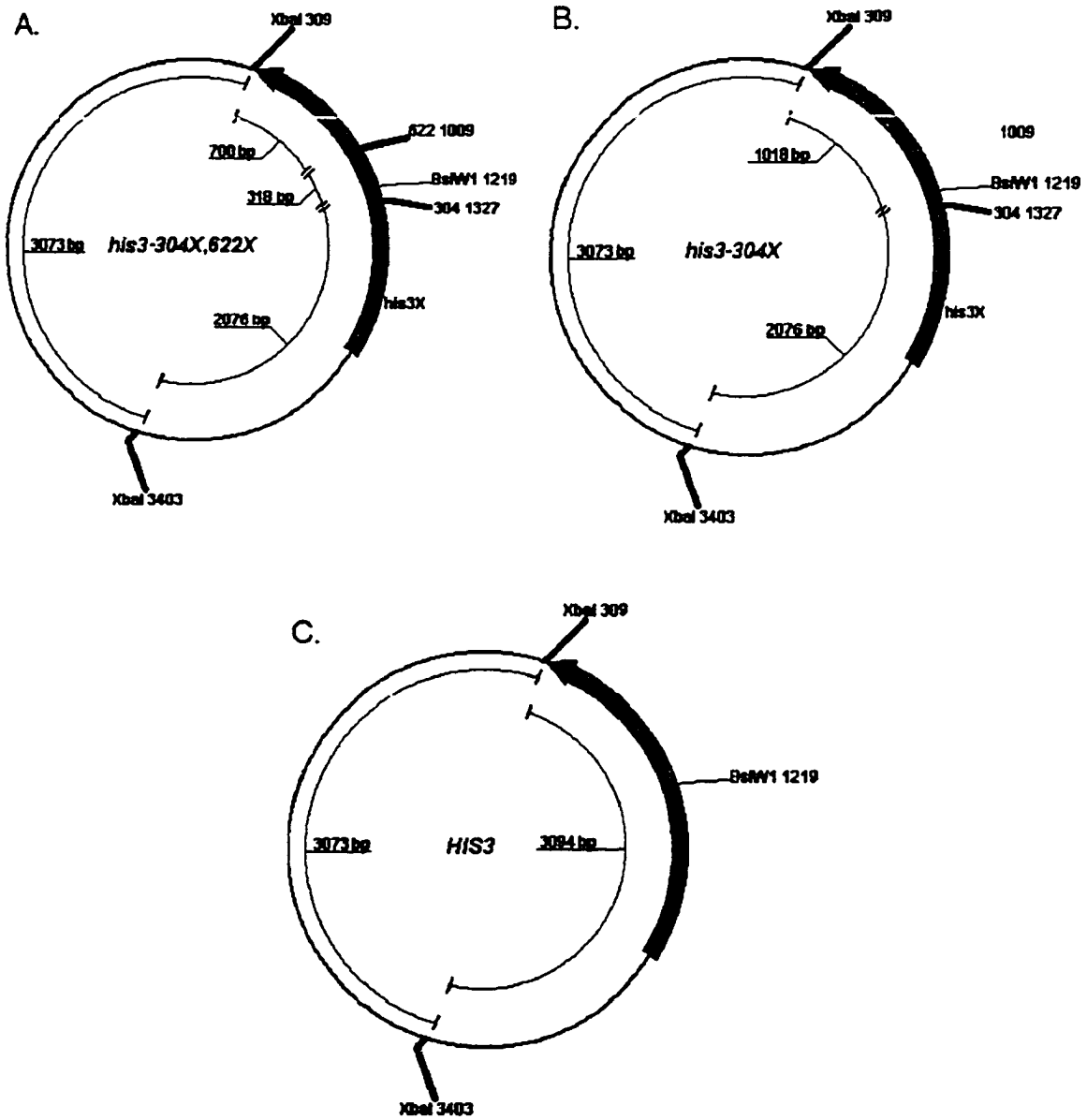

Figure 23. Non-crossover products arising from different gene conversion events.
A. Conversion to the chromosomal marker (partial conversion).
B. Conversion to the chromosomal allele (full conversion)
C. Conversion of the plasmid marker (wildtype allele)

on the form of inducing damage. Conversion tracts induced from psoralen crosslink damage preferentially extend upstream from the damage site while conversion tracts induced from a double strand break at the same site preferentially extend downstream from the damage site.

Conversion tracts are predominantly unidirectional in non-crossover products:

In both Type I and Type II arrangements, the chromosomal and plasmid borne markers flank the damage site. The use of flanking markers enables the measurement of the levels of unidirectional and bi-directional conversion tracts. Unidirectional conversion tracts, those that extend either upstream or downstream in only one direction, result in the conversion of only one of the two markers. If a conversion tract is bi-directional, extending in both directions from the damage site, both markers can be involved in a gene conversion event (see fig 11b. and fig 16).

Unidirectional conversion tracts account for all of the His^+ gene conversion events of Type I and Type II combinations due to the marker arrangements. His^- products however, can arise from either uni- or bi-directional conversion tracts. We have measured the levels of both uni- and bi-directional conversion tracts in the non-crossover products. Physical analysis has detected plasmid borne *his3* alleles that have been fully converted to the chromosomal allele. This could only happen if both markers are converted to the chromosomal sequence by a bi-directional gene conversion tract.

The overall level of bi-directional conversion tracts is shown in the gene conversion profiles. Bi-directional tracts are present in 2.5% to 11.3 % of the repaired plasmids. Of the total gene conversion events the level of bi-directional tracts are in the range of 7.3% to 20.4%. The majority of conversion tracts (79.6% to 92.7%) are therefore unidirectional. A difference in the level of uni- and bi-directional tracts as a function of the type of inducing damage was not observed.

Gene conversion profiles of crosslink and double strand break induced repair products are similar for the Type III arrangements:

The gene conversion profiles of the products from Type III combinations are shown in figs 24a,b. The profiles for both crosslink and double strand break repair products appear to be similar. Also, the marker arrangements in the Type III combinations impose restraints on gene conversion as discussed in the genetic analysis section. Only 2.5% to 5.7% of the repaired plasmids converted the plasmid marker by a discontinuous conversion tract.

The level of overall gene conversion in the Type III combinations is substantially lower compared to the levels observed for the Type I and Type II combinations. The average level of gene conversion in Type I and Type II combinations is 46.8%. The average level of gene conversion in Type III combinations is 15.1 %, where the gene conversion average is 24.5% in the *his3-304X* strain and only 6.4% in the *his3-207X* strain. The decline in overall gene conversion appears to be associated with the distance between the plasmid and chromosomal markers. As the distance between the markers decreases the level of

his3-75X in *his3-304X*: non-reciprocal products

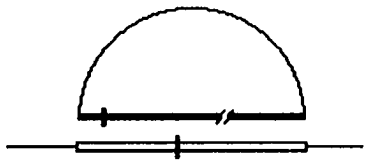

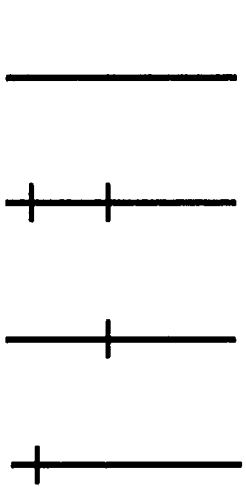

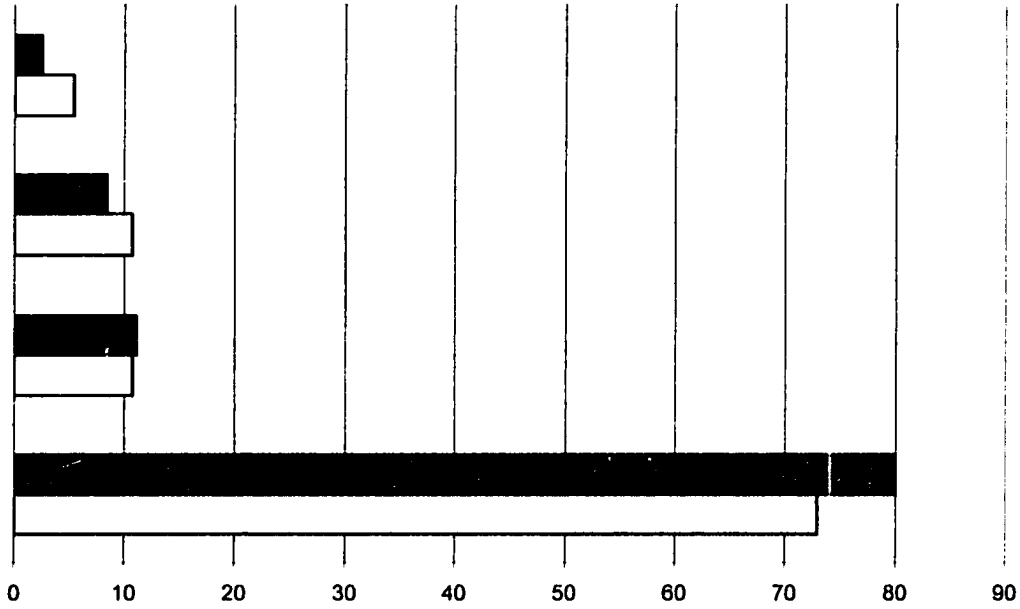

	No Change	Conversion at both sites	Conversion at 304	Conversion at 75
■DSB 80 (35)	80	11.1	8.4	2.5
□XL 102 (37)	73	10.8	10.8	5.4

his3-75X in *his3-207X*: non-reciprocal products

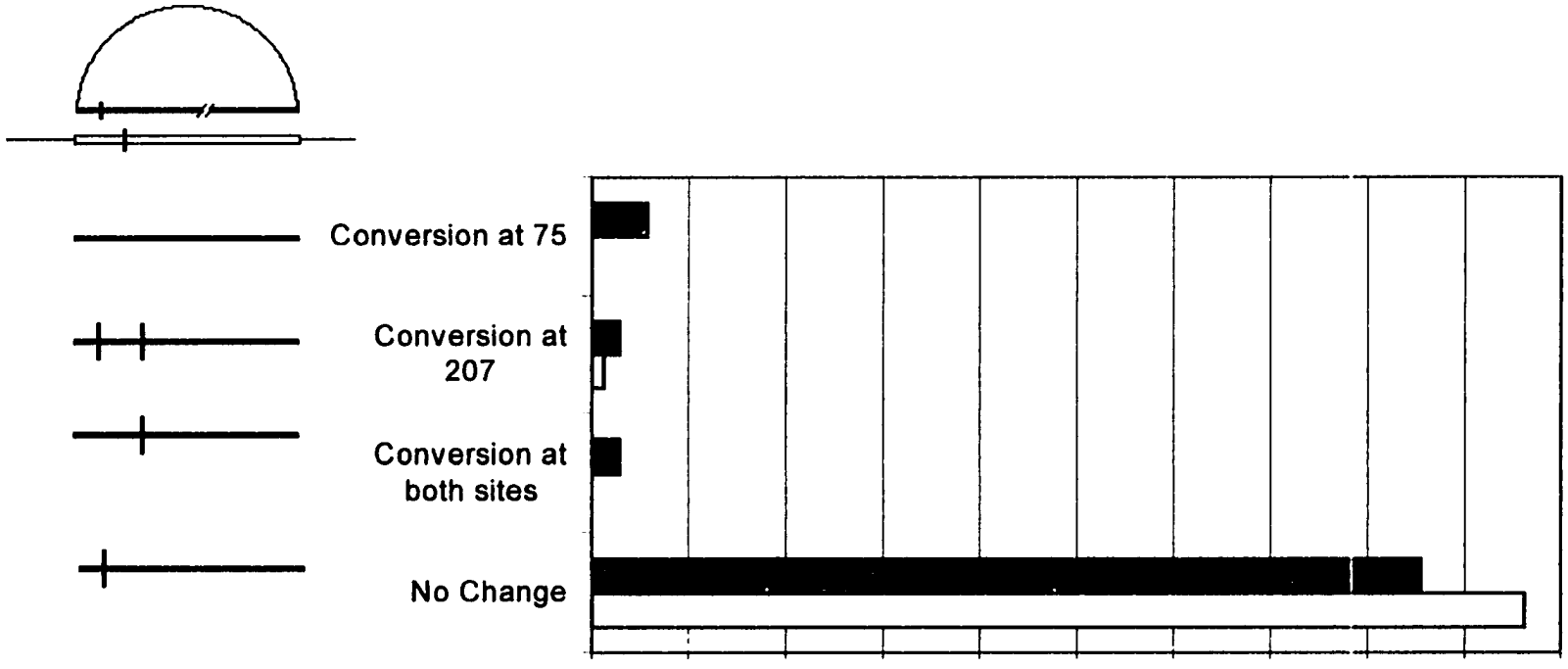

	No Change	Conversion at both sites	Conversion at 207	Conversion at 75
■DSB 113 (35)	85.5	2.9	2.9	5.7
□XL 111 (80)	96.2	0	1.2	0

Figure 24a - b. Gene conversion profiles for the non-crossover products of the Type III combinations. Left (top): Original plasmid and chromosomal marker locations. Left (bottom): Marker location(s) of XbaI marker(s) in the plasmid borne allele of non-crossover products isolated by plasmid rescue. Right: Percent of each product category and gene conversion event determined from genetic and physical analysis. The number of colonies used for the genetic analysis and physical analysis (in parenthesis) are included in the data tables.

gene conversion also decrease. This may be due to heteroduplex rejection caused by a decrease in local homology between the recombining sequences as the markers approach one another.

Mutations at the damage site are detected from psoralen crosslink damage but not double strand break damage.

*Xba*I restriction mapping identified four types of non-crossover products that show different patterns of the *Xba*I marker(s) in the *his3* gene. A fifth class of product was retrieved from *BsiW*I restriction mapping of the rescued plasmids. These products are plasmids that carry a mutation at the damage site (the *BsiW*I site within the *HIS3* gene) and were detected as plasmids resistant to restriction endonuclease digestion with *BsiW*I enzyme. The level of mutations at the *BsiW*I site for the non-crossover products from substrates that carried a psoralen crosslink was measured at 9.1% of the total products (table 5a).

Non-crossover products from double strand break induced repair were analyzed for mutations at the *BsiWI* site. Mutations were not detected, as all products were susceptible to *BsiW*I digestion (table 5b). Crossover products of crosslink induced repair were also analyzed for mutations at the *BsiW*I site. PCR was used to amplify a 900 bp. fragment of the *his3* gene. The PCR product was then treated with *BsiW*I restriction endonuclease to determine the integrity of the *BsiW*I site. All PCR products were cleaved into two fragments indicating that mutations at the *BsiW*I site in the crossover products of psoralen crosslink repair were not present.

TABLE 5

Targeted mutations of the *BsiWI* site within the *HIS3* coding sequence.

A

Strain	*his3-622X* substrate	*his3-75X* substrate
His3(75X)	1 (10.0%)	N.D.
His3(207X)	0	9 (11.3%)
His3(304X)	2 (11.1%)	3 (8.1%)
His3(622X)	N.D.	2 (6.5%)

B

Damage	Product	Total	Mutations
Psoralen Crosslink	Non-crossover	186	17 (9.1%)
Psoralen Crosslink	Crossover	82	0
Double strand break	Non-crossover	141	0

A. Percent of rescued plasmids resistant to *BsiWI* digestion indicating mutation at the *BsiWI* site for each substrate/strain combination. All substrates carried a psoralen crosslink at the *BsiWI* site. **B.** Total products analyzed for mutations at the *BsiWI* site. Non-crossover products were analyzed by plasmid rescue followed by digestion with *BsiWI* restriction endonuclease. Crossover products were analyzed by PCR amplification of the 900 bp. sequence surrounding the *BsiWI* site followed by *BsiWI* digestion of the PCR product. All PCR fragments synthesized from psoralen crosslink induced crossover recombination products were cut by the *BsiWI* enzyme.

We have analyzed the sequence of psoralen crosslink induced mutations and found that all mutations involve the psoralen-modified thymine residues in the *BsiW*I sequence. The mutations retrieved are shown in table 6. The 100 bp. sequence centered about the modified *BsiW*I site of 15 *BsiW*I-resistant products was analyzed. Ten products contained T:A → C:G transitions. Three T:A → G:C transversions, one T:A → A:T transversion and one GT → TG double transversion was observed. *Xba*I restriction mapping of the products containing mutations at the *BsiW*I site showed that all of these products retained the original *Xba*I frameshift marker and did not show any evidence of gene conversion at the chromosomal marker position.

Physical analysis of crossover recombination products:

Southern hybridization analysis of the crossover products was used to construct the gene conversion profiles for both crosslink and double strand break induced repair. Trp^+ stable colonies were grown in 10 ml cultures and genomic DNA was isolated. DNA samples were divided in half and subjected to both *Xba*I and *EcoR*I digestion. Digested DNA was run on agarose electrophoresis gels and transferred to nylon filters. pUC18-*HIS3* probe was hybridized to the filters to detect fragments containing both vector and *HIS3* sequences generated by the digestion of the genomic DNA. Restriction fragment lengths were determined against λ *BstE*II size standard or λ *Hind*III size standard included on each gel. Fragment lengths were used to construct restriction maps of the *HIS3* locus for

TABLE 6

Mutational spectrum from sequence analysis of *BsiW*I resistant plasmid products from psoralen crosslink repair.

(+) CAGGCCG*T*ACGCAGTTG
(-) GTCCGGCA*T*GCGTCAAC

Strand	T:A→C:G	T:A→ G:C	T:A → A:T	GT → TG
+	6	3	1	1
-	4	0	0	0

Sequence analysis of the 100 bp. region flanking the *his3 BsiW*I site of plasmids resistant to *BsiW*I digestion. All mutations involve the psoralen modified thymine residue of either the non-transcribed (+) strand or the transcribed (-) strand shown on top. Bottom: mutation spectrum from 15 products sequenced .

each product. The constructed restriction maps were compared to the restriction maps of the *his3* loci prior to crossover recombination (figure 25). Changes in the position(s) of the *Xba*I restriction sites in the repair products were identified and used to deduce the specific gene conversion event(s) required to produce the observed marker patterns. Products were classified according to these events. *EcoR*I blots were used to distinguish single and multiple integration products.

Southern hybridization analysis identifies 6 classes of crossover recombination products:

Six classes of crossover recombination products were identified by southern hybridization, three of which arise from gene conversion in the chromosome-to-plasmid direction. These three classes are products that have lost the plasmid marker, products that have gained the chromosomal marker, and products that have simultaneously lost the plasmid marker and gained the chromosome marker. The fourth class of products are those where gene conversion occurs in the plasmid-to-chromosome direction. Plasmids that have integrated without gene conversion comprise the fifth class and products that contain deletions or rearrangements at *his3* account for the sixth class. These six types of products have been identified in products showing both single and multiple plasmid integration. Examples of the alleles, marker arrangements, and deduced gene conversion events determined from the Southern hybridization analysis for some of the detected single integration products are shown in figure 26.

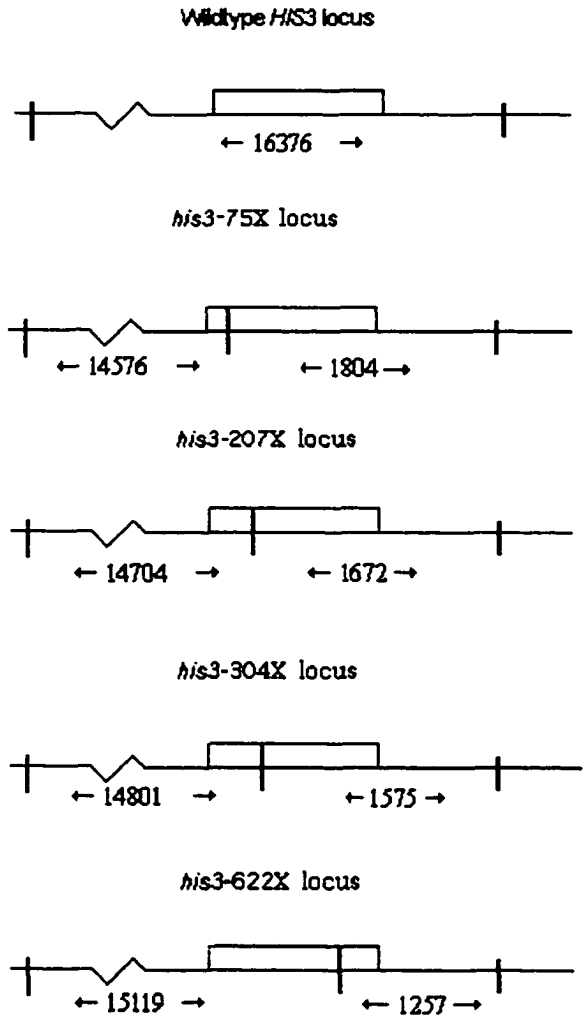

Figure 25. ***Xba*I restriction map of the wildtype and frameshift strains *HIS3* locus.**

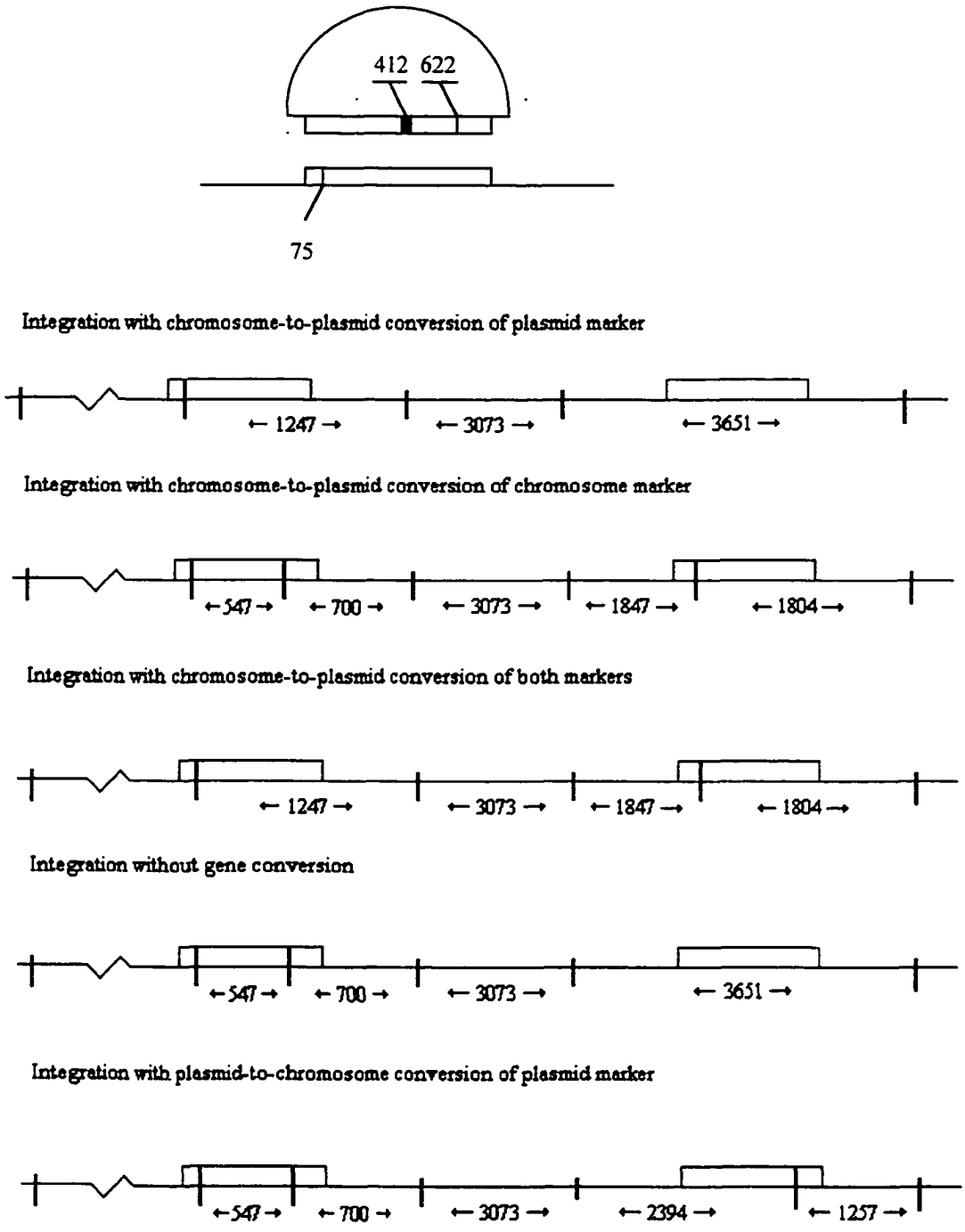

Figure 26. ***Xba*I restriction maps of some crossover recombination products (single integration).** Maps shown are for Type I combination of the *his3-622X* substrate transformed into the *his3-75X strain* (top) . Bottom: Maps deduced from Southern hybridization analysis of blots from genomic DNA digestions with *Xba*I.

The contribution of each product category to the total products obtained was calculated for and used to construct the gene conversion profile. Patterns retrieved from the profiles for both forms of damage were compared. Gene conversion profiles for the crossover products are shown in figures 27a - f. The trends obtained from the gene conversion profiles coincide with the trends observed from the genetic analysis.

The majority of gene conversion events occur in the chromosome-to-plasmid direction for crossover products:

In all of the combinations studied (all Type I, II, and III) the plasmid and chromosomal alleles of the *his3* gene carry *Xba*I markers at different locations. When a plasmid becomes integrated into the genome an additional allele, and an additional *Xba*I marker, are introduce to the *HIS3* locus. If gene conversion does not occur the two alleles will carry a total of two markers at the positions corresponding to the original chromosome and the original plasmid positions. Which allele carries which marker will depend on the crossover point during the integration which is a function of the resolution of the heteroduplex intermediate.

Gene conversion in the chromosome-to-plasmid direction can occur at either position, resulting in different products. If chromosome-to-plasmid conversion occurs at the plasmid marker position, the plasmid marker will convert to the chromosomal sequence and will be lost. The result is a decrease in the number of plasmid markers relative to the number of integrated plasmids. If

his3-622X in *his3-75X*: reciprocal products

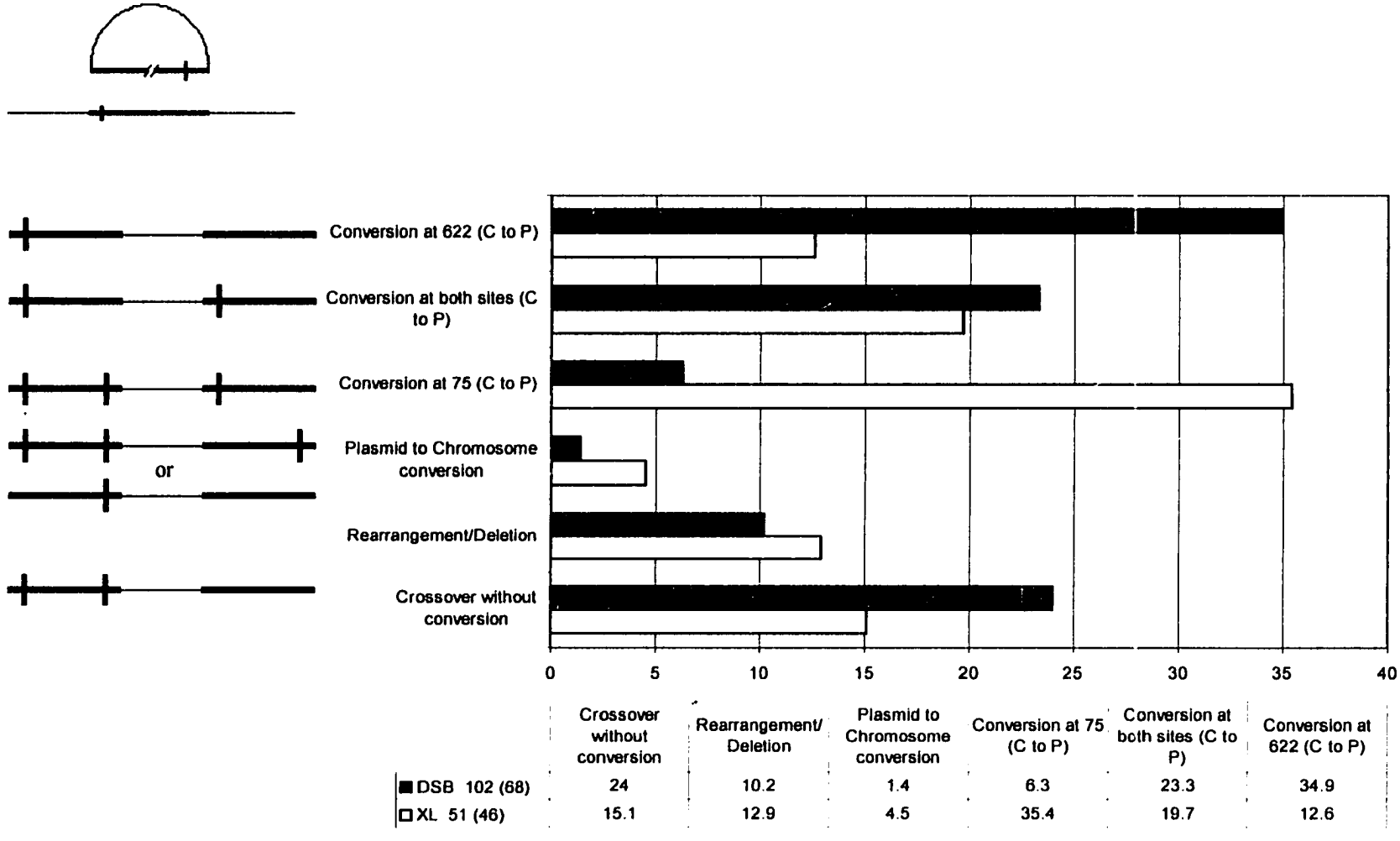

	Crossover without conversion	Rearrangement/ Deletion	Plasmid to Chromosome conversion	Conversion at 75 (C to P)	Conversion at both sites (C to P)	Conversion at 622 (C to P)
■ DSB 102 (68)	24	10.2	1.4	6.3	23.3	34.9
□ XL 51 (46)	15.1	12.9	4.5	35.4	19.7	12.6

his3-622X in *his3-207X*: reciprocal products

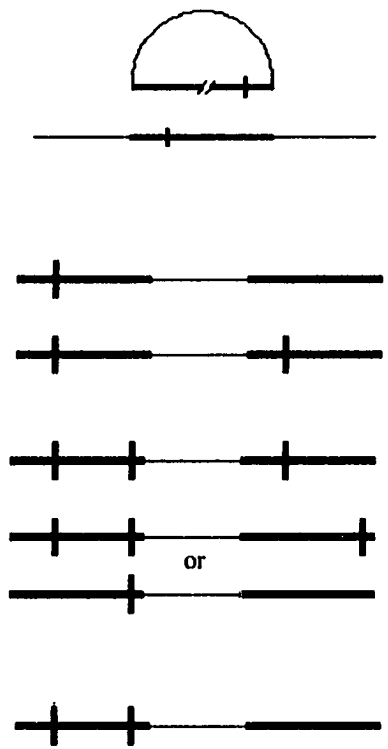

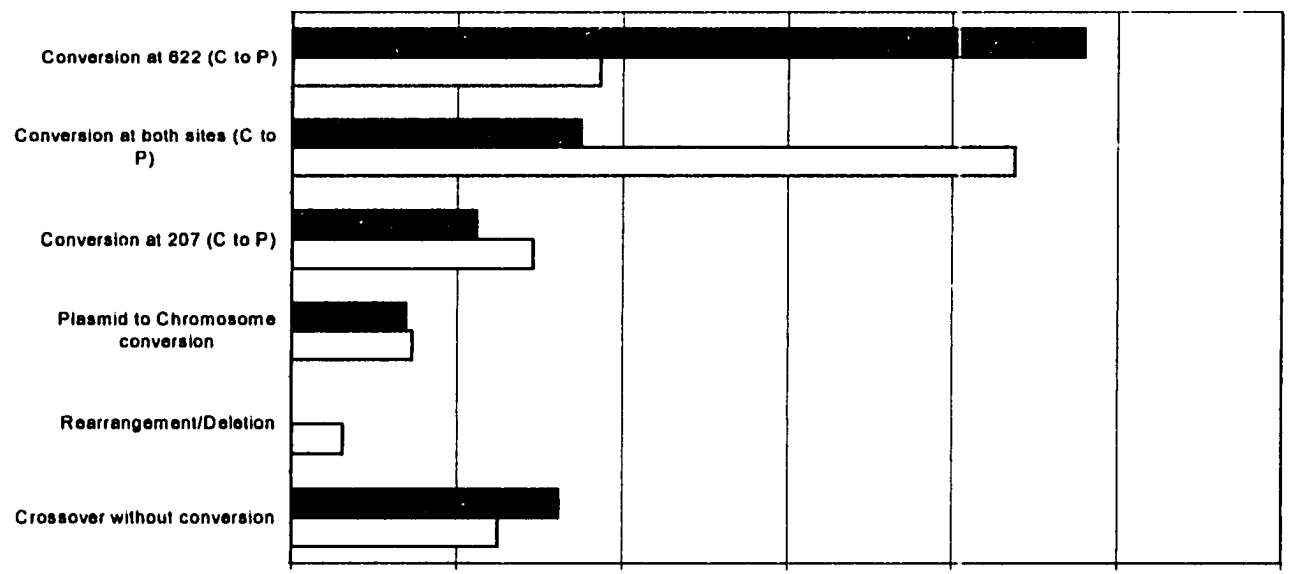

	Crossover without conversion	Rearrangement/Deletion	Plasmid to Chromosome conversion	Conversion at 207 (C to P)	Conversion at both sites (C to P)	Conversion at 622 (C to P)
■DSB 115 (51)	16.2	0	6.9	11.2	17.5	48
□XL 35 (20)	12.5	3.1	7.3	14.6	43.8	18.7

his3-622X in *his3-304X*: reciprocal products

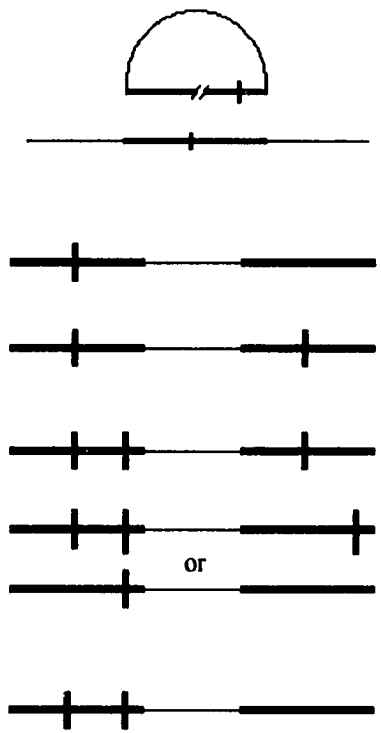

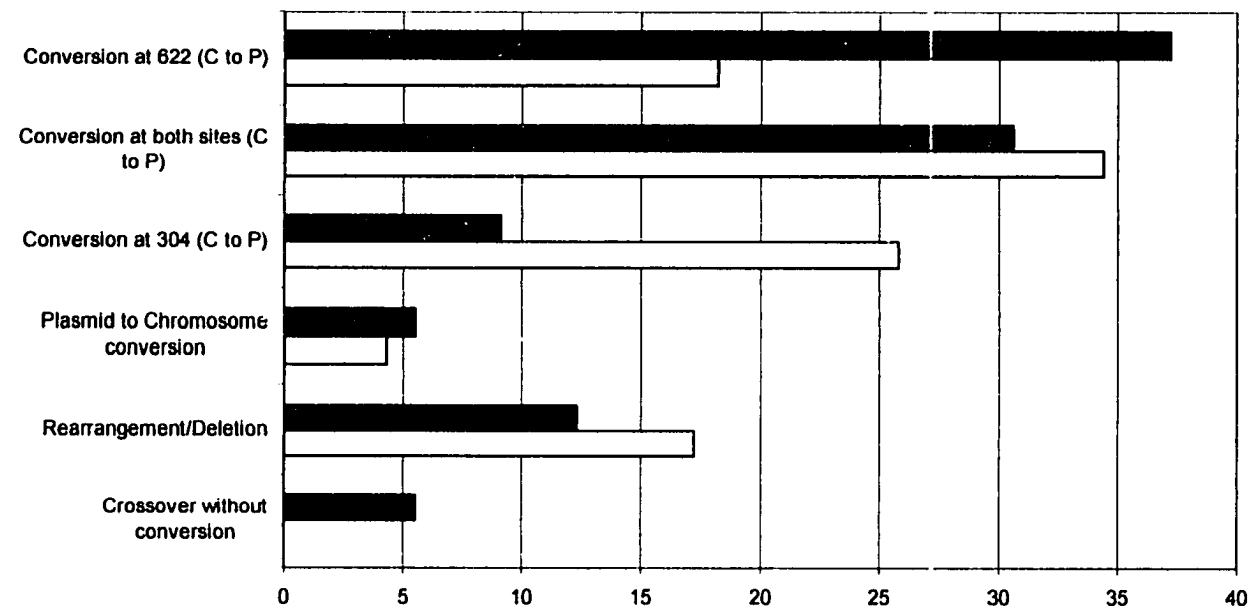

	Crossover without conversion	Rearrangement/ Deletion	Plasmid to Chromosome conversion	Conversion at 304 (C to P)	Conversion at both sites (C to P)	Conversion at 622 (C to P)
■DSB 103 (57)	5.5	12.3	5.5	9.1	30.6	37.2
□XL 33 (24)	0	17.2	4.3	25.8	34.4	18.2

his3-75X in *his3-622X*: reciprocal products

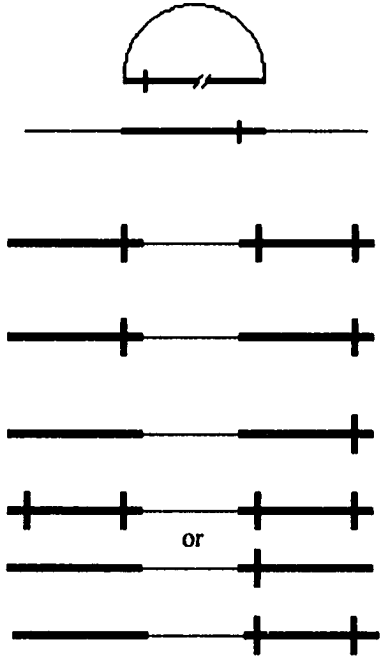

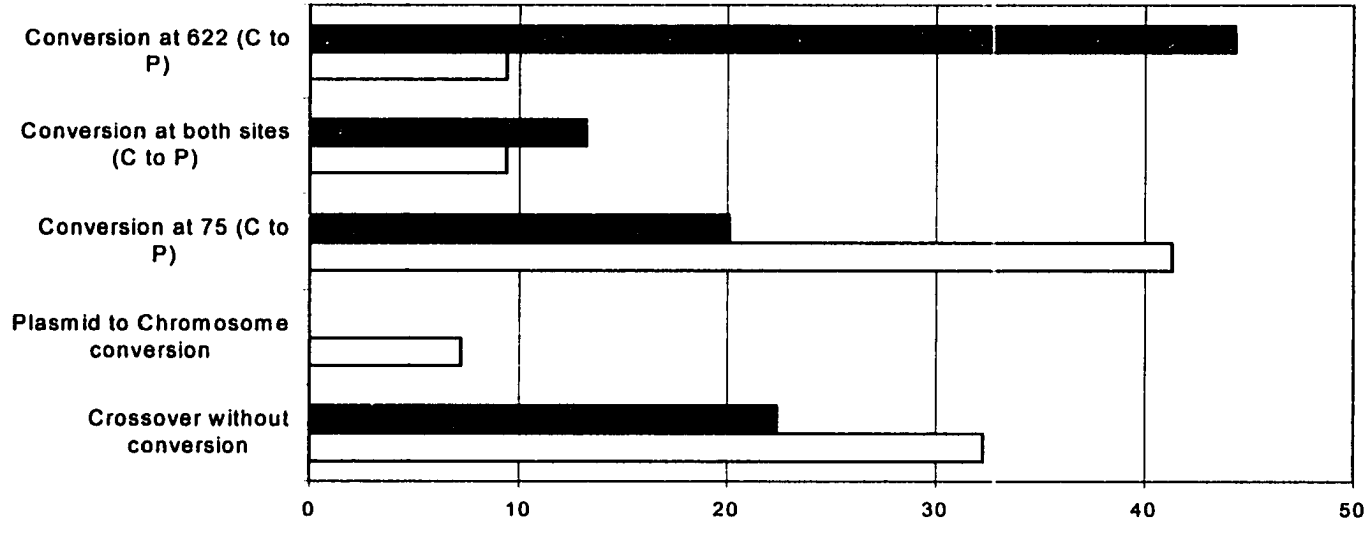

	Crossover without conversion	Plasmid to Chromosome conversion	Conversion at 75 (C to P)	Conversion at both sites (C to P)	Conversion at 622 (C to P)
■DSB 69 (46)	22.4	0	20.1	13.2	44.3
□XL 70 (27)	32.3	7.2	41.3	9.4	9.4

his3-75X in *his3-304X*: reciprocal products

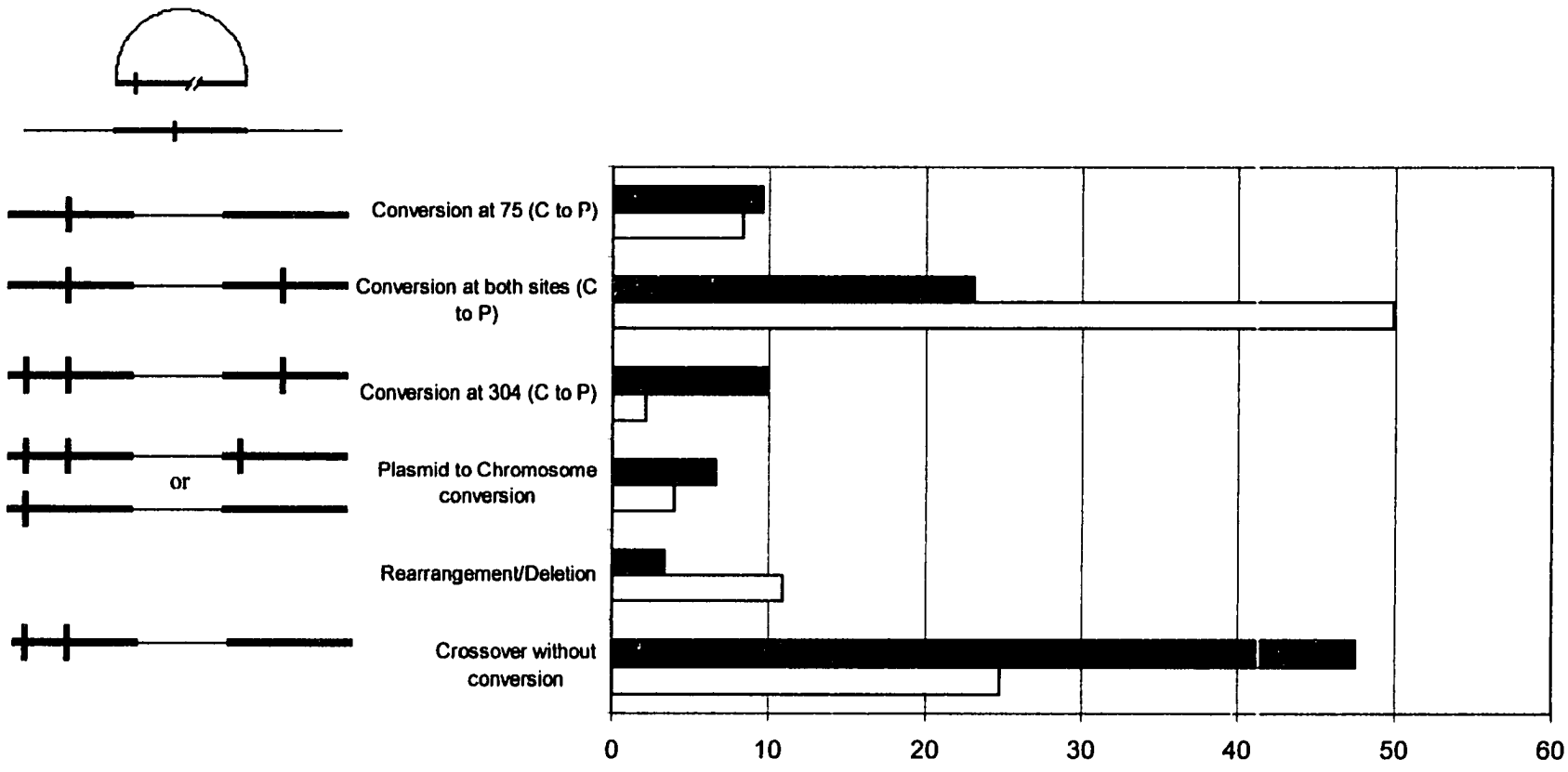

	Crossover without conversion	Rearrangement/ Deletion	Plasmid to Chromosome conversion	Conversion at 304 (C to P)	Conversion at both sites (C to P)	Conversion at 75 (C to P)
■ DSB 120 (36)	47.5	3.3	6.6	9.9	23.1	9.6
□ XL 109 (57)	24.8	10.9	3.9	2.1	49.9	8.3

his3-75X in *his3-207X*: reciprocal products

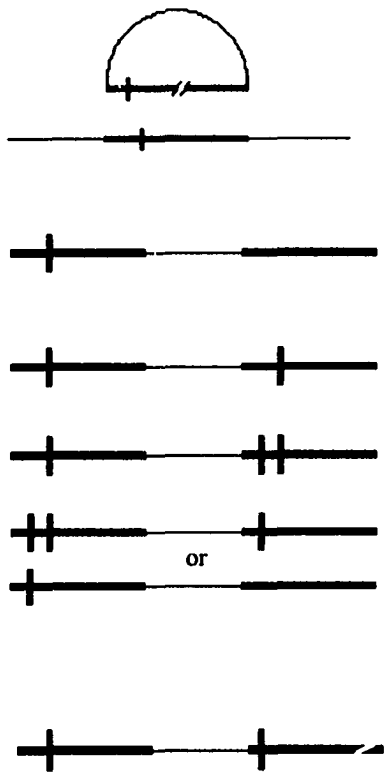

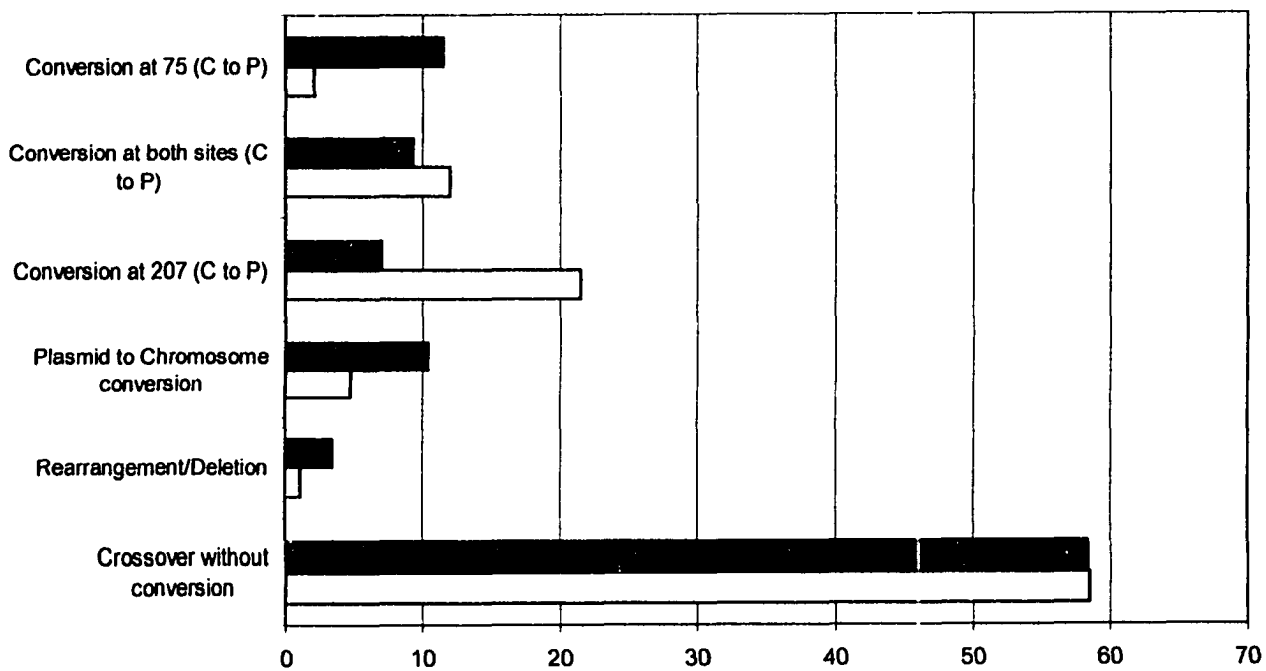

	Crossover without conversion	Rearrangement /Deletion	Plasmid to Chromosome conversion	Conversion at 207 (C to P)	Conversion at both sites (C to P)	Conversion at 75 (C to P)
■DSB 87 (44)	58.4	3.4	10.4	7	9.3	11.5
□XL 93 (44)	58.5	1.1	4.8	21.5	12	2.1

Figure 27 a-f. Gene conversion profiles for the crossover products of Type I (a-c), Type II (d), and Type III (e,f) combinations. Left (top): Original plasmid and chromosomal marker locations. Left (bottom): Marker location(s) of XbaI marker(s) in the plasmid borne allele of non-crossover products isolated by plasmid rescue. Right: Percent of each product category and gene conversion event determined from genetic and physical analysis. The number of colonies used for the genetic analysis and physical analysis (in parenthesis) are included in the data tables.

chromosome-to-plasmid conversion occurs at the chromosomal marker position it will be copied to the plasmid allele, increasing the number of markers at the chromosomal position. Both of these events have been used to identify chromosome-to-plasmid gene conversion for single and multiple integration products.

Plasmid-to-chromosome gene conversion has the reverse effect on the numbers of plasmid and chromosomal markers. When plasmid-to-chromosome gene conversion occurs at the plasmid marker position this marker is copied to the chromosome. The result is an increase in the number of plasmid markers relative to the number of integrated plasmids. Plasmid-to-chromosome conversion at the chromosomal marker position converts the chromosomal marker to the plasmid sequence resulting in the loss of the chromosomal marker. Both of these events have been used to identify plasmid-to-chromosome gene conversion for both single and multiple integration products.

The level of plasmid-to-chromosome gene conversion induced from both crosslink and double strand break damage is shown in the gene conversion profiles. For Type I and Type II combinations, plasmid-to-chromosome gene conversion occur in 1.4% to 7.3% of the products. Of the total gene conversion events the corresponding level of chromosome-to-plasmid gene conversion is 89.4% to 98.2%. For the Type III combinations the level of plasmid-to-chromosome gene conversion is slightly higher. 3.9% to 10.4% of the products show gene conversion in the plasmid-to-chromosome direction. Of the total gene

conversion events for the Type III combinations, the corresponding level of chromosome-to-plasmid gene conversion is 75.0% to 94.8%. The predominant direction of gene conversion is in the chromosome-to-plasmid direction for all combinations studied for gene conversion induced from both crosslink and double strand break damage. The level was independent of the inducing damage.

Conversion tracts in crossover products exhibit the same directional polarity as observed in the non-crossover products:

Damage induced conversion tracts in the non-crossover products of Type I and Type II combinations show polarity, which depends on the inducing damage. It was observed that conversion tracts induced from crosslink damage preferentially extend upstream from the damage site while conversion tracts induced from double strand break damage preferentially extend downstream from the damage site. In Type I and Type II combinations, the damage induced conversion tracts of the crossover products show the same polarity, which again is dependent upon the kind of inducing damage. The level of upstream conversion induced from crosslink damage is 2-to-5 fold higher than the level of upstream conversion induced from double strand break damage. The level of downstream conversion induced from double strand break damage is 2-to-5 fold higher than downstream conversion during crosslink repair. These results are consistent with the genetic analysis and account for the observed difference in His phenotype generation observed for the crossover products.

The difference in the polarity of gene conversion tracts, observed for both crossover and non-crossover products during damage-induced recombination, is the most notable distinction between gene conversion induced from psoralen crosslink damage and that induced from double strand break damage. Polarity of gene conversion tracts has been seen in other recombination systems, during both mitotic repair and meiotic gene conversion. Polarity during meiotic gene conversion is believed to be the result of specific recombination initiation sites within the gene at the high end of the polarity gradient (Malone *et al.*, 1992). During mitotic repair of double strand break damage polarity of gene conversion has been shown to result from differential end processing (see discussion). In our system, damage induced recombination initiates from the same site for substrates carrying both forms of damage. Therefore our results imply that a physical or mechanistic difference exists between the recombination intermediates of crosslink and double strand break damage, that gives rise to an opposite gene conversion polarity, possibly by causing differential end processing.

Differential end processing of the recombination intermediates may lead to the formation of extensive asymmetric hDNA on a specific side of the damage site in the Holliday structure, leading to mismatches on the side corresponding to the observed polarity for the specific form of damage. The difference in end processing may be due to either a physical difference between the recombination intermediates of crosslink and double strand break damage or may be due to mechanistic differences in the processing and/or excision steps leading to

differential resectioning in the recombination intermediates. A directional preference in resectioning can result if one of the terminal ends of the break is blocked due to the transcription and/or the excision repair machinery or the release of terminal ends from the excision machinery is ordered.

Gene conversion levels induced from crosslink and double strand break damage are similar in crossover products:

The only repair pathway that can produce plasmid integration is the recombinational pathway. Therefore, this pathway must mediate every repair event that results in a crossover product. This is not true for all extra-chromosomal products. Crosslink damage induces the mutagenic pathway in addition to the recombinogenic pathway. Both pathways lead to extra-chromosomal repair products. Products entering the mutagenic pathway do not enter the recombination pathway and therefore do not exhibit gene conversion, as conversion events are a consequence of recombination.

We have observed that the level of gene conversion in non-crossover products is lower for crosslink damaged substrates than for double strand break damaged substrates. Our results indicate that this is due, in part, to the shunting of substrates into the mutagenic pathway.

The level of gene conversion was measured for crossover products and is shown in fig 28. Both crosslink and double strand break damaged substrates exhibit similar levels of gene conversion. The similarity of the levels of gene

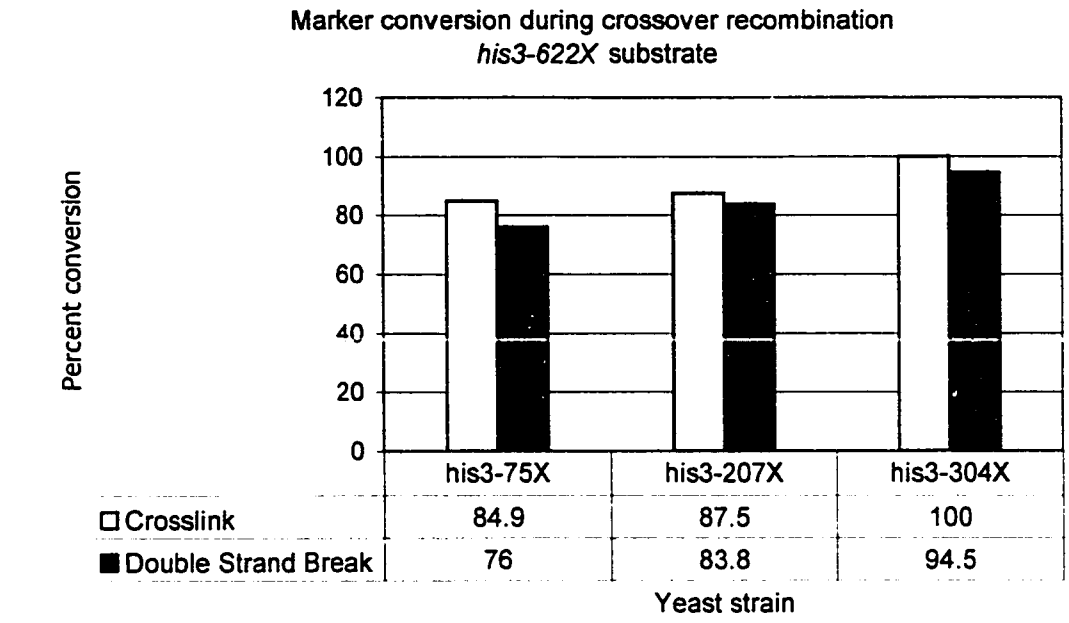

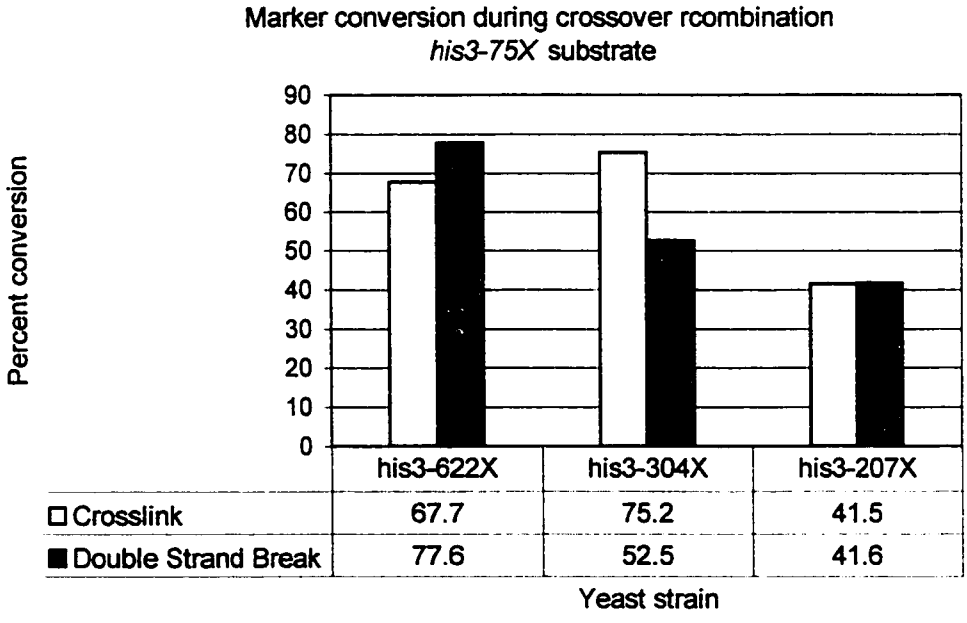

Figure 28. **Overall levels of marker conversion for crossover recombination products.** Total levels of conversion determined by Southern hybridization analysis of His^+ and His^- repair products are combined for the *his3-622X* substrate (top) and the *his3-75X* substrate (bottom).

conversion in the crossover products when both forms of damage are compared suggests that when recombination intermediates of either form of damage enter the recombination pathway, they exhibit a similar effectiveness of inducing gene conversion. Since the extra-chromosomal products of crosslink repair result from two different repair pathways, only one of which is associated with gene conversion, the level of gene conversion for crosslink substrates will be lower than double strand break substrates which are repaired exclusively by the recombination pathway.

The level of bi-directional conversion tracts increases in crossover products but unidirectional conversion tracts still predominate:

The level of bi-directional conversion tracts in the crossover products of Type I and Type II combinations is 2-to-7 times higher than the level of bi-directional conversion tracts in non-crossover products. The total level of unidirectional tracts in the crossover products is however higher than the level of bi-directional tracts (fig 29). For double strand break induced damage repair both the level of preferred downstream unidirectional conversion tracts and the level of total unidirectional conversion tracts are higher than bi-directional tracts in all Type I and Type II combinations. For crosslink induced repair, 2 of the 4 Type I and II combinations show a higher level of preferred upstream unidirectional tracts and 3 of the 4 arrangements show a higher level of total unidirectional tracts compared to bi-directional tracts.

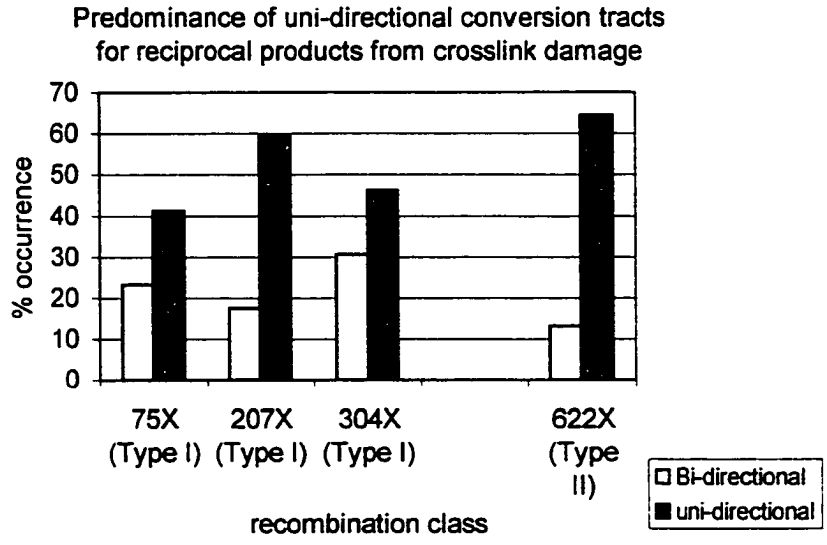

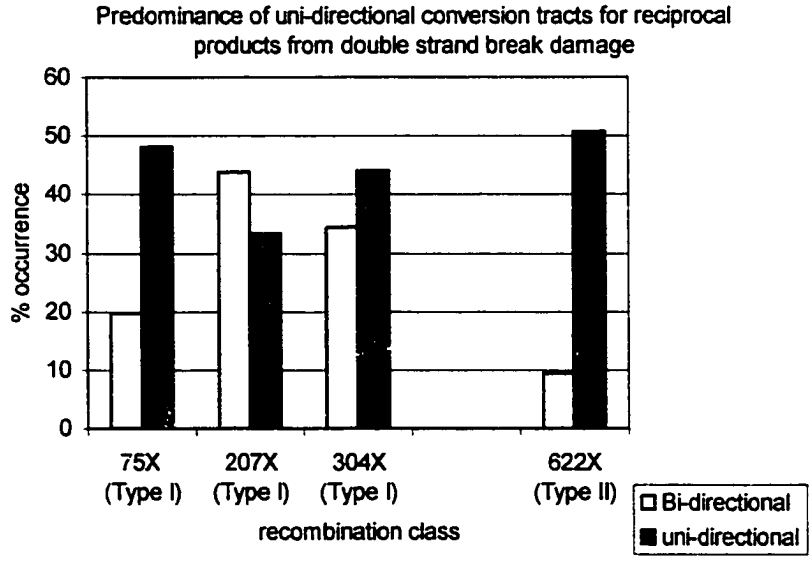

Figure 29. Percent of uni-directional and bi-directional conversion tracts for crossover products.

The level of gene conversion is reduced in the crossover products of the Type III arrangements and discontinuous conversion tracts are detected:

The gene conversion profiles of the crossover products of the Type III arrangements from both crosslink and double strand repair are similar to each other and to the gene conversion profiles of the non-crossover products of the Type III arrangements. The overall level of gene conversion appears to decline as the distance between the chromosomal and plasmid borne markers decreases. This may be due to heteroduplex rejection caused by an increase in non-homology when the markers are close to one another leading to a high probability that both markers are incorporated into the heteroduplex structure. While the cause of the decline in gene conversion level for the Type III arrangements is unknown, the phenomenon affects gene conversion induced by crosslinks and double strand breaks to the same degree.

Discontinuous conversion tracts have been detected in the crossover products of the Type III arrangements. As in the non-crossover products of the Type III arrangements a dependence of the level of discontinuous conversion tracts on the form of damage was not observed. Discontinuous conversion tracts have been detected in 2.1%-to-11.5% of the products for the Type III arrangements.

Discussion:

The collective results of previous studies tracking the repair, recombination, and gene conversion induced by psoralen modification suggest separate models for the repair of crosslinks and monoadducts. The repair of a crosslink is believed to initiate with an incision step catalyzed by the nucleotide excision repair pathway (Jachymczyk *et al.*, 1981; Magana-Schwencke *et al.*, 1982). In yeast, excision of the crosslink produces a double strand break intermediate (Jachymczyk *et al.*, 1981; Miller *et al.*, 1982). The resulting intermediate is a substrate for the recombinational repair pathway, which repairs the break using a homologous sequence as a template to direct repair synthesis. The model for monoadduct repair proposes that the adduct is a substrate of only the nucleotide excision repair pathway, which produces a single strand gap intermediate upon excision of the damage. The gapped intermediate does not require, but may stimulate recombination (Grant *et a*l., 1979; Averbeck and Moustacchi 1979,1980; Averbeck *et al.*, 1980; Saeki *et al.*, 1983; Cassier *et al.*, 1984). Repair of the gap proceeds through DNA polymerase-mediated repair synthesis using the undamaged strand as a template.

The models of psoralen induced repair make certain predictions of repair and recombination outcome. A single monoadduct should be repaired more efficiently than a single crosslink and should be non-recombinogenic. A crosslink should be repaired less efficiently than a double strand break but should produce similar recombination and gene conversion patterns. In a previous study, we

observed deviations from the predictions of these models due to a dose response to high levels of crosslink damage (Saffran *et al.*, 1994). At a low level of adducts (< 30 adducts/plasmid), crosslink damaged plasmids were shown to induce a higher level of transformation than monoadduct damaged plasmids. However, at higher adduct/plasmid levels, where the lethal effects of crosslink damage overwhelm the cellular repair capacity, monoadduct damaged plasmids induced higher levels of transformants. Dose responses have been observed in other systems, and have been shown to influence survival, gene conversion, and mutation levels (Averbeck and Averbeck 1978; Averbeck and Moustacchi 1979; Averbeck 1985).

Conventional techniques used to introduce psoralen modification to DNA, both in vivo and in vitro, produce modification at random sites throughout the genome and/or plasmid substrates used for repair studies. The randomness of modification within the population introduces a factor, in addition to the dose response, which has prevented verification of the models of psoralen repair. Random damage decreases the level of survival in the population and effects observable recombination levels when a particular gene is the focus of the study.

Analysis of the repair products resulting from substrates carrying a site specifically placed psoralen monoadduct, crosslink, and double strand break should provide the evidence needed to validate the models of psoralen repair. We have synthesized analogous repair substrates that contain a single damaging lesion (crosslink, monoadduct, or double strand break) at the same position to compare repair, recombination, and gene conversion patterns induced from each form of

damage on the molecular level. In doing so we have removed any dose-dependent response that may influence repair, recombination, and gene conversion patterns induced from psoralen modification. In this paper we present data that support the models of crosslink and monoadduct repair, but also provide evidence that there exist differences between repair induced by a single psoralen crosslink and repair induced by a single double strand break. These differences imply that the recombination intermediate of crosslink damage is not identical to the recombination intermediate of double strand break damage as the model predicts.

Properties and trends of crosslink and double strand break repair and recombination that support the model of crosslink repair:

By comparing the repair products of each form of damage, we have detected various properties and trends of repair, recombination, and gene conversion that are similar between crosslink and double strand break repair. Collectively, these trends suggest that similarities exist between the repair intermediates of the two forms of damage, which supports the model of psoralen crosslink repair. The trends and properties that support the model of crosslink repair are discussed below.

The toxicity of a single psoralen crosslink lesion is 2-3 times the toxicity of a single monoadduct lesion and a double strand break:

At equal doses of irradiation, equimolar concentrations of mono- and bi-functional psoralens produce different levels of lethality, and different levels of

mutagenic and recombinogenic effect in both diploid and haploid systems (Averbeck and Moustacchi 1979; Averbeck *et al.*, 1981). However, differences in the levels of adduct formation, depending on the specific psoralen derivative, creates a dose response which is partially responsible for the observed differences. Plots of genetic data versus the number of induced lesions have shown that bifunctional psoralens produce higher toxic, and genotoxic effects compared to monofunctional psoralens at equal numbers of adducts (Averbeck 1985). We have previously observed similar results in a plasmid x chromosome system (Saffran et al., 1994). The LD_{10} 3-CPs/LD_{10} 8-MOP has been reported as 2.5, indicating that the toxicity of psoralen crosslink damage is 2.5 times higher than psoralen monoadduct damage (Henriques and Moustacchi 1980)

In the present study, the repair of a double strand break and a single psoralen monoadduct resulted in different levels of colonies acquiring tryptophan prototrophy, indicating a difference in the toxicity for these two forms of damage. The repair of a single psoralen crosslink was substaintially lower, showing toxicity levels 2- 3 times higher than either a DSB or a monoadduct. The toxicity level of the single crosslink and monoadduct lesion observed in this system is in agreement with the LD_{10} ratio reported by Henriques and Moustacchi.

The model for the repair of psoralen crosslinks proposes that both the nucleotide excision repair pathway and the recombinational repair pathway are required in a sequential order to repair crosslink damage. Crosslinks are excised to produce a double strand break intermediate, which is then a substrate for the

recombinational repair pathway. We have observed that the repair efficiency of a psoralen crosslink is about 3 times lower than either a double strand break or a single psoralen monoadduct. This is in agreement with the model of crosslink repair. The model predicts that a single crosslink lesion will be repaired less efficiently than a double strand break or a monoadduct since two pathways are required to repair crosslink damage. The repair efficiency of a single psoralen crosslink may be lower than either a single monoadduct or double strand break since two independent pathways mediate the repair of this form of damage.

Crossover Recombination levels indicate a similarity between the recombinogenic intermediate of crosslink and double strand break damage:

The model for psoralen crosslink repair proposes that the recombinogenic intermediate for this form of damage is the double strand break intermediate produced by NER-mediated excision of the crosslink (Jachymczyk et al., 1981). In addition, the model predicts similarities between crosslink induced recombination and double strand break induced recombination since the recombination intermediate of crosslink repair is equivalent to a double strand break. We have compared levels of crossover recombination induced by both forms of damage and have found them to be statistically similar although double strand break induction is slightly higher (table 7).

The similarity of the recombination outcome induced by a single psoralen crosslink and a double strand break is in agreement with the model of crosslink

repair, and suggests that the recombinogenic intermediate of crosslink repair is equivalent to a double strand break.

While both crosslink damage and double strand break damage induced crossover recombination to a similar degree, monoadduct damage did not induce crossover recombination to an appreciable level. The repair intermediate from a single monoadduct-damaging lesion, the single strand gap, is shown here to be ineffective at inducing recombination in comparison to both crosslink and double strand break repair intermediates.

The recombinogenic nature of monoadduct damage has been documented (Averbeck and Moustacchi 1979; Averbeck *et al.*, 1981; Cassier *et al.*, 1984; Saffran *et al.* 1994). However, the results of these studies have shown that induced recombination from monoadduct damage is dose-dependent. It has also been documented that double strand breaks have been observed in intermediates of monoadduct repair (Dardalhon and Averbeck, 1995). The double strand breaks, however, have been observed only at high levels of adduct modification. It has been suggested that the accumulation of double strand breaks from monoadduct damage occurs due to overlapping excision of monoadducts on opposite strands and accounts for the recombinogenic nature of monoadduct damage.

Monoadduct repair is not affected by mutations in a number of the *RAD52* epistasis group genes, indicating that the recombinational repair pathway is not a

TABLE 7

Statistical comparison of crossover recombination levels for all recombination classes induced from crosslink damage (XL) and double strand break damage (DSB).

	his3-622X substrate			*his3-75X* substrate		
Strain	XL	DSB	P(χ^2)	XL	DSB	P(χ^2)
his3(75X)	51 (41.8)	102 (51.0)	.109	N.D.	N.D.	N.D.
his3(207X)	35 (53.0)	115 (57.5)	.526	93 (45.6)	87 (43.5)	.673
his3(304X)	33 (35.5)	103 (51.5)	.011	109 (51.7)	120 (60.0)	.089
his3(622X)	N.D.	N.D.	N.D.	70 (32.4)	69 (34.5)	.651

Chi-square analysis comparing psoralen and double strand induced crossover recombination for each combination. The number of crossover products for each combination is shown and the corresponding percentage out of the total repair products is shown in parentheses.

requirement for efficient repair of monoadduct damage (Henriques and Moustacchi, 1980). Our results show that the damage from a single psoralen monoadduct lesion is non-recombinogenic. The inability of a monoadduct lesion to induce recombination is consistent with the model of monoadduct repair.

Gene conversion is predominantly in the chromosome to plasmid direction for both forms of damage:

The undamaged DNA molecule has been observed to act as the primary donor of genetic information during gene conversion events in both double strand break-induced recombination systems and meiotic recombination systems (Detloff et al 1991; Sweetser et al 1994; Nelson et al 1996). It is not known how the damaged and undamaged strands are distinguished during gene conversion but it appears to be a common trend for gene conversion events induced by double strand breaks. It has been suggested that a tag exists which allows the cell to distinguish the donor and recipient molecules during conversion events (Nelson et al 1996). The tag for double strand break repair has been proposed to be the broken end(s) targeting the invading strands and designating the broken DNA molecule as the recipient. The identity of donating strand is influenced by the conversion event. If gene conversion occurs by repair synthesis of gaps produced from resectioning, the undamaged strand will act as the sole donor of genetic information. If gene conversion occurs by mismatch repair of heterduplex DNA prior to strand cutting for resolution (early MMR) the broken ends represent entry

points for the MMR machinery and again the undamaged strand will act as the sole donor of genetic information. Once resolution of the heteroduplex structure is initiated the undamaged strands contain nicks which can act as entry points for the MMR machinery (late MMR) (figure 4). The damaged strand will act as donor of genetic information if mismatch repair initiates at these entry points.

For the products analyzed in this study, the direction in which genetic information is transferred during gene conversion events occurs predominantly from the undamaged chromosome DNA molecule to the damaged plasmid molecule (table 8). This trend has been observed for both crossover and non-crossover products and is consistent for both crosslink and double strand break induced gene conversion. The high level at which the undamaged chromosome acts as the donor of genetic information is nearly identical for double strand break and crosslink damage and suggests that late MMR occurs only at a low level during damaged induced gene conversion.

Crosslinks and double strand breaks induce similar levels of uni- and bidirection conversion tracts:

In plasmid x chromosome recombination systems where gene conversion was induced by double strand break formation at an HO site carried on the plasmid, conversion tracts were predominantly unidirectional (Sweetser et al. 1994; Nelson et al., 1996). When DBS-induced gene conversion was compared between a plasmid x chromosome system and gene conversion between

TABLE 8

Percent of gene conversions in the chromosome-to-plasmid direction during damage induced recombination.

A

Damage	n	Chromosome-to-plasmid conversions	$P(\chi^2)$
Crosslink	21	20 (95.2)	
DSB	114	108 (94.7)	0.924

B

Damage	n	Chromosome-to-plasmid conversions	$P(\chi^2)$
Crosslink	157	146 (93.0)	
DSB	231	214 (92.6)	0.895

Overall percent of chromosome-to-plasmid gene conversion out of total gene conversion events. The number and percent of chromosome-to-plasmid conversions is shown for each damage form. Chi-square analysis was used to compare the results of both forms of damage. **A.** Type I non-crossover products. The total number of gene conversions producing His^+ was determined by genetic analysis. The stability of the His^+ phenotype was determined in correlation with the stability of the Trp^+ phenotype to indicate the recipient molecule in the gene conversion. **B.** The recipient DNA molecule during gene conversion was determined by Southern hybridization analysis for crosslink induced and double strand break (DSB) induced crossover recombination products.

chromosomal borne direct repeats, bidirectional conversion tracts occurred twice as often in the direct repeats than in the plasmid system (Cho et al., 1998). Chromosome environment was proposed to influence tract directionality.

We have observed that in the non-crossover repair products, gene conversion tracts are predominately unidirectional when induced from either a psoralen crosslink or a double strand break. The level of bi-directional conversion tracts in the crossover products are approximately doubled compared to the level observed for non-crossover products for both crosslink and double strand break induced gene conversion. However, unidirectional tracts are still the predominant types of conversion tracts observed. The percent of bi-directional conversion tracts observed in both crossover and non-crossover products is shown in table 9.

Conversion tract length is not limiting within the marker region for either form of damage:

Gene conversion tract structures have been studied in DSB-induced systems. In plasmid x chromosome crosses between *ura3* heteroalleles carrying silent RFLP markers at 100 bp. intervals, conversion tract lengths (and therefore hDNA formation) were shown to be limiting (Sweetser *et al.*, 1994; Weng *et al.*, 1996). RFLP marker conversion decreased with increasing distance from the damage site.

We have tested gene conversion tracts induced from crosslink damage to determine if hDNA formation is limiting and whether the inducing damage influences tract lengths. Gene conversion was measured at 100 base intervals by

TABLE 9

Overall level of bi-directional conversion tracts in Type I and Type II arrangements.

Damage	Non-crossover Products	Crossover Products
Crosslinks	14/115 (12.2%)	43/154 (27.9%)
DSB	32/228 (14.0%)	85/325 (26.2%)

Percent of bi-directional conversion tracts from total gene conversion events.

comparing conversion levels in the Type I series. Only a marginal decrease in the level of gene conversion occurred as the distance of the chromosomal marker from the damage site increased. Statistically the levels of gene conversion at the different distances are the same (table 10). This was observed for both crosslink induced and double strand break induced gene conversions leading to both His^+ and His^- colonies and implies that hDNA formation is not limiting over the 300 bp. span studied. The level of gene conversion in the Type II combination was similar to the levels observed for the Type I combinations. In the Type II combination, the distances of the conversion tracts are comparable to the longest tracts of the Type I arrangement. Gene conversion levels in the Type III combinations, however, were markedly different. When the *his3-75X* substrate is in combination with the *his3-304X* strain, the chromosomal and plasmid markers are separated by 219 bp. and are on the same side of the damage site. Gene conversion levels were observed to decline in this combination. The decline in gene conversion levels was more pronounced when the *his3-75X* substrate was in combination with the *his3-207X* strain, where the marker separation was only 132 bp.

The decline in conversion levels in the Type III combinations may be due to heteroduplex rejection (Alani et al., 1994) brought about by an increase in local non-homology as the markers approach on another. Mismatches in heteroduplex DNA has been reported to cause rejection. Heteroduplex rejection may be responsible for the conversion tract gradient observed by Sweetser et al., and

TABLE 10

Statistical analysis of gene conversion levels at 100 base pair intervals.

A. *his3-622X* crosslink damage substrate

Conversion Product	*his3-304X* (112 bp.)	*his3-207X* (209 bp.)	*His3-75X* (341 bp.)	P
His^-	22 (36.6)	10 (32.3)	21 (29.6)	0.688
His^+	12 (16.9)	4 (12.9)	4 (6.7)	0.206

B. *his3-622X* DSB damage substrate

Conversion Product	*his3-304X* (112 bp.)	*his3-207X* (209 bp.)	*His3-75X* (341 bp.)	P
His^-	18 (18.4)	22 (25.9)	24 (24.7)	0.415
His^+	45 (45.9)	24 (28.2)	39 (40.2)	0.046

Weng et al. As the silent RFLP's are incorporated into hDNA, the number of mismatches increases in the heteroduplex structure. If this stimulates rejection then a bias against longer conversion tracts, which produce a higher number of mismatches, is created. This would give rise to a conversion tract gradient.

In our system, conversion tracts in the Type I and Type II combinations proceed through a span of identical homology until the marker is encountered. There is no statistical difference between the levels of conversion tracts reaching each marker, for the combinations of the series. Conversion tracts (and hDNA formation) are not limiting through the span of identical homology.

Distinctions between crosslink induced repair and double strand break repair:

We have presented evidence that establishes common trends between crosslink and double strand break repair. The evidence suggests that there exist common physical and mechanistic properties between the repair intermediates of crosslink and DSB damage. The model of crosslink repair proposes that gene conversion trends should be similar between the two forms of damage since the repair intermediate of crosslink damage is a double strand break. The results presented thus far are all consistent with this model.

However, certain aspects of crosslink and double strand break induced repair that we have observed, exhibit different outcomes and suggest that physical and mechanistic properties between both the actual damage and the repair intermediates of the two forms of damage are different.

The physical analysis has detected 2 major factors that contribute to the differences in gene conversion levels and patterns obtained from crosslink and double strand break induced gene conversion.

1) Psoralen crosslinks, in addition to processing by the error free pathways of NER and recombination, are substrates for the mutagenic repair pathway while double strand break damage is only a substrate for the error free recombinational pathway.
2) The polarity of the conversion tracts induced from double strand break and crosslink damage occur in opposite directions, indicating a possible physical or mechanistic difference between the recombinational intermediates of double strand break and crosslink damage.

The significance and effects of these two factors on the model of crosslink repair is addressed below.

Gene Conversion levels suggest a difference between the recombination intermediates:

Since gene conversion events occur as the result of recombination it is expected that the gene conversion patterns induced by the two forms of damage during both crossover and non-crossover events should be similar, if the recombinogenic intermediates are similar. We have compared the overall gene conversion levels induced from both forms of damage for crossover and non-crossover repair products and have found a difference between crosslink and

double strand break induced gene conversion levels. The overall gene conversion levels are shown in table 11.

The frequency of gene conversion observed in the non-crossover repair products induced by double strand breaks is higher than the frequency of gene conversion induced by psoralen crosslinks. However, in the crossover recombination products, there is no significant difference in the overall levels of gene conversion. The difference in gene conversion levels during repair events leading to non-crossover products suggests that either the repair intermediates differ with respect to their capability of forming or sustaining hDNA, or a difference between the damaged substrates with respect to their ability to enter the recombination pathway exists. It is not a necessity that all extra-chromosomal repair products result from the homologous recombinational repair pathway. Repair mediated by the error-prone pathways can result in non-crossover products. Crossover products, however, arise only by the recombination pathway. Since the gene conversion levels observed for the crossover products, which have been exclusively mediated by the recombination pathway, are similar, the ability of each repair intermediate to induce gene conversion must be similar. The difference in conversion levels for non-crossover products is likely due to differences in the number of substrate molecules entering the recombination pathway. Non-homologous end joining may play a role in this observed difference.

TABLE 11

Statistical comparison of overall gene conversion levels for all recombination classes induce from crosslink damage (XL) and double strand break damage (DSB).

A

	his3-622X substrate			*his3-75X* substrate		
Strain	XL	DSB	$P\chi^2$	XL	DSB	$P\chi^2$
his3(75X)	31 (43.6)	63 (64.3)	.008	N.D.	N.D.	N.D.
his3(207X)	14 (45.2)	45 (52.9)	.458	1 (1.2)	16 (14.2)	.006
his3(304X)	19 (31.7)	61 (62.9)	.0001	10 (27.0)	7 (20.0)	.483
his3(622X)	N.D.	N.D.	N.D.	46 (31.5)	56 (42.7)	.053

B

	his3-622X substrate			*his3-75X* substrate		
Strain	XL	DSB	$P\chi^2$	XL	DSB	$P\chi^2$
his3(75X)	33 (71.7)	45 (66.1)	.531	N.D.	N.D.	N.D.
his3(207X)	15 (75.0)	43 (84.3)	.361	18 (66.7)	35 (76.1)	.384
his3(304X)	20 (83.3)	47 (82.5)	.924	40 (70.1)	20 (55.5)	.152
his3(622X)	N.D.	N.D.	N.D.	20 (43.5)	23 (52.3)	.404

Statistical comparison of overall gene conversion levels for non-crossover (A) and crossover (B) repair products. His^+ and His^- products were classified by physical analysis. **A.** The results of the physical analysis were combined with results of the genetic analysis and conversions to both His^+ and His^- were combined to achieve the overall levels of gene conversion. **B.** The results of the physical analysis were used directly in the statistical analysis.

Error-free and error-prone repair pathways compete for psoralen crosslink damage, which is mutagenic:

Physical analysis of the non-crossover products has revealed that a single psoralen crosslink is capable of inducing mutations resulting in both transitions and transversions of the modified bases in the *BsiW*I site of the plasmid borne *his3* allele. Further analysis of the products containing mutations at the *BsiW*I site has shown that all repair products undergoing mutagenic repair of the crosslink have retained the original *Xba*I marker and *his3* sequence. No evidence of gene conversion has been detected for substrates that have entered the mutagenic pathway. Mutations were not detected at the *BsiW*I site of the non-crossover repair products of double strand break damaged substrates.

The observed mutation level does not equal the difference in conversion levels between double strand break and crosslink damage, but it does account for a portion of the difference. The lack of gene conversion in products carrying mutations at the *BsiW*I site indicates that they have not entered the recombinogenic pathway but rather have been shunted into the mutagenic pathway. Some of the substrates that enter the mutagenic repair pathway are repaired correctly with an intact *BsiW*I site. These products escaped detection entirely and may account for the remaining difference observed in the levels of gene conversion since all products of the mutagenic pathway were detected as non-crossover recombination products without gene conversion by the genetic

analysis. This lowers the observed level of non-crossover gene conversion induced from crosslink damage.

The repair products of double strand break damage do not exhibit induced mutations. The mutagenic nature of the psoralen crosslink therefore originates from the psoralen molecule itself, prior to excision. In a *rad4* strain the level of induced mutations at the *BsiWI* site of the crosslink modified substrate increased about 3 fold (Sandra Thomas, personal communication). The increase in mutation level suggests that the NER and the mutational pathway compete for the crosslink substrate. If the mutagenic capacity of the crosslink damage arose due to NER processing a decrease of the mutation level would occur in the absence of NER. In the absence of NER, more substrate is available for entrance into the mutagenic pathway.

PCR analysis of the crossover recombination products from crosslink damage did not detect mutations at the *BsiWI* site of the *his3* alleles. Crossover products arise from the sequential processing by the error free pathways of NER and recombination. Plasmid integration occurs only as the result of the recombinational repair pathway. Since all crossover products must have entered the recombinational repair pathway we would not expect mutations in these products if the mutagenic pathway competes for substrate with the error free pathways. We have observed that non-integrated repair products, which have entered the mutagenic pathway, do not show gene conversion as these plasmids are not substrates of the recombinational pathway and therefore do not result in -

*gene conversion events. The absence of mutations in both crossover products from crosslink damage and the non-crossover products of double strand break damage, and the increased level of mutation from crosslink damage in an NER deficient strain imply that the error free and error prone pathways of crosslink repair are divergent prior to NER and compete for psoralen crosslink substrate.

The model for psoralen crosslink repair, based on our experimental data, incorporates the mutagenic nature of a single crosslink and the competition of the error-free and error-prone pathways for damaged substrates during the preliminary step(s) of the repair process prior to crosslink excision. The model is shown in figure 30.

The mutagenic nature of a single psoralen crosslink is a clear distinction between the physical nature of the damage produced from a psoralen crosslink lesion compared to an enzymatically produced double strand break. Chemical modification of DNA, such as a psoralen crosslink, is an unnatural condition and the induction of a mutagenic response to such damage represents one link to the pathogenic response induced by psoralen as well as other chemical carcinogens. In yeast, enzymatically produced double strand breaks represent a natural occurrence, at least during mating type switching where double strand break formation occurs by the HO endonuclease. However, double strand breaks produced by ionizing radiation, are associated with base damage and are mutagenic. Base damage does not occur from the enzymatic cleavage of DNA, which accounts for the absence of a mutagenic response to this form of double strand break damage.

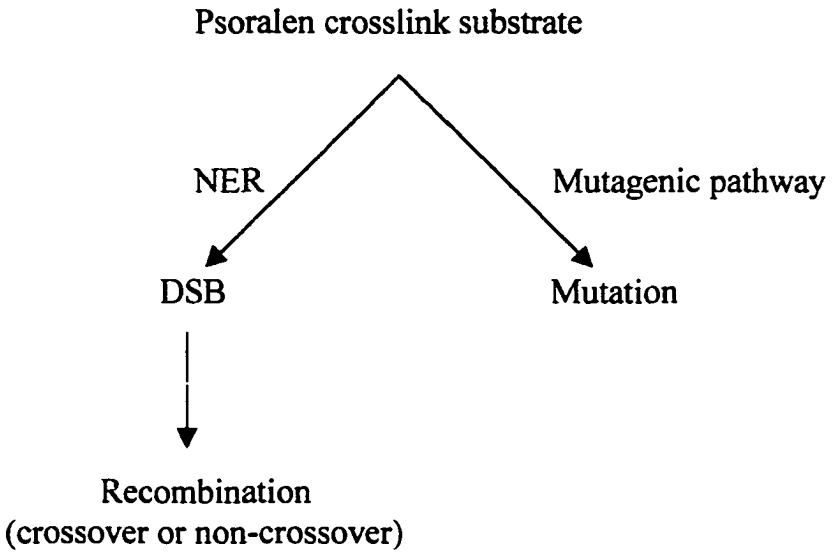

Figure 30. **General model for psoralen crosslink induced repair including mutagenic branch.**

The directional polarity of gene conversion tracts is the major distinction between recombination induced by repair intermediates of crosslink and double strand break damage:

We have observed a difference in the generation of His phenotype when the colonies arising from crosslink and double strand break damaged substrates carrying identical frameshift mutations are compared in the same strain. This appears to be the major difference with respect to gene conversion induced from both forms of damage and it suggests that there is a physical and/or mechanistic difference between the recombinogenic intermediates generated during repair of crosslink and double strand break damaged substrates. The genetic analysis of the Type I combinations has shown that repair events yielding a His^+ phenotype predominate the induced gene conversion events when the substrate carries a double strand break. The level of conversion leading to His^+ colonies was higher than the level of conversion leading to His^- colonies for double strand break substrates and was higher than the level of conversion leading to His^+ for crosslink damaged substrates. In contrast, the prevailing gene conversion events induced when substrates carry crosslink damage, in identical combinations of strain and substrate, lead to generation of His^- colonies. The level of conversion leading to His^- colonies was higher than the level of conversion leading to His^+ colonies for crosslink-damaged substrates and was higher than the level of conversion leading to His^- for double strand break damaged substrates. This trend is consistent in all

Type I combinations and has been observed in both the crossover and non-crossover products (table 12).

In the Type I combinations His^+ colonies arise from unidirectional conversion tracts extending downstream from the damage site. This is due to the arrangement of the markers in these combinations. The difference in phenotype generation suggests that conversion tracts exhibit a directional polarity, the direction of which depends on the form of the inducing damage.

Through physical analysis of the non-crossover products we have shown that the difference in gene conversion outcome occurs due to a polarity in the direction of unidirectional conversion tracts. The results show that unidirectional gene conversion tracts induced from double strand break damage preferentially extend downstream from the damage site while unidirectional conversion tracts induced from crosslink damage preferentially extend upstream from the damage site (table 13a). Physical analysis of the crossover products of Type I combinations shows that unidirectional gene conversion tracts exhibit the same directional polarity as seen in the non-crossover products (table 13b).

The directional polarity of conversion tracts is directly related to the inducing damage. In the Type II combination the marker orientation is reversed. Unidirectional conversion tracts extending downstream from the damage site will yield His^- colonies while unidirectional tracts extending upstream from the damage site will yield His^+ colonies. The observed trend of His phenotype generation is reversed in the Type II arrangement compared to the Type I

TABLE 12

Statistical comparison of His phenotype generation during Type I recombination induced from psoralen crosslink and double strand break damage.

A

	Crosslink damage			Double strand break damage			
Strain	n	His^+ unstable	His^- unstable	n	His^+ unstable	His^- unstable	$P(\chi^2)$
His3(75X)	71	12 (16.9)	21 (**29.6**)	98	45 (**45.9**)	18 (18.4)	.0009
His3(207X)	31	4 (12.9)	10 (**32.3**)	85	24 (**28.2**)	22 (25.9)	.1211
His3(304X)	60	4 (6.7)	22 (**36.6**)	97	39 (**40.2**)	24 (24.7)	.0001

B

	Crosslink damage			Double strand break damage			
Strain	n	His^+ stable	His^- stable	n	His^+ stable	His^- unstable	$P(\chi^2)$
His3(75X)	51	16 (31.4)	35 (**68.6**)	102	57 (**55.9**)	45 (44.1)	.0042
His3(207X)	35	12 (34.3)	23 (**65.7**)	115	71 (**61.7**)	44 (38.3)	.0042
His3(304X)	33	6 (18.2)	27 (**81.8**)	103	45 (**43.8**)	58 (56.3)	.0084

C

	Crosslink damage			Double strand break damage			
Product	n	T+H+	T+H-	n	T+H+	T+H-	$P(\chi^2)$
Non-crossover	162	20 (12.3)	53 (**32.7**)	280	108 (**36.8**)	64 (22.8)	<.0001
Crossover	119	34 (28.6)	85 (**71.4**)	320	173 (**54.1**)	147 (45.9)	<.0001

A: Chi-square comparison of His phenotype generation in each strain during Type I damage-induced non-crossover recombination. The number and percent of each product is shown for crosslink and double strand break-induced recombination. **B:** Chi-square comparison of crossover recombination products. **C:** Combined results indicating a significant bias for His^- generation from crosslink damage and a significant bias for His^+ generation from double strand break damage.

TABLE 13

Comparison by physical analysis of conversion tract direction during Type I recombination induced from crosslink and double strand break damage.

A

	Crosslink damage		Double strand break damage	
Strain	Conversion Upstream	Conversion Downstream	Conversion Upstream	Conversion Downstream
His3(75X)	**17.8%**	16.9%	7.8%	**45.9%**
His3(207X)	**25.8%**	12.9%	14.6%	**28.2%**
His3(304X)	**18.3%**	8.7%	13.3%	**40.2%**

B

	Crosslink damage		Double strand break damage	
Strain	Conversion Upstream	Conversion Downstream	Conversion Upstream	Conversion Downstream
His3(75X)	**35.4%**	12.6%	6.3%	**34.9%**
His3(207X)	**14.6%**	11.2%	18.7%	**48.0%**
His3(304X)	**25.8%**	9.1%	18.2%	**37.2%**

A: Percent of upstream and downstream conversion tracts determined from physical analysis of non-crossover products by plasmid rescue and restriction mapping. Polarity of conversion tract direction accounts for the observed preference in His phenotype generation. **B:** Percent of upstream and downstream conversion tracts determined from physical analysis of crossover products by Southern hybridization analysis.

arrangements (table 14a). The frequency of His^+ colonies generated during crosslink-induced repair (for both the non-crossover and crossover products) is higher than the frequency of His^+ colonies generated during double strand break-induced repair. Physical analysis of both the crossover and non-crossover products shows that conversion tracts preferentially extend upstream from the damage site when induced from a psoralen crosslink and downstream when induced from a double strand break (table 14b). The directions of the observed polarities in the Type II combination are the same as the polarities observed in Type I combinations.

Polarity of gene conversion tracts has been observed in a number of double strand break-induced recombination systems (Priebe et al 1994, Nelson et al. 1996, Ferguson and Holloman 1996, Weng and Nicoloff 1997). Nelson et al observed high polarity of the unidirectional conversion tracts in an HO-induced *URA3* recombination system containing silent RFLP markers spaced at 100 base intervals, where the terminal ends produced by HO endonuclease cleavage contained non-homology to the intact homolog. When the degree of homeology in the sequences flanking the terminal non-homology was increased, the level of bi-directional conversion tracts increased. However, when substrates contained only terminal homeology, conversion tracts again were highly polar and unidirectional. One-ended invasion coupled with mismatch repair and/or precise Rad1/10 cleavage at homology/non-homology borders was proposed to explain the high directionality of conversion tracts in this system. Differential end processing by

TABLE 14

Statistical comparison of His phenotype generation during Type II recombination induced from psoralen crosslink and double strand break damage.

A

	Crosslink damage			Double strand break damage			
Product	n	T+H+	T+H-	n	T+H+	T+H-	$P(\chi^2)$
Non-crossover	146	31 (**21.2**)	115 (78.8)	131	10 (7.6)	121 (**92.4**)	.0015
Crossover	70	47 (**67.1**)	23 (32.9)	69	32 (46.4)	37 (**53.6**)	.0135

B

	Crosslink damage		Double strand break damage	
Product	Conversion Upstream	Conversion Downstream	Conversion Upstream	Conversion Downstream
Non-crossover	**28.0%**	0	7.6%	**31.9%**
Crossover	**41.3%**	9.4%	20.1%	**44.3%**

A: Chi-square comparison of His phenotype generation for crossover and non-crossover products of the Type II arrangement. Pattern is the reverse of the Type I arrangements.

B: Percent of upstream and downstream conversion tracts determined from the physical analysis.

MMR and/or Rad1/10 endonuclease activity due to the degree of homology/homeology at the terminal ends accounted for the formation of uni- and bi-directional tracts and for the observed polarity.

In our system, polarity of conversion tracts has been observed for both double strand break induced conversion and psoralen crosslink induced conversion. However, the polarities for double strand break induced gene conversion and crosslink-induced gene conversion are in opposite directions. Since gene conversion initiates from the same site in the respective substrates, neither sequence effects nor chromosomal environment could give rise to the different polarities, as these factors are identical for both substrates. In addition, the terminal ends of the recombination intermediates, independent of the inducing damage, have complete homology with the intact homolog. Therefore, the invading end or ends are not subject to MMR and/or Rad1/Rad10 cleavage. Also, the total homology of the terminal ends relieves any pressure against two-ended invasion. If differential end processing gives rise to the opposite polarities of conversion tracts in these experiments, it is not due to sequence differences at the terminal ends of the repair intermediates as reported by Weng *et al.* (1997). The difference in tract direction cannot be the result of chromosomal environment as reported by Averbeck *et al.* (1985) since the location of the damage and the nature of the homolog are identical during repair of both forms of damage. We believe that structural differences and/or mechanistic differences due to the processing or

formation of the recombination intermediates may account for the differential end processing leading to the opposite polarities.

There is evidence that the structural asymmetry of bi-functional psoralen molecules gives rise to differential processing by the nucleotide excision repair machinery of humans (Kumaresan *et al.*, 1995). Incisions were detected on both the 3' and 5' sides of a lesion when DNA substrates carrying either a furan side TMP monoadduct, a pyrone side TMP monoadduct, or a TMP crosslink were treated with human chromatin-associated protein extracts. Incision on the 3' side of both the furan side and pyrone side adducts was similar, occurring at either the 4^{th} or 5^{th} phosphodiester bond from the adducted thymine. However, the incision on the 5' side of the adducted thymine depended on the type of adduct present. The 5' incision occurred at the 5^{th} or 6^{th} phosphodiester bond at sites of a furan side adduct but occurred at the 13^{th} or 14^{th} phosphodiester bond at sites of a pyrone side adduct.

The structural asymmetry of the psoralen molecule has also been implicated as the cause of differential processing and repair in *S. cerevisiae* (Barre *et al.*, 1999). Using triple-helix-forming oligonucleotides to deliver a site specific and end oriented psoralen crosslink to a plasmid borne *URA3* gene it was shown that the mutational frequency and spectra depended on the orientation of the crosslink with respect to the transcribed strand. Bypass of pyrone side adducted thymine yielded T→A or T→C substitutions and A insertions while bypass of furan side adducted thymine yielded T→G substitutions or G insertions. The results suggest

that the cell repair machinery recognize psoralen crosslinks in an asymmetric manner, where the furan side of a lesion is excised more easily than the pyrone side. It has been speculated that the preference of incisions arises due to the geometry of the distortion produced at the site of a crosslink in conjunction with the geometry of the NER machinery.

It is possible that the orientation of the asymmetric psoralen molecule gives rise to differential end processing which in turn gives rise to the polarity of gene conversion tracts observed in our system. Our substrates have been synthesized to exclusively contain a crosslink where the furan side of the adduct is on the sense strand and the pyrone side of the adduct is on the transcribed strand. To test whether the orientation of the psoralen crosslink is involved in the observed polarity the experiments can be repeated using substrates containing the crosslink in the reverse orientation. By synthesizing repair substrates using 14-mer non-sense strand primers carrying MAF adducts and sense strand phagemids to direct second strand synthesis, the trends of repair and recombination obtained with these substrates can be compared to our results presented here. If the orientation of the psoralen crosslink affects conversion tract direction, the polarity should be reversed.

Determining the physical structure of NER-mediated repair intermediates from psoralen damaged substrates may provide evidence of the nature of the directional polarity of psoralen induced gene conversion. Treating substrates carrying psoralen crosslinks in both orientations with the components of NER

shown to reconstitute in vitro bimodal incision (Gudzer et al., 1995) will allow the structures of these intermediates to be isolated and studied. Conversion tract polarity may arise if incision position is dependent on the orientation of the adduct, as observed with a reconstituted, in vitro, NER system prepared from human cell extracts.

The *PSO* genes are involved during psoralen crosslink repair (review Friedberg *et al.*, 1988, 1995) but the role of these genes in the repair of psoralen damage has not been determined. A *pso2* mutant, which was shown to be proficient in the preferential incision of a psoralen crosslink at the MATα locus versus the HMLα locus, lacked the ability to perform complete repair of the damage (Meniel *et al.*, 1995). This suggests an intermediary role of the *PSO2* gene product acting between NER and recombination. One possible role for this gene product, and other *PSO* gene products, may be processing of the NER product into a recombination intermediate. End processing directed by the *PSO* genes, along with the Rad1/Rad10 complex may lead to the directional preference of gene conversion tracts.

The effects of the *PSO* genes on the repair and gene conversion trends observed from psoralen crosslink induced repair can be addressed by analyzing the structure of psoralen crosslink substrates treated with in vitro excision systems prepared from cell extracts from wildtype and strains carrying mutations of the *PSO* genes. Using substrates that carry the crosslink in both orientations will explore the effects of the structural asymmetry of the molecule in conjunction with

the role of NER and the *PSO* gene products. If complete excision can be reconstituted in vitro, the structure of the intermediates can be determined and compared. Transformation of the purified intermediates into wildtype and *PSO* mutant strains will link the structure of the intermediate to the trends and patterns of gene conversion.

Finally, differential end processing may arise from the consistent release of a specific end from the nucleotide excision machinery due to the mechanism of excision itself. The processing machinery may act upon this end while the NER machinery is still associated with the other end, thereby producing end blocking. The release of a specific end from the NER machinery may be related to the orientation of the psoralen crosslink, as the orientation of the crosslink may be responsible for the order of incisions. Members of the *PSO* genes may also play a role in this process.

End blocking leading to differential end processing may also arise from the transcription machinery as well. The activity of the nucleotide excision repair pathway is coupled to transcription (Friedberg *et al.*, 1995) and a stalled RNA polymerase is believed to be involved during the signaling of DNA damage requiring the NER pathway. The association of components of the transcription machinery with DNA undergoing NER could lead to end blocking. End labeling reactions on substrates during in vitro NER can distinguish ends of the recombination intermediate if end blocking occurs during NER.

In summary, we have compared repair, recombination, and gene conversion induced from a site-specifically placed psoralen crosslink, psoralen monoadduct, and double strand break on the molecular level. We have shown that a psoralen monoadduct and a double strand breaks induce similar levels of repair, and therefore have a similar level of toxicity. A psoralen crosslink is less efficiently repaired, indicating a higher level of toxicity for this form of damage, measured nearly 3 times the toxic level of a DBS. However, a psoralen crosslink and a double strand break induce similar levels of recombination and gene conversion, while a single monoadduct was an ineffective at inducing either event.

Recombination and gene conversion induce from both a psoralen crosslink and a double strand break has been shown to produce similar trends, which suggest that similarities exist between the repair intermediates of these forms of damage. The repair intermediate of a single psoralen monoadduct was shown to be non-recombinogenic, and is therefore distinct from the repair intermediates of crosslink and DSB damage. These finding are in support of the models of both psoralen crosslink and monoadduct repair.

Two major differences between psoralen crosslink and double strand break induced repair have been detected. Psoralen crosslinks have been shown to induce the mutagenic repair pathway in addition to the error free pathways of nucleotide excision repair and recombinational repair. The mutagenic capacity of psoralen damage has been shown to be the psoralen molecule itself, rather than the

intermediate produced by the excision of the adduct. Mutations were not induced from double strand break damage.

Although the levels of recombination and overall gene conversion were similar for both crosslink and double strand break induced repair, gene conversion tracts induced from these forms of damage exhibited a directional polarity in opposite directions. Tracts induced from psoralen crosslinks preferentially extended upstream from the damage site while tracts induced from double strand breaks preferentially extended downstream from the damage site. This phenomenon was independent of the marker arrangements. The difference in conversion tract polarity indicates that the repair intermediate of psoralen crosslink repair is distinct from the repair intermediate of double strand break repair. The results suggest that conversion tract polarity, in part, arise from either a structural aspect of the specific recombination intermediate or from a mechanistic difference in the processing of a repair substrate into a recombination intermediate which is linked to the form of damage initiating the conversion.

Bibliography

Alani E., R. Thresher, J.D. Griffith, and R.D. Kolodner 1992. Characterization of DNA-binding and strand exchange stimulation properties of y-RPA, a yeast single-strand-DNA-binding protein. *J. Mol. Biol.* 227:54-71

Alani E., R. A. Reenan, and R.D. Kolodner 1994. Interaction between mismatch repair and genetic recombination in *Saccharomyces cerevisiae*. *Genetics* 137:19-39

Averbeck D., 1985. Relationship between lesions photoinduced by mono- and bi-functional furocoumarins in DNA and genotoxic effects in diploid yeast. *Mutat. Res.* 151:217-233

Averbeck D., and S. Averbeck 1978. Dose-rate effects of 8-metoxypsoralen plus 365-nm irradiation on cell killing in *Saccharomyces cerevisiae*. *Mutat. Res.* 50:195-206

Averbeck D., S. Averbeck, and F. Dall'Acqua 1981. Mutagenic activity of three monofunctional and three bifunctional furocoumarins in yeast (*Saccharomyces cerevisiae*). *Farmaco* 36:492-505

Averbeck D., S. Averbeck, and E. Cundari 1987. Mutagenic and recombinogenic action of DNA monoadducts photoinduced by the bifunctional furocoumarin 8-methoxypsoralen in yeast (*Saccharomyces cerevisiae*). *Photochem. Photobiol.* 45:371-379

Averbeck D., and S. Averbeck 1998. DNA photodamage, repair, gene induction and genotoxicity following exposures to 245 nm UV and 8-methoxypsoralen plus UVA in a eukaryotic cell system. *Photochem. Photobiol.* 68:289-295

Averbeck D., E. Cundari, M. Dardalhon, F. Dall'Acqua, and D. Vedaldi 1990. Genetic effects and repair of DNA photo-adducts induced by 8-methoxypsoralen and homopsoralen (pyranocoumarin) in diploid yeast. *J. Photochem. Photobiol. B.* 5:179-195

Averbeck D., and E. Moustacchi 1975. 8-Methoxypsoralen plus 365nm light effects and repair in yeast. *Biochim. Biophys. Acta* 395:393-404

Averbeck D., and E. Moustacchi 1979. Genetic effects of 3-carbethoxypsoralen, angelicin, psoralen, and 8-methoxypsoralen plus 365-nm irradiation in *Saccharomyces cerevisiae*: induction of reversions, mitotic crossing-over, gene conversion, and cytoplasmic "petite" mutations. *Mutat. Res.* 68:133-148

Averbeck D., E. Moustacchi, and E. Bisagni 1978. Biological effects and repair of damage photoinduced by a derivative of psoralen substituted at the 3,4 reaction site. *Biochim. Biophys. Acta* 518: 464-481

Averbeck D., M. Dardalhon, N. Magana-Schwencke, L.B. Meira, V. Meniel, S. Boiteux, and E. Sage 1992. New aspects of the repair and genotoxicity of psoralen photoinduced lesions in DNA. *J. Photochem. Photobiol. B.* 14:47-63

Bankmann M., and M. Brendel 1989. UVA-induced binding of 8-methoxypsoralen to *Cells* of *Saccharomyces cerevisiae*: seperation and characterization of DNA photoadducts. *J. Photochem. Photobiol.* 3:33-52

Bankmann M., L. Prakash, and S. Prakash 1992. Yeast RAD14 and human xeroderma pigmentosum group A DNA-repair genes encode homologous proteins. *Nature* 355:555-558

Bardwell, A.J., L. Bardwell, A.E. Tomkinson, and E.C. Friedberg 1994c. Specific cleavage of model recombination and repair intermediates by the yeast Rad1-Rad10 DNA endonuclease. *Science* 265:2082-2085

Barre F.X., U. Asseline, and A. Harel-Bellan 1999. Asymmetric recognition of psoralen interstrand crosslinks by the nucleotide excision repair and the error-prone repair pathways. J. Mol. Biol. 12:1379-1387

Baynton K., A. Bresson-Roy, and R.P.P. Fuchs 1998. Analysis of damage tolerance pathways in *Saccharomyces cerevisiae*: A requirement for Rev3 DNA polymerase in translesion synthesis. *Mol. Cell. Biol.* 18:960-966

Beggs J.D. 1978. Transformation of yeast by a replicating hybrid plasmid. *Nature* 275:104-108

Bessho T., D. Mu, and A. Sancar 1997. Initiation of DNA interstrand cross-link repair in humans: the nucleotide excision repair system makes dual incisions 5' to the cross-linked base and removes a 22-to-28-nucleotide-long damage-free strand. *Mol. Cell. Biol.* 17:6822-6830

Boyer V., E Moustacchi, and E. Sage 1988. Sequence specificity in photoreaction of various psoralen derivatives with DNA: role in biological activity. *Biochemistry* 27:3011-3018

Brash D.E., J.A. Rudolph, J.A. Simon, A. Lin, G.J. McKenna, H.P. Baden, A.J. Halpern, and J. Ponten 1991. A role for sunlight in skin cancer: UV-induced p53 mutations in squamous cell carcinoma. *Proc. Natl. Acad. Sci.*. 88:10124-10128

Buratowski, S. 1994. The basics of basal transcription by RNA polymerase II. *Cell* 77:1-3

Cadet J., P. Vigny, and W.R. Midden 1990. Photoreactions of furocoumarins with biomolecules. J. Photochem. Photobiol B. 6:197-206

Cao L., E. Alani, and N. Kleckner 1990. A pathway for generation and processing of double-strand breaks during meiotic recombination in *S. cerevisiae*. *Cell* 61:1089-1101

Cassier C., R. Chanet, and E. Moustacchi 1984. Mutagenic and recombinogenic effects of DNA cross-links induced in yeast by 8-methoxypsoralen photoreaction. *Photochem. Photobiol.* 39:799-803

Cech T., and M.L. Pardue 1977. Cross-linking of DNA with trimethylpsoralen is a probe for chromatin structure. *Cell* 11:631-640

Cech T.R., and K.M. Karrer 1980. Chromatin structure of the ribosomal RNA gene of tetrahymena thermophila as analyzed by trimethylpsoralen crosslinking in vivo. J Mol Biol 136:395-416

Chanet R., C. Cassier, and E. Moustacchi 1985. Genetic control of the bypass of mono-adducts and of the repair of cross-links photoinduced by 8-methoxypsoralen in yeast. *Mutat. Res* 145:145-155

Chanet R., C. Cassier, N. Magana-Schwencke, and E. Moustacchi 1983. Fate of photo-induced 8-methoxypsoralen mono-adducts in yeast. Eviidence for bypass of these lesions in the absence of excision repair. *Mutat Res.* 112:201-204

Cheng S., B. Van Houten, H.B. Gamper, A. Sancar, and J.E. Hearst 1988. Use of psoralen-modified oligonucleotides to trap three-stranded RecA-DNA complexes and repair of these cross-linked complexes by ABC excinuclease. *J. Biol. Chem.* 263:15110-15117

Cho J.W., G.J. Khalsa, and J.A. Nickoloff 1998. Gene-conversion tract directionality is influenced by the chromosome environment. *Curr. Genet.* 34:269-279

Chomczynski P., and P.K. Qasba 1984. Alkaline transfer of DNA to plastic membrane. *Biochem. Biophys. Res. Commun.*122:340-344

Cimino G.D., H.B. Gamper, S.T. Isaacs, and J.E. Hearst 1985. Psoralens as photoactive probes of nucleic acid structure and function: Organic chemistry, Photochem.istry, and *Biochemistry. Ann Rev. Biochem.* 54:1151-1193

Cole R.S. 1971. Psoralen monoadducts and interstrand cross-links in DNA. *Biochem Biophys Acta* 254:30-39

Cole R.S. 1973. Repair of DNA containing interstrand crosslinks in Escherichia coli: sequential excision and recombination. *Proc. Natl. Acad. Sci.* USA 70:1064-1068

Conaway R.C., and J.W.Conaway 1993. General initiation factors for RNA polymerase II. *Annu. Rev. Biochem.* 62:161-190

Cox B.S., and J.M. Parry 1968. The isolation, genetics and survival characteristics of ultraviolet light sensitive mutants in yeast. *Mutat. Res* 6:37-55

Dall'Acqua F., M. Terbojevich, S. Marciani, D. Vedaldi, and M. Recher 1978. Investigation of the dark interaction between furocoumarins and DNA. *Chem. Biol. Interact.* 21:103-115

Dardalhon M ., and D. Averbeck 1995. Pulsed-field gel electrophoresis analysis of the repair of psoralen plus UVA induced DNA photoadducts in *Saccharomyces cerevisiae*. *Mutat. Res* 336:49-60

Davies A.A., E.C. Friedberg, A.E. Tomkinson, R.D. Wood, and S.C. West 1995. Role of the Rad1 and Rad10 proteins in nucleotide excision repair and recombination. *J. Biol. Chem.* 270:24638-24641

de Andrade H.H., E. Moustacchi, and J.A. Henriques 1989. The *PSO3* gene is involved in error-prone intragenic recombinational DNA repair in *Saccharomyces cerevisiae*. *Mol. Gen. Genet.* 219:75-80

DeFrascesco L., and G. Attardi 1981. In situ Photochem.ical crosslinking of HeLa cell mitochondrial DNA by a psoralen derivative reveals a protected region near the origin of replication. *Nuc. Acids. Res.* 9: 6017-6030

Detloff P., J.Sieber, and T.D. Petes 1991. Repair of specific base pair mismatches formed during meiotic recombination in the yeast *Saccharomyces cerevisiae*. *Mol. Cell. Biol.* 11:737-745

Detloff P., M.A. White, and T.D. Petes 1992. Analysis of a gene conversion gradient at the *HIS4* locus in *Saccharoymces cerevisiae*. *Genetics* 132:113-123

Feaver W.J., J.Q. Svejstrup, L. Bardwell, A.J. Bardwell, S. Buratowski, K.D. Gulyas, T.F. Donahue, E.C. Friedberg, and R.D. Kornberg 1993. Dual roles of a multiprotein complex from S. cerevisiae in transcription and DNA repair. *Cell* 75:1379-87

Fishman-Lobell J., and J.E. Haber 1992. Removal of nonhomologous DNA ends in double-strand break recombination: the role of the yeast ultraviolet repair gene RAD1. *Science* 258:480-484

Friedberg E.C. 1988. Deoxyribonucleic acid repair in the yeast *Saccharomyces cerevisiae*. *Microbiol. Rev.* 52:70-102

Friedberg E.C., G.C. Walker, and W. Siede 1995. DNA repair and mutagenesis. ASM Press, Washington D.C.

Ferguson D.O., and W.K. Holloman 1996. Recombinational repair of gaps in DNA is asymmetric in *Ustilago maydis* and can be explained by a migrating D-loop model. *Proc. Natl. Acad. Sci.* USA 93:5419-5424

Gaboriau F., P. Vigny, and J. Moron 1989. Secondary structure of DNA modified by monofunctional psoralen derivatives. *Biochemistry* 28:5801-5807

Gaboriau F., P. Vigny, J. Cadet, L. Voituriez, and E. Bisagni 1987. Photoreaction of monofunctional 3-carbethoxypsoralen with DNA: identification and conformational study of the predominant cis-syn furan side monoadduct to thymine. *Photochem. Photobiol.* 45:199-207

Game J.C., and R.K. Mortimer 1974. A genetic study of x-ray sensitive mutants in yeast. *Mutat. Res.* 24:281-292

Game J.C., T.J. Zamb, R.J. Braun, M. Resnick, and R.M. Roth 1980. The role of radiation (*rad*) genes in meiotic reombination in yeast. *Genetics* 94:51-68

Gia O., E. Uriarte, G. Zagotto, F. Baccichetti, C. Antonello, and S. Marciani-Magno 1992a. Synthesis and photobiological activity of new methylpsoralen derivatives. *J. Photochem. Photobiol. B.* 14:95-104

Gia O., S.M. Magno, A. Garbesi, F.P. Colonna, and M. Palumbo 1992b. Sequence specificity of psoralen photobinding to DNA: a quantitative approach. *Biochemistry* 31:11818-11822

Gilbertson L.A., and F.W. Stahl 1996. A test of the double-strand break repair model for meiotic recombination in *Saccharomyces cerevisiae*. *Genetics* 144:27-41

Grant E.L., R.C. von Borstel, and M.J. Ashwood-Smith 1979. Mutagenicity of cross-links and monoadducts of furocoumarins (psoralen and angelicin) induced by 360-nm radiation in excision-repair-defective and radiation-insensitive strains of *Saccharomyces cerevisiae*. *Environ. Mutagen.* 1:55-63

Guthrie, and G. Fink 1984. Methods in Enzymology Vol 184; A Guide to Yeast Genetics and Molecular Biology

Guzder S.N., P. Sung, L. Prakash, and S. Prakash 1998. Affinity of yeast nucleotide excision repair factor 2, consisting of the Rad4 and Rad23 proteins, for ultraviolet damaged DNA. *J. Biol. Chem.* 273:31541-31546

Guzder S.N., P. Sung, V. Bailly, L. Prakash, and S. Prakash 1994. RAD25 is a DNA helicase required for DNA repair and RNA polymerase II transcription. *Nature* 369:578-581

Guzder S.N., Y. Habraken, P. Sung, L. Prakash, and S. Prakash 1995. Reconstitution of yeast nucleotide excision repair with purified rad protein, replication protein A, and trasncription factor TFIIH. *J Biol. Chem.* 270:12973-12976

Guzder,S.N., P Sung, L. Prakash, and S. Prakash. 1993. Yeast DNA-repair gene RAD14 encodes a zinc metalloprotein with affinity for ultraviolet-damaged DNA . *Proc. Natl. Acad. Sci.*USA 90:5433-5437

Habraken Y., P. Sung, L. Prakash, and S. Prakash 1993. Yeast excision repair gene RAD2 encodes a single-stranded DNA endonuclease. *Nature* 366:365-368

Hallick L.M., C.V. Hanson, J.O. Cacciapuoti, and J.E. Hearst 1980. Photoaddition of trimethylpsoralen as a probe for the intra*Cell*ular organization of *Escherichia coli* DNA. *Nuc. Acids Res.* 8:611-622

Han E.K., and W.A. Saffran 1992. Differential repair and recombination of psoralen damaged plasmid DNA in *Saccharomyces cerevisiae*. *Mol. Gen. Genet.* 236:8-16

Hanson C.V., C.K. Shen, and J.E. Hearst 1976. Cross-linking of DNA in situ as a probe for chromatin structure. *Science* 193:62-64

Haynes R.H., and B.A. Kunz 1981. DNA repair and mutagenesis in yeast. In: J. Strathern, E.W. Jones, and J.R. Broach (Eds.), The Molecular Biology of the Yeast Saccharomyces, Life Cycle and Inheritance. Cold Spring Harbor Laboratory, Cold Spring Harbor, NY, pp 371-414

Hearst J.E., S.T. Isaacs, D. Kanne, H. Rapoport,and K Straub 1984. The reaction of the psoralens with deoxyribonucleic acid. *Q. Rev. Biophys.* 17:1-44

Henriques J.A., H.H. Andrade, M. Bankmann, and M. Brendel 1989. Reassessing the genotoxic potential of 8-MOP + UVA-induced DNA damage in the yeast *Saccharomyces cerevisiae*. *Curr. Genet.* 16: 75-80

Henriques J.A.P., and E. Moustacchi 1980. Sensitivity to photoaddition of mono- and bifunctional furocoumarins of X-ray sensitive mutants of *Saccharomyces cerevisiae*. *Photochem. Photobiol.* 31:557-563

Higgins D.R., S. Prakash, P. Reynolds, R. Polakowska, S. Weber, and L. Prakash 1983. Isolation and characterization of the RAD3 gene of *Saccharomyces cerevisiae* and inviability of rad3 deletion mutants. *Proc. Natl. Acad. Sci.* USA 80:5680-5684

Higgins N.P., K.Kato, and B. Strauss 1976. A model for replication repair in mammalian cells. *J. Mol. Biol.* 101:417-425

Hollstein M.C., D. Sidransky, B. Vogelstein, and C.C. Harris 1991. p53 mutations in human cancers. *Science* 253:49-53

Hollstein M.C., L. Peri, A.M. Mandard, J.A.Welsh, R. Montesano, R.A. Metcalf, M. Bak, and C.C. Harris 1991. Genetic analysis of human esophageal tumors from two high incidence geographic areas: frequent p53 bas substitutions and absence of ras mutations. *Cancer Res.* 51:4102-4106

Isaacs S.T., C.J. Shen, J.E. Hearst, and H. Rapoport 1977. Synthesis and characterization of new psoralen derivatives with superior photoreactivity with DNA and RNA. *Biochemistry* 16:1059-1064

Isaacs S.T., G. Wiesehahn, and L.M. Hallick 1984. In vitro characterization of the reaction of four psoralen derivatives with DNA. *Natl. Cancer Inst. Monogr.* 66:21-30

Jachymczyk W.J., R.C. von Borstel, M.R.A. Mowat, and P.J. Hastings 1981. Repair of interstrand cross-links in DNA of *Saccharomyces cerevisiae* requires two systems for DNA repair: The *RAD3* system and the *RAD51* system. *Mol. Gen. Genet.* 182:196-205

Jansen L.E., R.A. Verhage, and J. Brouwer 1998. Preferential binding of the yeast Rad4.Rad23 complex to damaged DNA. *J. Biol. Chem.* 273:33111-33114

Johnston B.H., M.A. Johnston, C.B. Moore, and J.E. Hearst 1977. Psoralen-DNA photoreaction: controlled production of mono- and diadducts with nanosecond ultraviolet laser pulses. *Science* 197:906-908

Kanne D., K. Rapoport, and J.E. Hearst 1984. 8-Methoxypsoralen-nucleic acid photoreaction. Effect of methyl substitution on pyrone vs. furan photoaddition. *J. Med. Chem.* 27:531-534

Kanne D., K. Straub, H. Rapoport, and J.E Hearst 1982. Psoralen-deoxyribonucleic acid photoreaction. Characterization of the monoaddition products from 8-methoxypsoralen and 4,5',8-trimethylpsoralen. *Biochemistry* 21:861-871

Kittler L., and G. Lober 1995. Sequence specificity of DNA-psoralen photoproduct formation in supercoiled plasmid DNA (pUC19). *J Photochem. Photobiol. B.* 27:161-166

Knox C.N., E.J. Land, and T.G. Truscott 1988. Triplet state properties and triplet-state-oxygen interactions of some linear and angular furocoumarins. *J Photochem. Photobiol. B.* 1:315-321

Kolodkin A.L., A.J. Klar, and F.W. Stahl 1986. Double-strand breaks can initiate meiotic recombination in *S. cerevisiae*. *Cell* 46:733-740

Kumaresan K.R., B. Hang, and M.W. Lambert 1995. Human endonucleolytic incision of DNA 3' and 5' to a site-directed psoralen monoadduct and interstrand crosslink. *J. Biol. Chem.* 270:30709-30716

Lamb B.C., 1998. Gene conversion disparity in yeast: its extent, multiple origins, and effects on allele frequencies. *Heredity* 80:538-552

Lawrence C.W., and D.C. Hinkle 1996. DNA polymerase zeta and the control of DNA damage induced mutagenesis in eukaryotes. *Cancer Surv.* 28:21-31

Lee J.M., and A. Bernstein 1993. p53 mutations increase resistance to ionizing radiation. *Proc. Natl. Acad. Sci.* USA 15:5742-5746

Levine A.J., J. Momand, and C.A. Finlay 1991. The p53 tumor suppressor gene. *Nature* 351:453-456

Lin L., D.N. Cook, G.P. Wiesehahn, R. Alfonso, B. Behrman, G.D. Cimino, L.Corten, P.B. Damonte, R. Dikeman, K. Dupuis, Y.M. Fang, C.V. Hanson, J.E. Hearst, C.Y. Lin, H.F. Londe, K. Metchette, A.T. Nerio, J.T.Pu, A.A. Reames, M. Rheinschmidt, J. Tessman, S.T. Isaacs, S. Wollowitz and L. Corash 1997. Photochem.ical inactivation of viruses and bacteria in platelet concentrates by use of a novel psoralen and long-wavelength ultraviolet light. *Transfusion* 37:423-435

Lin L., H. Londe, C.V. Hanson, G. Wiesehahn, S. Isaacs, G. Cimino, and L. Corash 1993. Photochemical inactivation of cell-associated human immunodeficiency virus in platelet concentrates. *Blood* 82:292-297

Magana-Schwencke N., and D. Averbeck 1991. Repair of exogenous (plasmid) DNA damaged by photoaddition of 8-methoxypsoralen in the yeast *Saccharomyces cerevisiae*. *Mutat. Res.* 251:123-131

Magana-Schwencke N., J.A.P. Henriques, R. Chanet, and E. Moustacchi 1982. The fate of 8-methoxypsoralen photoinduced crosslinks in nuclear and mitochondrial yeast DNA: Comparison of wild-type and repair-deficient strains. *Proc. Natl. Acad. Sci.* USA. 70:1722-1726

Malone R.E., S. Bullard, S. Lundquist, S.Kim, and T. Tarkowski 1992. A meiotic gene conversion gradient opposite the direction of transcription. *Nature* 359: 154-155

Maniatis T., E.F. Fritsch, and J. Sambrook 1982. *Molecular Cloning: A Laboratory Manual*. Cols Spring Harbor Laboratory Press, Cold Spring Harbor

Mantulin W.W. and P.S. Song 1973. Excited states of skin-sensitizing coumarins and psoralens. Spectroscopic studies. *J. Am. Chem. Soc.* 95:5122-5129

Meniel V., N. Magana-Schwencke, and D. Averbeck 1995. Preferential repair in yeast after induction of interstrand cross-links by 8-methoxypsoralen plus UVA. *Mutat. Res.* 329: 121-130

Miller R.D., L. Prakash, and S. Prakash 1982. Genetic control of excision of *Saccharomyces cerevisiae* interstrand DNA cross-links induced by psoralen plus near-UV light. *Mol. Cell. Biol.* 2:939-948

Moore T.A., A.B. Montgomery, and A.L. Kwiram 1976. Triplet electronic structure and photoreactivity of 8-methoxypsoralen. *Photochem. Photobiol.* 24:83-86

Nelson H.H., D.B. Sweetser,and J.A. Nickoloff 1996. Effects of terminal nonhomology and homeology on double-strand-break-induced gene conversion tract directionality. *Mol. Cell. Biol.* 16:2951-2957

Nelson J.R., C.W. Lawrence, and D.C. Hinkle 1996a. Thymine-thymine dimer bypass by yeast DNA polymerase zeta. *Science* 272:1646-1649

Nelson J.R., C.W. Lawrence, and D.C. Hinkle 1996b. Deoxycytidyl transferase activity of yeast *REV1* protein. *Nature* 382:729-731

Nickoloff J.A., and M.F. Hoekstra 1997. Double-strand break and recombinational repair in *Saccharomyces cerevisiae*, in *DNA Damage and Repair*. Humana Press, Totowa NJ.

O'Donovan A., A.A. Davies, J.G. Moggs, S.C. West, and R.D. Wood 1994. XPG endonuclease makes the 3' incision in human DNA nucleotide excision repair. *Nature* 371:432-435

Orr-Weaver T.L., and J.W. Szostak 1983. Yeast recombination: the association between double-strand gap repair and crossing-over. *Proc. Natl. Acad. Sci.* USA 80:4417-21

Ou C.N., and P.S. Song 1978. Photobinding of 8-methoxypsoralen to transfer RNA and 5-fluorouracil-enriched transfer RNA. *Biochemistry* 21:1054-1059

Ou C.N., C.H. Tsai, K.J. Tapley, and P.S. Song 1978. Photobinding of 8-methoxypsoralen and 5,7-dimethoxypsoralen to DNA and its effect on template activity. *Biochemistry* 21:1047-1053

Paques F., and J.E. Haber 1997. Two pathways for removal of nonhomologous DNA ends during double-strand break repair in *Saccharomyces cerevisiae*. *Mol. Cell. Biol.* 17:6765-6771

Pearlman D.A., S.R. Holbrook, D.H. Pirkle, and S.H. Kim 1985. Molecular models for DNA damaged by photoreaction. *Science* 227:1304-1308

Peckler S., B. Graves, D. Kanne, H. Rapoport, J.E. Hearst, and S.H. Kim 1982. Structure of a psoralen-thymine monoadduct formed in photoreaction with DNA. *J Mol. Biol.* 162:157-72

Prakash S., L. Prakash, W. Burke, and B.A. Montelone 1980. Effects of the RAD52 gene on recombination in *Saccharomyces cerevisiae*. *Genetics* 94:31-50

Priebe S.D., J. Westmoreland, T. Nilsson-Tillgren, and M.A. Resnick 1994. Induction of recombination between homologous and diverged DNAs by double-strand gaps and breaks and role of mismatch repair. *Mol. Cell. Biol.* 14:4802-4814

Ramaswamy M., and A.T. Yeung 1994. The reactivity of 4,5',8-trimethylpsoralen with oligonucleotides containing AT sites. *Biochemistry* 33:5411-5413

Resnick M.A., and P. Martin 1976. The repair of double-strand breaks in the nuclear DNA of *Saccharomyces cerevisiae* and its genetic control. *Mol. Gen. Genet.* 143:119129

Resnick, M.A., 1968. Genetic control of radiation sensitivity in *Saccharomyces cerevisiae*. *Genetics* 62:519-531

Reynolds R.J., D.R. Higgins, L. Prakash, and S. Prakash 1985. The nucleotide sequence of RAD3 gene of *Saccharomyces cerevisiae*: a potential adenine nucleotide binding amino acid sequence and a nonessential acidic carboxyl terminal region. *Nuc. Acids Res.* 13:2357-2372

Roche H., R.D. Gietz and B.A. Kunz 1995. Specificities of the *Saccharomyces cerevisiae* rad6,rad18, and rad52 mutators exhibit different degrees of dependence on the REV3 gene product, a putative nonessential DNA polymerase. *Genetics* 140:443-456

Rodighiero G., and F. Dall'Acqua 1976. Biochemical and medical aspects of psoralens. *Photochem. Photobiol.* 24:647-653

Rodighiero G., and F. Dall'Acqua 1986. Present aspects concerning the molecular mechanisms of Photochem.otherapy with psoralens. *Drugs Exp. Clin. Res.* 12:507-515

Rodriguez K., Z. Wang, E.C. Friedberg, and A.E. Tomkinson 1996. Identification of functional domains within the RAD1/RAD10 repair and recombination endonuclease of *Saccharomyces cerevisiae*. *J Biol. Chem.* 271:20551-20558

Rothstein R.J. 1983. Meth. Enzymol., 101:202-211

Rupp W.D., and P. Howard Flanders 1968. Discontinuities in the DNA synthesized in an excision-defective strain of *Escherichia coli* following ultraviolet irradiation. *J. Mol. Biol.* 31:291-304

Saeki T., C. Cassier, and E. Moustacchi 1983. Induction in *Saccharomyces cerevisiae* of mitotic recombination by mono and bifunctional agents: Comparison of the pso2-1 and rad52 repair deficient mutants to the wild-type. *Mol. Gen. Genet.* 190:255-264

Saffran W.A., C.R. Cantor, E.D. Smith, and M. Magdi 1992. Psoralen damage-induced plasmid recombination in *Saccharomyces cerevisiae*: dependence on *RAD1* and *RAD52*. *Mutat. Res.* 274:1-9

Saffran W.A., R.B. Greenberg, M.S. Thaler-Scheer, and M.M. Jones 1994. Single strand and double strand DNA damage-induced crossover recombination in yeast. Dependence on nucleotide excision repair and *RAD1* recombination. *Nuc. Acids Res.* 22:2823-2829

Salet C., T.M. De Sa E Melo, R. Bensasson, and E.J. Land 1980. Photophysical properties of aminoethylpsoralen in presence and absence of DNA. *Biochim. Biophys. Acta* 607:379-383

Sancar A. 1996. DNA excision repair. *Annu. Rev. Biochem.* 65:43-81

Schauber C., L. Chen, P. Tongaonkar, I. Vega, D. Lambertson, W. Potts, and K. Madura 1998. Rad23 links DNA repair to the ubiquitin/proteasome pathway. *Nature* 391:715-718

Shen C.K., and J.E. Hearst 1976. Psoralen-crosslinked secondary structure map of single-stranded virus DNA. *Proc. Natl. Acad. Sci.* USA 73:2649-2653

Shen C.K., and J.E. Hearst 1979. A technique for relating long-range base pairing on single-stranded DNA and eukaryotic RNA processing. *Anal. Biochem.* 95:108-116

Sherman F., G.R. Fink, and J.B. Hicks 1984. *Methods in Yeast Genetics.* Cold Spring Harbor Press, Cold Spring Harbor

Shim S.C., and Y.Z. Kim 1983. Photoreaction of 8-methoxypsoralen with thymidine. *Photochem. Photobiol.* 38:265-271

Shim S.C., J.S. Koh, and H.K. Shim 1983. Photoreaction of 4'5'-dihydropsoralen with thymine. *Photochem. Photobiol.* 38:369-372

Sinden R.R., and D.E. Pettijohn 1981. Chromosomes in living Escherichia coli *Cells* are segregated into domains of supercoiling. *Proc. Natl. Acad. Sci.* USA 78:224-228

Sinden R.R., J.O. Carlson, and D.E. Pettijohn 1980. Tortional tension in the DNA double helix measured with trimethylpsoralen in living E. coli *Cells*: analogous measurements in insect and human Cells. *Cell* 21:773-783

Sinden R.R., S.S. Broyles, and D.E. Pettijohn 1983. Perfect palindromic lac operator DNA sequence exists as a stable cruciform structure in supercoiled DNA in vitro but not in vivo.

Sladek F.M., A. Melian, and P. Howard-Flanders 1989. Incision by UvrABC excinuclease is a step in the path to mutagenisis by psoralen crosslinks in Escherichia coli. *Proc. Natl. Acad. Sci.* USA 86:3982-3986

Sogo J.M., H. Stahl, T. Koller, and R. Knippers 1986. Structure of replicating simian virus 40 minichromosomes. The replication fork, core histone segregation and terminal structures. *J. Mol. Biol.* 189:189-204

Song P.S. 1984. Photoreactive states of furocoumarins. *Natl. Cancer Inst. Monogr.* 66:15-19

Song P.S., and H. Baba 1974. Excited states of biomolecules II. *Photochem. Photobiol.* 20:527-532

Song P.S., and K.J. Tapley Jr. 1979. Photochem.istry and photobiology of psoralens. *Photochem. Photobiol.* 29:1177-1197

Song P.S., and R.D. Fugate 1975. Excited states of biomolecules III. *Photochem. Photobiol.* 22:277-285

Song P.S., and W.H. Gordon III 1970. A spectroscopic study of the excited state of coumarin. *J. Phys. Chem.* 74:4234-4240

Song P.S., M.L. Harter, T.A. Moore, and W.C. Herndon 1971. Luminescence spectra and photocycloaddition of the excited coumarins to DNA bases. *Photochem. Photobiol.* 14:521-530

Spielmann H.P., D.Y. Chi, N.G. Hunt, M.P. Klein, and J.E. Hearst, 1995c. Spin-labeled psoralen probes for the study of DNA dynamics. *Biochemistry* 34:14801-14814

Spielmann H.P., T.J. Dwyer, J.E. Hearst, and D.E. Wemmer 1995a. Solution structures of psoralen monoadducted and cross-linked DNA oligomers by NMR spectroscopy and restrained molecular dynamics. *Biochemistry* 34:12937-12953

Spielmann H.P., T.J. Dwyer, S.S. Sastry,J.E. Hearst, and D.E. Wemmer 1995b. DNA structural reorganization upon conversion of a psoralen furan-side monoadduct to an interstrand cross-link: implications for DNA repair. *Proc. Natl. Acad. Sci.* USA 92:2345-2349

Summary of the 8th report on carcinogens, U.S. Dept. of health and human services

Sun H., D. Treco, and J.W. Szostak 1991. Extensive 3'-overhanging, single-stranded DNA associated with the meiosis-specific double strand breaks at the ARG4 recombination initiation site. *Cell* 64:1155-1161

Sun H., D. Treco, N.P. Schultes, and J.W. Szostak 1989. Double-strand breaks at an initiation site for meiotic gene conversion. *Nature* 338:87-90

Sung P., L. Prakash, S. Weber, and S. Prakash 1987a. The RAD3 gene of *Saccharomyces cerevisiae* encodes a DNA-dependent ATPase. *Proc. Natl. Acad. Sci.* USA 84:6045-6049

Sung P., L. Prakash, S.W. Matson, and S. Prakash 1987b. RAD3 protein of *Saccharomyces cerevisiae* is a DNA helicase. *Proc. Natl. Acad. Sci.*USA 84:8951-8955

Sung P., P. Reynolds, L. Prakash, and S. Prakash 1993. Purification and characterization of the *Saccharomyces cerevisiae* RAD1/RAD10 endonuclease. *J. Biol. Chem.* 268:26391-26399

Sweetser D.B., H. Hough, J.F. Whelden, M. Arbuckle, and J.A. Nickoloff 1994. Fine-resolution mapping of spontaneous and double-strand break-induced gene conversion tracts in Saccharomyces cerevisiae reveals reversible mitotic conversion polarity. *Mol. Cell. Biol.* 14:3863-3875

Szostak J.W., T.L. Orr-Weaver, R.J. Rothstein, and F.W. Stahl 1983. The double-strand-break repair model for recombination. *Cell* 33:25-35

Tessman J.W., S.T. Isaacs, and J.E.Hearst 1985. Photochem.istry of the furan-side 8-methoxypsoralen-thymidine monoadduct inside the DNA helix. Conversion to diadduct and to pyrone-side monoadduct. *Biochemistry* 24:1669-1676

Thompson J.F. and J.E. Hearst 1983. Structure of E. coli 16S RNA elucidated by psoralen crosslinking. *Cell* 32:1355-1365

Van Houten B., H. Gamper, S.R. Holbrook, J.E. Hearst, and A. Sancar 1986. Action mechanism of ABC excision nuclease on a DNA substrate containing a psoralen crosslink at a defined position. *Proc. Natl. Acad. Sci. USA* 83:8077-8081

Van Scott E.J. 1975. Therapy of psoriasis 1975. *JAMA* 235:197-198

Watkins J.F., P. Sung, L. Prakash, and S. Prakash 1993. The *Saccharomyces cerevisiae* DNA repair gene RAD23 encodes a nuclear protein containing a ubiquitin-like domain required for biological function. *Mol. Cell. Biol.* 13:7757-7765

Weng Y.S. and J.A. Nickoloff 1996. Evidence for independent mismatch repair processing on opposite sides of a double strand break in *Saccharomyces cerevisiae*. *Genetics* 148:59-70

Wiesehahn G., and J.E. Hearst 1978. DNA unwinding induced by photoaddition of psoralen derivatives and determination of dark-binding equilibrium constants by gel electrophoresis. *Proc. Natl. Acad. Sci.* USA 75:2703-2707